



Lorenzo Pellizzer

Synthesis of cellulose-based flocculants and performance tests

Master's thesis in the scientific area of Chemical Engineering, supervised by Professor Doctor Maria da Graça Bomtempo Vaz Rasteiro and Doctor José António Ferreira Gamelas, Department of Chemical Engineering, Faculty of Science and Technology, University of Coimbra

July 2016



UNIVERSIDADE DE COIMBRA

Lorenzo Pellizzer

Synthesis of cellulose-based flocculants and performance tests

Master's thesis in the scientific area of Chemical Engineering, submitted to the Department of Chemical Engineering, Faculty of Science and Technology, University of Coimbra

Supervisors:

Professor Doctor Maria da Graça Bomtempo Vaz Rasteiro

Doctor José António Ferreira Gamelas

Institutions:

Department of Chemical Engineering, Faculty of Science and Technology, University of Coimbra

Financing:

Marie Curie Initial Training Networks (ITN) – European Industrial Doctorate (EID)

Grant agreement FP7-PEOPLE-2013-ITN- 604825

Coimbra, 2016

Acknowledgements

This work represents a big step in my academic career. It is not only my merit, but also of who has supported me and helped during this intense period. Therefore, I would like to thank:

Professor Doctor Maria da Graça Rasteiro for accepting me as Erasmus student and to give me the opportunity to be part of a Marie Curie project, to be my supervisor in this work, for the availability, for all the suggestions and corrections;

Professor José António Ferreira Gamelas for the help in the analytical procedures and the evaluation of the results as well as all the suggestions and corrections to my work;

PhD student Kinga Grenda, for the availability and the patience in teaching me the proper work in a laboratory, and for all the important tips;

The financial support from Marie Curie Initial Training Networks (ITN) – European Industrial Doctorate (EID), through Grant agreement FP7-PEOPLE-2013-ITN- 604825.

Abstract

One of the objectives of this work was to synthesize water soluble cellulose-based flocculants using extracted cellulose from *Eucalyptus* Kraft bleached pulp. Both cationic and anionic flocculants have been synthesized based on information from the literature. To increase cellulose reactivity, it was applied cellulose alkalization with NaOH aqueous solution and oxidation by sodium periodate. The cationization of cellulose was performed by using CHPTAC (3-chloro-2-hydroxypropyl trimethylammonium chloride) as reagent. The anionization was performed by using sodium metabisulfite as reagent. Some reaction variables have been changed in order to synthesize flocculants with different characteristics.

Once the water soluble flocculants were obtained, they have been characterized according to several techniques in order to determine the effective cellulose modification and other characteristic of the flocculants synthesized. To detect the modification spectroscopy techniques such as FTIR and ^1H NMR were used. To characterize the flocculants techniques like DLS (Dynamic Light Scattering), SLS (Static Light Scattering) and ELS (Electrophoretic Light Scattering) were used, to determine, respectively, the average hydrodynamic diameter of the coils, the molecular weight and the zeta potential. Moreover, from the elemental analysis measurements the degree of substitution (DS) was calculate. The characterization has shown a certain variability of the flocculants obtained in terms of charge and DS as a confirmation that their characteristic can be modulated by tuning the reaction variables.

The industrial application of the obtained cellulose-based flocculants was verified in wastewater treatment, in particular in the color removal from model effluents. The dyes selected for the performance test are among the ones frequently industrially used: Crystal Violet (liquid), Malachite Green (liquid) and Duasyn Direct Red 8 BLP (liquid) and Flora red 4bs, Orange 2, Acid Black 2, Basic Green 1 and Brilliant Yellow in the solid state. The performance has been evaluated calculating the percentage of color removed as a function of time, based on the decrease of absorbance of the supernatant water. The results show that both for CC (cationized cellulose) and ADAC (anionic dialdehyde cellulose) color removal percentages over 90% can be obtained for most dyes. Thus, these natural based polyelectrolytes can constitute good alternatives to the use of synthetic non- biodegradable flocculants in the treatment of very common and industrially frequent colored effluents.

Index

Acknowledgements	5
Abstract	6
Figures index	10
Tables index	12
Nomenclature and Symbols	14
1 Introduction	15
2 State of the Art	16
2.1 Wastewater treatment	16
2.2 Direct Flocculation	16
2.3 Mechanisms of flocculation	18
2.3.1 Bridging	19
2.3.2 Charge neutralization	21
2.3.3 Electrostatic patch	21
2.4 Factors influencing flocculation performance	22
2.4.1 Polymer dosage	22
2.4.2 Influence of pH and ionic strength	22
2.4.3 Shear degradation of polymers in solution	22
2.4.4 Polymer-cation complex formation in solution	23
2.4.5 Degradation of polymer by free radical attack	23
2.5 The natural polymers used in flocculation	23
2.5.1 Chitosan	24
2.5.2 Tannins	26
2.5.3 Gums and mucilage	26
2.5.4 Sodium alginate	27
2.5.5 Starches	27
2.5.6 Cellulose	28
2.6 Modification of natural polymers based flocculants	28
2.6.1 Starches modification	28
2.6.2 Tannins modification	30
2.6.3 Chitosans modification	31
2.6.4 Gums and mucilages modification	32

2.6.5 Cellulose modifications.....	33
3 Experimental work	37
3.1 Overview.....	37
3.2 Materials and chemicals	37
3.2.1 Cellulose.....	37
3.2.2 Chemicals and solvents.....	37
3.2.3 Color removal materials.....	38
3.3 Synthesis of cationic cellulose-based flocculants	38
3.3.1 Cationization of cellulose in NaOH aqueous solution	38
3.3.2 Attempt of cationization of DAC with CHPTAC	39
3.4 Synthesis of anionic cellulose-based flocculant.....	40
3.5 Determination of the aldehyde content of DAC and assessment of carboxyl's	40
3.6 Characterization procedures.....	41
3.7 Characterization of dyes.....	53
3.8 Performance tests: color removal	53
4 Results and discussion	56
4.1 Synthesis of cationic cellulose-based flocculants	56
4.1.1 Preliminary experimental work	56
4.1.2 Definitive Experimental work	61
4.1.3 Attempt to synthesis of cationic DAC	65
4.1.4 Color removal tests of CC.....	65
4.1.5 Color removal tests with undissolved CC.....	70
4.2 Synthesis of anionic cellulose-based flocculant.....	72
4.2.1 Synthesis of DAC	72
4.2.2 Synthesis of ADACs.....	73
4.2.3 Color removal tests with ADAC.....	75
5 Conclusions and future work.....	79
5.1 Conclusions	79
5.2 Future works.....	80
6 References	82
7 Appendix A	91
8 Appendix B	98
9 Appendix C	100

Figures index

Figure 1 - influence of polymer on particle adsorption and interactions leading to flocculation or dispersion. ¹³	20
Figure 2 - (a) Negatively charged particles. (b) Cationic flocculants. (c) Charge neutralization by patch mechanism (arrows show the attraction of opposite charges). ²	21
Figure 3 - Schematic view of a charge neutralization. ²¹	21
Figure 4 - Classification of flocculants. ³	23
Figure 6 - Mannich reaction with tannins. ⁶⁷	30
Figure 7 – Probable chemical structure of <i>Tanfloc</i> . ⁶⁹	31
Figure 8 - Periodate oxidation of cellulose. ⁸⁷	34
Figure 9 - Periodate and chlorite oxidation of cellulose. ⁸⁹	34
Figure 10 - Periodate oxidation of cellulose followed by the metabisulfite sulphonation reaction. ⁹¹	35
Figure 11 - Cationization of cellulose by Girard's reagent T. ⁹²	35
Figure 12 - Synthesis of amphoteric cellulose (QACMC) via etherification of CMC with EPTMAC.	36
Figure 13 - Schematic of cellulose oxidation and oxime reaction. ⁹⁹	40
Figure 14 - A multiple reflection ATR system. ¹⁰¹	42
Figure 15 – Example of the PSD by number required when there is not good <i>quality report</i> , on the left. The corresponding PSD by intensity, on the right.....	45
Figure 16 – Example of Debye Plot.....	47
Figure 18 - As the applied magnetic field increases, so does the energy difference between α - and β -spin state. ¹⁰⁷	50
Figure 17 – Spin energy state. ¹⁰⁷ The arrow representing B_0 points North.	50
Figure 19 – NMR spectrum: shielded nuclei come into resonance at lower frequencies than de-shielded nuclei. Upfield means farther to the right-hand side of the spectrum, and downfield means farther to the left-hand side of the spectrum. ¹⁰⁸	51
Figure 20 – Reaction scheme of the two-step cellulose cationization with CHPTAC. ⁹⁴	60
The range reported for the zeta potential was calculated as the half than difference between the higher and the lower value of measured zeta potential.	62
Figure 23 – Diagram of DS and zeta potential of CC samples in function of time from CC19 to CC24.	63

Figure 24 – Centrifuge tube after centrifugation of reaction solution with CHPTAC. Note the difference between supernatant CC24 and precipitated CC24u.....	64
Figure 25 – FTIR spectrum of CC17.....	64
Figure 26 - ¹ H NMR spectrum of CC22.....	65
Figure 27 – Pictures of color removal tests of CC19 with Acid Black. The numbers correspond to the samples in Table 10 (0 is the initial effluent).	67
Figure 30 – ¹ H NMR spectrum of ADAC3-1.....	75
Figure 31 – Pictures of color removal tests of Acid Black with ADAC3-1.....	76

Tables index

Table 1 - Parameters to be controlled for process optimization. ¹⁰	17
Table 2 - Comparison between coagulation-flocculation and direct flocculation. ³	18
Table 3 - Flocculation mechanisms for different types of flocculants. ³	19
Table 4 - Application of natural flocculants in wastewater treatment. ³	25
and 3-chloro-2-hydroxypropyltrimethylammonium chloride. ⁵⁷	29
Table 5 – Trials for cellulose dissolution in NaOH-based aqueous solution.*	57
*More information are reported in Table 5.....	59
Table 7 – Trials of cationized cellulose starting from Cellulose-NaOH-Urea solution of Table 6.*.....	59
Table 8 – Reaction data for synthesis of cationic cellulose-based flocculant.*	62
Table 9 – Characterization results of CC and undissolved CC.*	63
Table 10 – Data from dyes characterization.*.....	65
Table 11 – Color removal test of Acid Black with CC19. Experimental conditions and performance after 5 min,	
Table 12 - Color removal test of Acid Black with CC21. Experimental conditions and performance after 5 min, 1 h, 24 h.....	67
Table 13 - Color removal test of Methylene Blue with CC19. Experimental conditions and performance after 5 min, 1 h, 24 h.....	68
Table 14 - Color removal test of CC19 with Basic Green 1. Experimental conditions and performance after 5 min, 1 h, 24 h.....	68
Table 15 - Color removal test of Brilliant Yellow with CC16. Experimental conditions and performance after 5 min, 1 h, 24 h.....	69
Table 16 - Color removal test of Flora Red 4bs with CC17. Experimental conditions and performance after 5 min, 1 h, 24 h.....	69
Table 17 - Color removal test of Acid Black with CC21u. Experimental conditions and performance after stirring.....	70
Table 18 - Color removal test of CC21u with Brilliant Yellow. Data and performance after stirring.....	71
Table 19 - Color removal test of Flora Red 4bs with CC21u. Experimental conditions and performance after stirring.....	71

Table 20 - Color removal test of Orange 2 with CC21u. Experimental conditions and performance after stirring.	71
Table 21 – Reaction data and substitution degree for synthesis of DACs.....	73
Table 23 - Color removal test of Methylene Blue with ADAC3-1. Experimental conditions and performance after 5 min, 1 h, 24 h.....	75
Table 24 - Color removal test of Acid Black with ADAC3-1. Experimental conditions and performance after 5 min, 1 h, 24 h.	76
Table 25 - Color removal test of Flora Red 4bs with ADAC3-1. Data and performance after 5 min, 1 h, 24 h.....	77
Table 26 - Color removal test of Brilliant Yellow with ADAC3-1. Experimental conditions and performance after 5 min, 1 h, 24 h.....	77

Nomenclature and Symbols

Nomenclature/Acronyms

ADAC	Anionic DAC
AGU	Anhydroglucose unit
ATR	Attenuated total reflectance
CC	Cationic cellulose
CDAC	Cationic DAC
CHPTAC	3-chloro-2-hydroxypropyl trimethylammonium chloride
COD	Chemical oxygen demand
DAC	Dialdehyde cellulose
DLS	Dynamic light scattering
DMSO	Dimethyl sulfoxide
DP	Polymerization degree
DS	Substitution degree
EA	Elemental analysis
ELS	Electrophoretic light scattering
EPTAC	2,3-epoxypropyltrimethylammonium chloride
FTIR	Fourier transform infrared spectroscopy
NMR	Nuclear magnetic resonance
CPAA	Cationic polyacrylamide
PDI	Polydispersity index
SLS	Static light scattering
TSS	Total suspended solid
UV-VIS	Ultraviolet–visible spectroscopy

1 Introduction

Flocculants are widely used to achieve efficient solid-liquid separations in many industries such as pharmaceuticals, water treatment, and papermaking. They are used to increase size and density of the aggregates and promote the settling rate and dewaterability of suspensions. The most part of them are synthetic polyelectrolytes derived from oil with a scarce biodegradability and adverse impact on human health which is associated with their degradation products. Consequently, there is a growing interest in replacing oil-based flocculants with more sustainable alternatives based on raw materials such as cellulose, chitin, starch, and their derivatives. Among naturally occurring polysaccharides, cellulose has great potential as one of the most environmentally friendly non-food sources to be used in the production of a wide range of eco-friendly products. Among the major concerns in the use of cellulose are its limited solubility in water and poor reactivity due to its highly ordered hydrogen bond network and high crystallinity. To overcome these problems, many modifications can be set up, both homogeneously, in solvent systems, or heterogeneously, in aqueous medium. The last one is preferred because of the advantages regarding toxicity, volatility and price. One way to improve cellulose reactivity is to synthesize the dialdehyde cellulose (DAC) in water solution. Starting from this more reactive form, the cellulose can be further modified to obtain many potential polyelectrolytes. Another way, it is to perform cellulose alkalization using sodium hydroxide aqueous solution. One possibility to produce cationic polyelectrolytes is to conduct a reaction with CHPTAC which introduces quaternary ammonium groups into the cellulose. On the other hand, to produce anionic polyelectrolytes one possibility is to performed a reaction with sodium metabisulfite to produce sulfonated cellulose. There are several suitable reactions of cellulose with different monomers, each of them requires specific conditions and need tuning many adjustable variables in order to generate plenty of distinct flocculants. In literature, it is well known that both degree of substitution and distribution of functional groups influence the properties of the modified cellulose. This versatility gives a wide spectre of products and likewise applications, not only as flocculants.

The aims of this work is to synthesize water soluble cellulose-based flocculants, using extracted cellulose from Eucalyptus bleached Kraft pulp and set up performance test on model effluents. The work is divided into three parts:

1. Synthesis of water soluble cellulose-based flocculants, both cationic and anionic, by increasing cellulose reactivity and further introducing substitution groups in its backbone;
2. Characterization of the flocculants obtained with several techniques such as DLS, SLS, ELS, FTIR spectroscopy, ¹H NMR and elemental analysis;
3. Performance tests on model effluents (dyes suspensions/solutions) to assess the capability of the flocculants in color removal.

2 State of the Art

2.1 Wastewater treatment

Wastewater treatment is a process to convert wastewater into an effluent that can be either returned to the water cycle with minimal environmental issues or reused. The wastewater treatments are currently composed of a series of methods like biological treatment, membrane processes, wet air oxidation treatment, photocatalytic technique, chemical and electrochemical oxidation techniques etc., which are always expensive and high energy consumption. The wastewater produced from different kinds of industries normally contains very fine suspended solids, dissolved solids, inorganic and organic particles, metals and other impurities. Due to the very small size of the particles and presence of surface charge, the task to make these particles larger with a heavier mass for settling and filtration becomes challenging.¹ Among the methods to enable the solid-liquid separation in the wastewater treatment, the coagulation/flocculation is one of the most widely used. In this process, after the addition of a coagulant and/or flocculant, finely divided or dispersed particles are aggregated or agglomerated together to form large particles of such a size (flocs) which settle and cause clarification of the system.² Nowadays, the use of polymeric flocculants is preferred with respect to inorganic coagulants to facilitate separation process due to its higher effectiveness.³ At the time being, synthetic and natural polymeric flocculants are becoming very popular in industrial effluent treatment due to their natural inertness to pH changes, high efficiency with a low dosage, and easy handling.⁴ However, the synthetic polymeric flocculants have the main problems of non-biodegradability and unfriendly to the environment⁵, while the with natural flocculants are related to moderate efficiency and short shelf life. Recently, the so-called modified natural flocculants have been synthesized and studied in order to combine the best properties of synthetic and natural polymers.

The research of the most cost-effective flocculants is the main challenge in many studies. In fact, flocculants play the major role in flocculation processes and their performance depends on specific variables. The common variables to control flocculation efficiency are: settling rate of flocs, sediment volume (SVI), percent solid settled, turbidity or supernatant clarity, the percentage of pollutants removal or water recovery.⁶

2.2 Direct Flocculation

The conventional treatment method of coagulation/flocculation is going to be substituted by the more cost/time effective direct flocculation. As reported in some studies, the treatment of

residues after coagulation may cause several health hazards. Inorganic coagulants have high poisoning factor for encephalopathy, neurodegenerative illnesses⁷ and Alzheimer's disease. Moreover, the synthetic polyelectrolytes are also toxic and carcinogenic.⁸ Due to those issues, there is a strong need in replacement of inorganic and organic coagulants with alternative natural coagulants/flocculants.

The flocculation process is aimed at treating fine colloidal particles to create larger aggregates or flocs, which settle rapidly and are easily removable by secondary optional processes such as filtration and thickening. This process of aggregation of suspended particles is performed by polyelectrolytes (cationic, anionic, or amphoteric) mainly by either a bridging or a patch mechanism. Depending on the type of industrial unit operation, different properties of the flocs are required. For example, for filtration is essential strong porous and less dense flocs whereas, in the sedimentation process, dense large flocs with minimum porosity are preferred.⁹ The properties of flocs have been discussed in the literature and the important parameters to be controlled for process optimization are reported on **Table 1**.¹⁰

Table 1- Parameters to be controlled for process optimization.¹⁰

PHYSICAL FACTORS	CHEMICAL FACTORS
state of particle dispersion	type of charge on polymer
initial particle size	charge density
intensity of shear	structure of the polymer
type of shear	molecular weight of polymer
time of agitation	pH of the suspension
rate of polymer addition	species in solution
polymer dosage	
pulp density	

The physical factors (pulp density, intensity and time of shear, rate of addition and concentration of the polymer, initial particle size) and the chemical factors (nature of charge, charge density, molecular weight of the polymer, pH of the suspension and solution species, etc.) determine the kinetics of the flocculation, floc growth and also control the floc morphology. In order to separate one specific component of the mixed slurry it is necessary a well-defined polymer as well as in-depth understanding of the mode of attachment of the functional groups onto the specific surfaces sites. Unfortunately, the selective flocculation technique was found to have some strong limitations and there are few commercial scale processes in operation.¹¹ The problems regard the non-specific adsorption on the solid

surfaces, particle entrapment in the flocs, coating of impurities on the particles resulting from interferences between constituents, etc. This, in general, leads to poor separation efficiency, but if these problems are solved the method of separation offers great potential. Nevertheless, in direct flocculation the polymers used are workable in a wide range of pH values and they produce less volume of sludge in respect to the coagulation-flocculation.³ In addition, if they are natural-based polymers, some of the sludge generated is readily for disposal after simple treatment that leads to the reduction of overall treatment cost.¹² Despite the advantages, the direct flocculation application is mostly limited to organic-based wastewater with high concentration of suspended and colloidal solids; such as food, paper and pulp, and textile effluents. On a general point of view, each treatment has its own pros and cons that depend also on the type of wastewater. An overview of the differences between coagulation–flocculation and direct flocculation and the general procedures for each process are presented in **Table 2.**³

Table 2 - Comparison between coagulation-flocculation and direct flocculation.³

Comparison criteria	Coagulation-flocculation	Direct flocculation
Application	Inorganic and organic based wastewater	Organic based wastewater
Treatment Ability	Suspended and dissolved solid particles	Suspended and colloidal solid particles
Types of chemicals to be used	Coagulant(s)(e.g. inorganic metal salt(s)) followed by polymeric flocculant(s) (usually anionic)	Cationic or anionic polymeric flocculants (usually cationic)
Treatment process	More complicated, requires the pH adjustment	Simpler without pH adjustment
Sludge generated	More sludge is produced, may contain metals and monomer residue	Less sludge is produced, may contain monomers residue
Overall treatment cost	More expensive due to chemicals cost (coagulant and flocculant) and large sludge treatment cost	Less expensive because only one chemical is used and less sludge treatment cost
Flocculation mechanism	Charge neutralisation (coagulation) followed by bridging (flocculation)	Charge neutralisation and bridging occur concurrently

2.3 Mechanisms of flocculation

A qualitative explanation of the process of polymeric flocculation is very complicated because of the physiochemical complexity of the process. Generally, many different types of mechanism are involved but flocculation has the most influence on floc structure. As mention before, the two main flocculation mechanisms involved are the bridge flocculation and the patch neutralization, instead the destabilization process due to an increase in Van

der Waals attraction or a decrease in electrostatic repulsion are not predominant. Anyway, other flocculation mechanisms have been proposed in some studies, such as depletion flocculation, displacement flocculation, etc.^{13 14} The flocs formed by the bridge mechanism are entirely different from those formed by the charge-patch neutralization, which are similar to flocs formed by inorganic coagulants. Usually, the most common mechanism is charge neutralization, where the flocculant and adsorbed pollutants are of opposite charge.

Table 3 - Flocculation mechanisms for different types of flocculants.³

Category of flocculants	Type of flocculant	Flocculation mechanism
Chemical coagulants	Inorganic metal salts	Charge neutralisation
Chemical flocculants	Polyelectrolytes with low MW and low CD	Charge neutralisation
	Polyelectrolytes with high MW and low CD	Bridging
	Polyelectrolytes with low MW and high CD	Electrostatic patch
	Polyelectrolytes with high MW and high CD	Electrostatic patch+ Bridging
Bio/flocculants	Cationic (chitosan)	Charge neutralisation+ Bridging
	Anionic (cellulose, tannin, sodium alginate)	Bridging
	Anionic/Neutral plant based flocculants	Bridging
Grafted flocculants	Amphoteric/cationic/anionic graft copolymers	Charge neutralisation+ Bridging/bridging only

The majority of particles in wastewater are hydrophobic and characterized by negative charge. As consequence, applying cationic polyelectrolytes leads to a reduction of the surface charge of particles and, by decreasing electrostatic the repulsion, the aggregation can start. Moreover, the type of mechanism varies according to the type of flocculants and they are summarized in **Table 3**.³

2.3.1 Bridging

In general, polymer bridging takes place when long chain polymers with high molecular weight and low charge density¹⁵ adsorb on particles in such a way that long loops and tails create links between particles. In this way the polymers are adsorbed on particles through several segments with the remaining part free to move in the solution (**Figure 1a**). There are two possible types of bridging mechanisms. The first when two particles are linked by the long chains of one polymer or when the link is formed by the separate adsorption of polymers on different particle surfaces.^{16 17} The later case can happen when the surface of the particles is very covered, the loops and tails are long and the degree of association between polymer chains is strong. The combination of these mechanism allows the formation of the aggregates

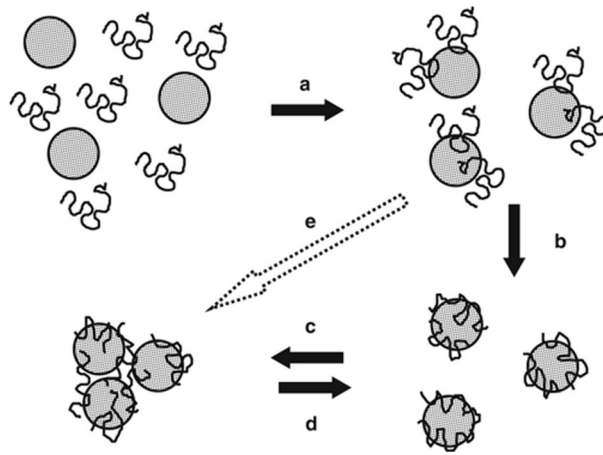


Figure 1- influence of polymer on particle adsorption and interactions leading to flocculation or dispersion.¹³

(**Figure 1e**). Two additional factors can influence the polymer coiling which are: solution pH and the presence of counterions. In particular, if the ionic strength grows up the polymer could coil-up and this weakens the bridging bonds. In some cases, if the entire polymer is adsorbed on the surface of the particle it cannot operate as a bridge anymore (**Figure 1b**) or, if the surface is completely covered there are no more sites for adsorption. This unwanted case leads to redispersion of the particles in the solution. Another case of redispersion is caused by the rupture of flocs caused by agitation and the following back-adsorption of polymers extended part in the same particle (**Figure 1d**).

In summary, to guarantee an effective bridging process it is essential a long polymer chain (high molecular weight) in order to permit a sufficient extension of the chains from one particle to another.¹⁸ Besides, there should be sufficient free sites on a particle for attachment of segments of polymer chains adsorbed on other particles. Furthermore, the amount of polymer should not be too much, otherwise the particle surfaces will be completely covered and it would be impossible to create any bridge between particles.¹⁹ So, it is not recommended an excessive amount of polymer but also insufficient amount may avoid forming enough bridges among particles. Based on these considerations the concept of an optimum polymer dosage for bridging flocculation is necessary.¹³ Finally, bridging mechanism can give much larger and stronger aggregates than those formed in other ways. In addition, bridging contacts are also more resistant to breakage at elevated shear levels.

2.3.2 Charge neutralization

This mechanism takes place when the flocculant and the adsorption site are of opposite charge. The flocculation could occur simply as a result of the reduced surface charge of the particles (reduction of zeta potential) and hence a decreased electrical repulsion force between colloidal particles, which allows the formation of Van der Waals forces of attraction to encourage initial aggregation of colloidal and fine suspended materials to form microflocs (**Figure 2**). In many studies, it has been found that optimum flocculation occurs at polyelectrolytes dosages around that needed to just neutralize the particle charge, or to give a zeta potential close to zero (isoelectric point). At this point, the particles would tend to agglomerate under the influence of the Van der Waals' forces and the colloidal suspension becomes destabilized.²⁰ If too much polymer is used, however, a charge reversal can occur and the particles will again become dispersed, but with a positive charge rather than negatively charged. Sometimes, the flocs formed with charge neutralization are loosely packed and fragile and settle slowly. Thus, the addition of another high molecular weight polymer with bridging effect is necessary to bond the microflocs together for fast sedimentation and high water recovery.²¹

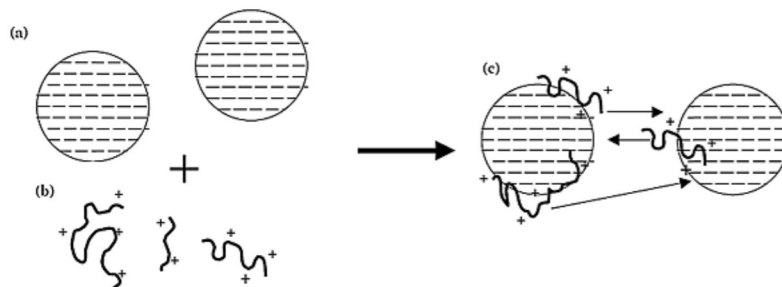


Figure 2 - (a) Negatively charged particles. (b) Cationic flocculants. (c) Charge neutralization by patch mechanism (arrows show the attraction of opposite charges).²

2.3.3 Electrostatic patch

This flocculation mechanism concerns with the use of high charge density polyelectrolytes that have low molecular weight. The polymers are adsorb on negative surfaces of the particles with a fairly low density of charged sites, but since they are much smaller than the surface area of the particles, bridging capability is reduced and it is formed a sort of patch on the surface.²² An

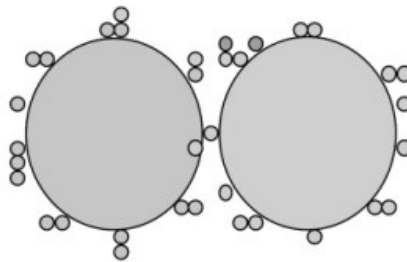


Figure 3 - Schematic view of a charge neutralization.²¹

important consequence of ‘patchwise’ adsorption is that, as particles approach closely, there is an electrostatic attraction between positive patches and negative areas, which can give particle attachment and hence flocculation (**Figure 3**).¹³ Floccs produced in this way are not as strong as those formed by bridging, but stronger than floccs formed in the presence of metal salts or by simple charge neutralization. Anyway, the bridging flocculation becomes more likely if the charge density is reduced.²³

2.4 Factors influencing flocculation performance

2.4.1 Polymer dosage

The amount of polymer and the dosage technique are important parameters controlling the flocculation process. As already mentioned, the optimum amount of polymer is crucial, nevertheless the method of addition has its own importance. For example, multi-stage additions can lead to using lower polymer concentrations compared to an addition all at once. The multi-stage additions can ensure a more efficient uptake of the polymer by the particles and faster rate of flocc growth. However, the floccs may break up more easily and to a high rate of addition may lead to insufficient mixing in the suspension and then an ineffective flocculation.

2.4.2 Influence of pH and ionic strength

The pH can control both the charges on the polymer and on the particle surface. As a case of study, the flocculation of alumina using a pyrene labeled PAA polymer suggested that the pH variation offers a means of controlling the flocculation efficiency.²⁴ The ionic strength is also very important since the compression of the double layer results in a reduction in the interparticle separation and this would lead to flocculation by Van der Waals attraction, the charge patch or bridging flocculation. At low ionic strength and low pH, the polymer is strongly coiled in solution but on adsorption, the tails can extend to some extent from the surface. In low ionic strength, the size of the polymer coils increases so it may extend in solution and favor bridging.

2.4.3 Shear degradation of polymers in solution

A molecular weight reduction of polymers can be caused by shear degradation consequently of the pumping of polymer solution around the plant. From this point view, it is important to understand the effect of shear rate on the polymer system with the aim to reduce it. Factors such as shear time, concentration, polymer type and ionic strength can influence the polymer structure. An extensive study on loss of flocculation efficiency of polyacrylamide flocculants has shown that the polymer degradation increases with polymer solution concentration.²⁵

2.4.4 Polymer-cation complex formation in solution

The formation of complexes between multivalent cations and carboxyl groups on anionic polyacrylamides has been reported throughout the literature.²⁶ In fact, this mechanism has frequently been used to explain the binding of anionic flocculants to negative charge surface. Some cations such as Cu form chelate by bonding to two carbonyl ligands, instead Ca and Mg do not affect the polymer conformation but they only form complexes with carboxyl groups. The interior crosslink of the molecular coils leads to a change in the number of polar groups in sterically exposed positions, which cause changes in conformation and degree of chelation. As consequence, it is observed a precipitation of the polymer from solution at high cation concentrations.

2.4.5 Degradation of polymer by free radical attack

The action of free radical over an extended period of time can lead to molecular degradation.²⁶

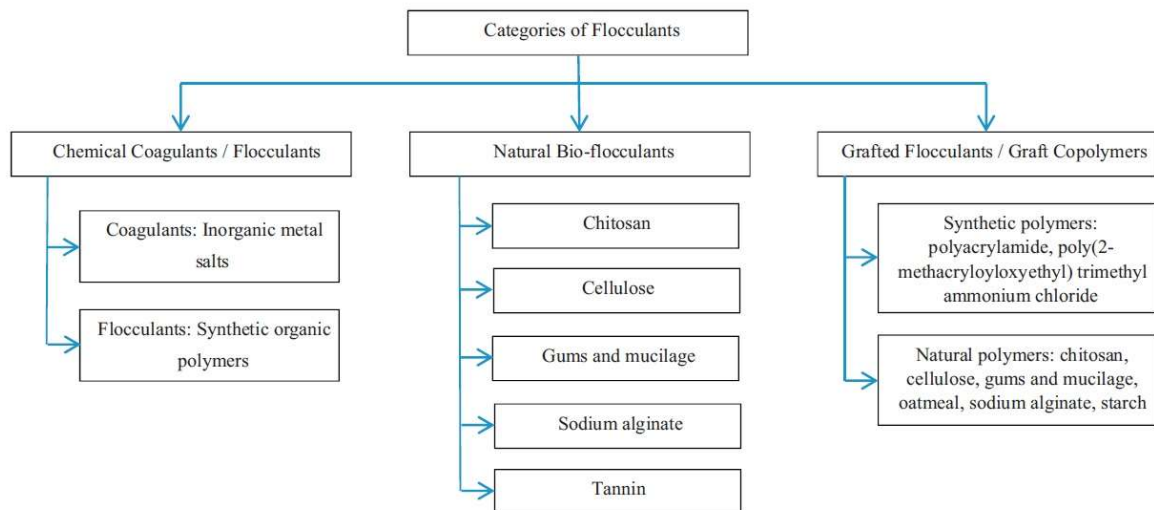


Figure 4 - Classification of flocculants.³

However, this has in general a mild effect on the flocculation performance. The use of small amount of ethanol or methanol to wet the dry polymer beads during solution preparation has shown to prevent this behavior.

2.5 The natural polymers used in flocculation

As reported in Figure 4, the flocculants applied in wastewater treatment can be divided in three categories: chemical coagulants/flocculants, natural bio-flocculants and grafted flocculants.³ Chemical coagulants/flocculants are conventionally applied in wastewater treatment and derived from synthetic materials. The conventional chemical coagulants/flocculants that are widely applied in industrial wastewater treatment can be classified into two major groups: inorganic mineral additives/metal salts which are used as

coagulants and organic polymeric materials that are employed as flocculants. Grafted flocculants have been investigated recently and synthesized by combining the properties of chemical and natural flocculants.

Natural bio-flocculants have been extensively explored on the past few years and sourced from natural materials. In fact, biodegradability, nontoxicity, eco-friendly behaviour and sustainability became the main goals in the development of natural bio-flocculants and their grafted derivatives. Based on this characteristics, the demand for application in treating water and wastewater continue to increase and they have emerged to be promising alternative materials to replace conventional flocculants. Furthermore, compared with conventional chemical flocculants, bio-flocculants present also a fairly shear stability, easy availability from reproducible agricultural resources and no production of secondary pollution.¹³ In addition, as biopolymers are biodegradable, the sludge can be efficiently degraded by microorganisms.¹⁴ Thus, they can be applied not just in water and wastewater treatment but also in food and fermentation processes, pharmaceuticals as well as in cosmetics. Natural organic flocculants are mostly based on polysaccharides or other natural polymers. They have the ability to destabilize the colloidal particles by increasing the ionic strength and decreasing the thickness of the diffuse part of the electrical double layer. Or, since they have particular macromolecular structures with a variety of functional groups (e.g. carboxyl and hydroxyl groups) they can adsorb specifically counterions to neutralize the particle charge.²⁷ The multitude of polar groups (anionic, cationic, nonionic) that polymers contain can change with the solution pH and the type of chemical modification. This changes the solubility of the macromolecules in water that is a fundamental feature for application as flocculants. Many biopolymers based flocculants such as starches, chitosan, tannins, cellulose, alginate, gums and mucilage have been studied and majority is listed in **Table 4**.

2.5.1 Chitosan

There are several naturally occurring polymers that have inherent cationic properties or, alternatively, the polymer can be modified to yield a cationic polyelectrolyte. The most prominent of these is chitosan, a biopolymer extracted from shellfish sources. This is partially deacetylated chitin which is a 1:4 random copolymer of N-acetyl- α -D-glucosamine and a D-glucosamine.²⁸ Chitosan does not present solubility in either water or organic solvents but it is soluble in dilute organic acids such as acetic acid and formic acid and inorganic acids (with the remarkable exception of sulphuric acid).^{29,14} Thanks to the high cationic charge density (presence of primary amino groups)³⁰ and long polymer chains with high molecular weight, it

can be an effective coagulant and/or flocculant for the removal of contaminants in the suspended and dissolved state.^{31,14} It can be quite effective at NOM (Natural Organic Matter) removal,^{32,33,34} even though it can be slightly charged (17%) at neutral pH levels. The use of chitosan in water purification applications generally has been extensively reviewed, with references to its use in decolorizing dye-containing effluents³⁵ or textile wastewater,²⁹ the treatment of food processing wastes, organic matter (e.g. lignin and chlorinated compounds) in pulp and paper mill wastewater,³⁶ metal ion removal and sludge conditioning.³⁷ Chitosan is

Table 4 - Application of natural flocculants in wastewater treatment.³

Bio product	Flocculant	Effluent/Wastewater	Optimum results	Bio product
Chitosan	Chitosan	Pulp and paper mill wastewater	Turbidity COD	10-1.1NTU 1303-516mg/L
	Chitosan	Cardboard industry wastewater	Turbidity COD	85% removal 80% removal
	Chitosan	Dye containing solution	Dye	99% removal
Tannin	Anionic tannin	Drinking water	Turbidity	300-2FTU
	Anionic tannin	Ink/containing effluent from cardboard box/making factory	Dye	99% removal
	Modified tannin (cationic)	Polluted surface water	COD Cu ²⁺ , Zn ²⁺ , Ni ²⁺	84% removal 90%, 75%, 70% removal
	Modified tannin (cationic)	Municipal wastewater	Turbidity COD BOD*	100% removal 50% removal 50% removal
Gums and mucilage	Anionic Psyllium mucilage	Sewage effluent	TSS	95% removal
	Neutral Fenugreek mucilage	Tannery effluent	TSS	85-87% removal
	Tamarind mucilage	Golden yellow dye and direct fast scarlet dye	TDS* Dye	40% removal 60% and 25% removal
	Mallow mucilage	Biologically treated effluent	Turbidity	67% removal
	Anionic Okra gum	Biologically treated effluent	Turbidity	74% removal
	Anionic Isabgol mucilage	Semi/aerobic landfill leachate	COD Colour TSS	64% removal 90% removal 96% removal
Cellulose	Anionic sodium carboxymethylcellulose	Drinking water	Turbidity	93% removal
	Anionic dicarboxylic acid nanocellulose	Municipal water	Turbidity COD	40-80% removal 40-60% removal

*BOD is the biological oxygen demand, COD is the chemical oxygen demand and TDS is the total dissolved solids in the wastewater.

efficient in cold water at very low concentrations, producing reduced volume of sludge, which is easily degraded by microorganisms. It acts according to two flocculation mechanisms: charge neutralization (it has positively charged amino group) and bridging.

Results already described in the literature indicate that chitosan can be a potential substitute for metallic salts and synthetic polyelectrolytes in treating drinking water and wastewaters.¹⁴ The development of chitosan-based materials as useful coagulants and flocculants is still an expanding field in the area of water and wastewater treatment.

2.5.2 Tannins

Tannins are biodegradable anionic polymers³⁸ which come from polyphenolic secondary metabolites such as bark, fruits, leaves and others.³⁹ The most common commercial tannins are mimosa bark tannin, quebracho wood tannin, pine bark tannin and eucalyptus species bark tannin. They have been widely applied in several industries, through medical uses, to uses in the food industry, as well as in ink manufacture, dye industry, plastic resins, water purification, manufacture of adhesives, surface coatings and manufacture of gallic acid, etc. Tannins are often classified into two groups: the first group is the one of hydrolyzable tannins, which are esters of sugar and are usually further divided into two groups: the gallotannins and the ellagitannins; The second group is the one of condensed tannins, which are derivatives of flavan and are mainly extracted from larch (*Larix gmelinii*), black wattle (*Acacia mearnsii*), quebracho, and chestnut.⁴⁰ The application of tannins as coagulant has been tested many times in different fields such as removal of suspended and colloidal materials in drinking water treatment,²⁷ removal of suspended matters from synthetic raw water,³⁸ and removal of dyes, pigments and inks from ink-containing wastewater.⁴¹ However, in these studies tannin was coupled with aluminium sulfate as coagulant to obtain the destabilization of the negatively charged colloidal particles. In fact, a study demonstrates that the combination of aluminium sulfate as coagulant and tannin as flocculant significantly reduced the required doses of the coagulant.²⁷ Recently, in order to avoid the necessity of coagulant, modified tannins (*Tanfloc* flocculant) have been tested to remove heavy metals from polluted surface water and in municipal wastewater treatment.³⁹ Thanks to quaternary nitrogen along the chain it has a cationic character, thus, it can be used for direct flocculation without coagulant and pH adjustment.

2.5.3 Gums and mucilage

A safer and environmental friendly alternative to synthetic chemical flocculants is derived from several plants gums and mucilage. These plant-based flocculants are generally obtained through aqueous extraction, precipitation with alcohol and drying. Good performances are

exhibited in many cases like the treatments of landfill leachate,⁴² biologically treated effluent,⁴³ textile wastewater,⁴⁴ tannery effluent and sewage effluent.^{45,46} In these studies, they are claimed to perform minimum 85% of TSS removal, 70% of turbidity removal, 60% of COD reduction and 90% of colour removal. Moreover, these bio-flocculants were also able to remove 85% of suspended solids from sewage water and up to 90% of colour from tested effluents, with the flocculation efficiency equal to synthetic poly-acrylamide.⁴⁷

2.5.4 Sodium alginate

The sodium alginate is a linear water-soluble anionic polymer derived from the sodium salt of alginic acid.⁴⁸ It seems like a gelling polysaccharide and is extracted from seaweeds. Most of the large brown seaweeds are potential sources of alginate, their properties being different from one species to another. The most important technical properties of alginates are their thickening character (increase in the solvent viscosity upon dissolution), their ionic exchange aptitude, and their gel-forming ability in the presence of multivalent counterions. These features are a direct consequence of the fact that alginates are polyelectrolytes and follow, therefore, the usual behaviour of charged polymers. Based on this behaviour, the flocculation efficiency has been tested in the treatment of industrial textile wastewater and synthetic dye wastewater by using aluminium sulfate as coagulant. The results reveal that the polymer is capable of more than 90% colour removal and 80% of COD reduction.

2.5.5 Starches

Starches have attracted attention for industrial use for wastewater treatment purposes because of its renewability, biodegradability and low cost. In its natural form, starch consists of a mixture of two polymers of hydroglucose units, amylose and amylopectin, and is one of the most abundant natural polymers in the world.⁴⁹ The application in the treatment of real industrial wastewater as coagulation-flocculation agent is divided between the use of modified and unmodified starch. Studies conducted upon the direct utilization of unmodified starches are very limited. Only recently a study demonstrates the performance of unmodified starches used as natural coagulant in coagulation–flocculation treatment of POME (palm oil mill effluent).⁵⁰ Although modified starch may provide higher efficiency in wastewater treatment, the potentially hazardous chemicals used to modify the structure of starch such as formaldehyde, highly corrosive caustic soda and high amount of solvent are the main drawbacks for commercialization.⁵¹ The natural and unmodified starch can still be considered as a preferable choice in wastewater treatment because it can eliminate or reduce the use of harmful inorganic coagulants without the need of chemical modifications. In fact, it performed well in the

treatment of real industry wastewater, either as a primary coagulant or as a flocculant aid. Anyway, studies on the characteristics of the flocs produced from the treatment of real industrial wastewater using starch are limited.⁵⁰ In recent years, a study has investigated adsorption and flocculation behavior of amphiphilic cationic starch derivatives in dispersions of the most important papermaking fillers.⁵²

2.5.6 Cellulose

This homopolymer, a linear chain of polysaccharide formed by repeated connections of D-glucose building blocks, and having biodegradable properties, is promising as a feedstock for the production of chemicals with applications in various industries.⁵³ Cellulose can be obtained from a variety of sources such as wood, annual plants, microbes, and animals. These include seed fibers (cotton), wood fibers (hardwoods and softwoods), bast fibers (flax, hemp, jute, and ramie), grasses (bagasse, bamboo), algae, and bacteria. Cellulose has good water purification effects because it has abundant free –OH groups on the chain, enabling efficient removal of metal ions and organic matters from water for excellent chelating effect. However, owing to poor water solubility and relatively low chemical reactivity, application of cellulose as a flocculant is always limited. To overcome those shortcomings, modified cellulose materials have been manufactured, and carboxymethylation is a conventional and useful method for chemical modification. The water-soluble (hydrophilic) modified cellulose plays a very important role as a potential replacement of oil-based flocculants. Some cellulose derivatives were already successfully tested in order to remove suspended solids. There is also a growing interest in developing low-cost biomass (cellulosic) absorbents for treating dye-contaminated wastewater (colour removing) from various types of wastewater (agricultural, industrial, municipal wastes). For example, anionic sodium carboxymethyl-cellulose (CMCNa) that was prepared from an agricultural waste date palm rachis was tested as an eco-friendly flocculant coupled with aluminium sulfate as coagulant for removal of turbidity in drinking water treatment.⁵⁴ In another study, anionized dicarboxylic acid nanocellulose (DCC) flocculant was produced and examined its flocculating properties with ferric sulphate as coagulant, in municipal wastewater.⁵⁵

2.6 Modification of natural polymers based flocculants

2.6.1 Starches modification

There are many reports in literature on preparation of flocculants from chemical modification of starches. For example, starch phosphates are derivatives obtained with phosphoric acid and include mono-, di- and tri-starch phosphate esters. Monoesters can be produced by the reaction

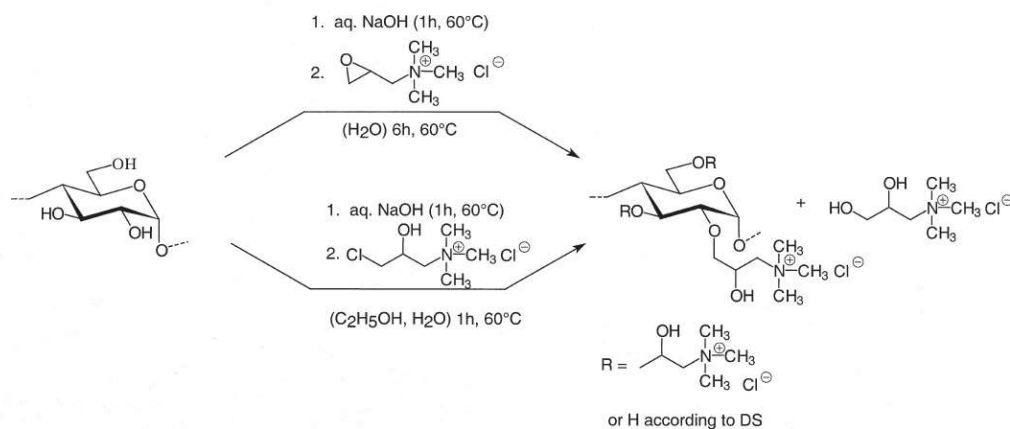


Figure 5 – Reaction scheme for the cationization of starch with 2,3-epoxypropyltrimethylammonium chloride and 3-chloro-2-hydroxypropyltrimethylammonium chloride.⁵⁷

of starch with inorganic phosphates, with or without urea and with organic phosphorus containing reagents. These products are anionic compounds that are used also for the flocculation as well as adhesives in papermaking, textiles, pharmaceuticals, foods, agriculture.⁵⁶ On the other hand, cationic starches are obtained by the reaction of starch with reagents containing amino, imino, ammonium or sulphonium groups. The two main types of commercial products are the tertiary amino and quaternary ammonium starch ethers (**Figure 5**).⁵⁷ Among the reagents that can add quaternary ammonium groups to starch, probably the most popular is the EPTAC. This compound has the characteristics that it can establish an ether bond with the OH groups of starch. Thus, it reacts with starch so as to form a compound that is stable over a very wide pH range. From the point of view of reaction media, the wet process seems to promise better product quality, whereas homogeneous phase cationization can be complicated by the high viscosity of starch paste. On the other hand, the use of heterogeneous systems preserves better starch granules structure⁵⁸ and it was shown that cationized starches that maintained the structure of native starch were better flocculants.⁵⁹ As starch is less expensive than the cationizing reagent, the cost of the latter can mainly influence the price of cationized starch, and thus it is essential to maximize reaction efficiency in order to turn this product competitive with regard to synthetic polymers. Kavaliauskaite et al.⁶⁰, managed to improve previous efficiency values and obtained cationized starches, precrosslinked or not, with substitution degree (DS) between 0.2 and 0.85 and reaction efficiencies between 82 and 93%. Reactions were carried out in heterogeneous conditions, with preservation of granule structure, employing monosaccharide units: EPTAC: NaOH: H₂O = 1: (0.3–2):(0–0.175): (0–11) molar ratios.⁶⁰ Hebeish et al. showed that for the case of starch DS and reaction efficiency follow the order: aqueous medium > aqueous/nonaqueous medium > semidry method > nonaqueous medium.

These authors also tested different bases for the reaction and found that effectiveness followed the order $\text{NaOH} > \text{Na}_2\text{CO}_3 > \text{NaHCO}_3$. Evaluating different organic amines as bases, the effectiveness order was diethylamine $>$ ethylamine $>$ methylamine. Diethylamine was as effective as NaOH, not causing as much alkaline hydrolysis of the epoxide as NaOH.⁶¹ The cationized starch is applied as flocculants with at least a DS higher than 0.2. Ellis et al.⁶² prepared several cationic starch derivatives from oxidized and esterified starches by reaction with tetraethyl ammonium bromide and pyridine respectively.⁶² The ability of these starch derivatives to remove suspended particles from surface water was comparable to the one of aluminium sulfate.⁶² In another report Nishiuchi et al.⁶³ prepared a cationic flocculant for kaolin suspensions by reaction of corn or potato starch successively with epichlorohydrin and triethylamine.⁶³ Cationic starch with DS of 0.29 or 0.36, were succinylated to a DS of 0.11–0.34, to obtain amphoteric products. These were tested in the flocculation of kaolin suspensions and the sedimentation of wastewater sludge. Amphoteric starch presented the advantage of a broader range of efficient phase separation conditions (flocculation “window”) when compared to cationic starch.⁶⁴

2.6.2 Tannins modification

As previously mentioned, tannins are classified into two groups: hydrolysable and condensed. Because of their negative charge, condensed tannins are not used directly as flocculants to remove anionic pollutants in water or wastewater.⁶⁵ To improve their flocculant capacity, the tannins can be modified by aldehydes, amines, or other cationic reagents,⁶⁶ and most of the modification methods and performance data are patented. The mechanism of the modification is the Mannich reaction, which involves the introduction of a quaternary nitrogen into the tannin’s complex structure, mainly in the 6,8-resorcinol A rings (**Figure 6**).⁶⁷ The resulting tannin polymer possesses higher molecular weight and amphoteric character due to the presence of both cationic amines and anionic phenols on the polymer. After modification, tannin flocculants can be used alone to remove pollutants in water. After polymerizing tannin with formaldehyde and monoethanolamine, Quamme and Kem observed that the polymer products

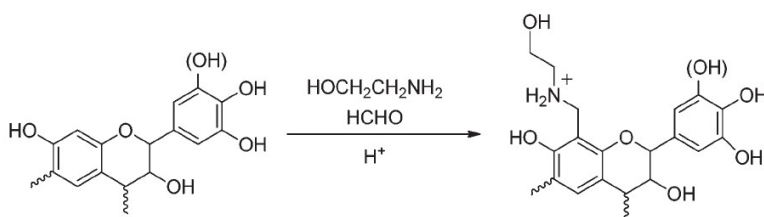


Figure 6 - Mannich reaction with tannins.⁶⁷

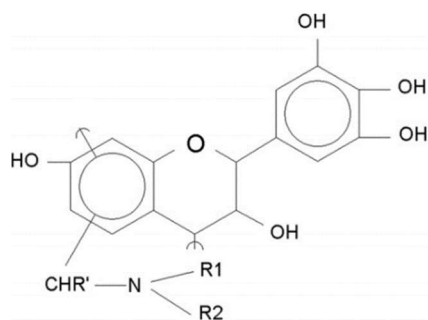


Figure 7 – Probable chemical structure of *Tanfloc*.⁶⁹

were more effective in the treatment of river water to remove turbidity and color than alum and ferric chlorides.⁶⁸ Already Beltran-Heredia and Sánchez-Martín conducted the clarification of raw water from a treatment plant using flocculant derived tannins, commercially called *Tanfloc*, belonging to Brazilian company TANAC. The product is obtained from the bark of the acacia tree common in Brazil, a tannin-based compound, consisting of flavonoid structures with an average molecular weight of 1.7 kDa, and positively charged nitrogen in its structure, as shown in **Figure 7**.⁶⁹ Even if the industrial production process of *Tanfloc* is protected by intellectual patents, similar procedures are referred to as Mannich-based reactions. It involves tannin polymerization through the addition of formaldehyde (37%), ammonium chloride, and commercial hydrochloric acid. The resulting product, obtained under specific temperature conditions, has a viscous appearance and contains 36% of active material. In the research, the efficiency of *Tanfloc* in water clarification process is not dependent to the temperature. It allows the effective removal of BOD, COD, turbidity levels (up to 80%), with application of 40 mg L⁻¹, and removing about 30% of anionic agent surfactant, and generate little sludge volume, being biodegradable. Another flocculant obtained by tannins modification is *SilvaFLOC*, a trademark that belongs to Silvateam (Italy). This tannin-based product is modified by a physico-chemical process and has a high flocculation power. It is obtained from *S. balansae* bark and the production process is under intellectual patent law. According to Silvateam information, *SilvaFLOC* is a compound based on *Quebracho* tannin extract, 2-aminoethanol, hydrochloric acid and formaldehyde. It is presented as a dark brown liquid with a 16% solid content.

2.6.3 Chitosans modification

Chitosan is a cationic biopolymer and is the deacetylated derivative of chitin. Chitin deacetylation is performed by the hydrolysis of the acetamide groups at high temperature in a strongly alkaline medium. The reaction is generally carried out heterogeneously using concentrated (40–50 per cent) NaOH or KOH solutions at temperatures above 100°C, preferably in an inert atmosphere or in the presence of reducing agents, such as NaBH₄ or

thiophenol, in order to avoid depolymerization. The specific reaction conditions depend on several factors, such as the starting material, the previous treatment and the desired degree of acetylation. Nevertheless, with only one alkaline treatment, the maximum deacetylation degree attained will not surpass 75–85 per cent. Prolonged treatments cause the degradation of the polymer without resulting in an appreciable increase in the deacetylation degree (Figure 8). , The degree of N-acetylation influences not only the physicochemical characteristics, but also the biodegradability and immunological activity of chitosan. In a recent study, CHPTAC was incorporated onto chitosan in an aqueous alkaline solution. In this way, the flocculation performance of the chitosan could be altered by the incorporation of the CHPTAC moiety. The study showed that not all the modified chitosans had superior flocculation performance versus the native chitosan. It was demonstrated that the modified chitosan with a moderate molecular weight and a moderate charge density showed the best flocculation performance in both model suspensions.

2.6.4 Gums and mucilages modification

In the most part of the studies, gums and mucilage are used as flocculating agents directly without any modification of the native raw material. The performances are quite good in all selected application, considering also all the common advantage of natural polymers as biodegradability. Anyway, a gum-grafted polyelectrolyte has been synthesized recently in order to produce a green flocculant.⁷⁰ The work reports the under pressure preparation of reduced *gum rosin* and the further grafting with polyacrylamide. The modification steps consist in the initial conversion of *gum rosin* acids into alcohols by using sodium borohydride. Then polyacrylamide grafted reduced *gum rosin* was synthesized under pressure with potassium persulphate (KPS) as thermal initiator. The process followed is claimed to be eco-friendly as all the reactions are carried out in aqueous solvent and the backbone used is a biodegradable natural source. In another paper, pure *Tamarindus* mucilage and its PAA grafted copolymer were tested as flocculants for color removal. The copolymer was synthesized by grafting acrylamide onto tamarind mucilage by a radical polymerization method in aqueous system, using ceric ion/nitric acid redox initiator. Grafting of polyacrylamide did not affect the biodegradability of *Tamarindus* mucilage although the shelf life was improved. The grafted copolymer, Tam-g-PAA, showed better flocculation efficiency for dye removal than the pure mucilage.⁷¹

2.6.5 Cellulose modifications

Native cellulose has a relatively low reactivity towards adsorption or flocculation in water treatment.⁷² Thus, the introduction of new functional groups on the surface of cellulose can increase its surface polarity and hydrophilicity, which can, in turn, enhance the adsorption of polar adsorbents and the selectivity of the cellulose for the target pollutant.⁷³ However, the chemical modification of this natural polymer is slightly difficult because of the low reactivity. This is influenced also by the large number of hydrogen bonds which decrease the potential solubility in most common solvents. Commonly, the modification of cellulose fibers is performed by heterogeneous synthesis that may lead to unexpected byproducts or cellulose decomposition since is poorly controllable. However, using special cellulose solvents it is possible to conduct the reactions in homogenous state. For instance, LiCl in DMSO⁷⁴ or tetrabutylammonium fluoride in DMSO (TBAF/DMSO)⁷⁵, are able to disrupt the hydrogen bonds of cellulose and further dissolve cellulose. As it is known the properties of cellulose strongly depend on the types of substituent groups and on their degree of substitution, as well as on their distribution in the cellulose backbone.

One of the most known cellulose-based water soluble anionic polyelectrolyte is sodium carboxymethylcellulose (CMC). CMC, which is a water soluble polymer obtained from the reaction of hydroxyl groups at the 2, 3, and 6 positions of the AGUs of cellulose with chloroacetic acid, is one of the most important cellulose ethers because it is relatively inexpensive, nontoxic, highly biocompatible, and biodegradable. More in detail, the synthesis of CMC involves two reaction stages: mercerization and etherification. The reactions are commercially carried out in water-alcohol mixture, usually as a slurry process at 10% pulp consistency. In the first stage the pulp is treated with NaOH at 20 to 30°C and the alcohol is usually ethanol or isopropanol. The product of this stage is called alkali cellulose (Na-cellulose) and is highly reactive towards monochloroacetic acid (MCA), or its sodium salt, which is added in the following etherification stage. The reaction between alkali cellulose and the etherification agent is normally carried out at about 50 to 70 °C.⁷⁶ Nowadays, the original two-step dry process of mercerization and etherification has been widely substituted by a one-step slurry process that incorporates the use of an alcohol as co-solvent. The DS is an important CMC parameter, determining, for example, its solubility in water. The theoretical maximum of the DS value for cellulose/CMC is 3.0, but the range of commercially available CMC grades is generally in the range 0.4 to 1.5.⁷⁷ Increasing the DS enhances solubility in water, in particular CMC shows a good water solubility for DS above 0.6.⁷⁸

Another way to confer anionic character to cellulose is through the introduction of sulphonate groups (-SO₃⁻). Zhu et al.⁷⁹ proposed the direct sulphonation of cellulose in *N,N*-dimethylformamide (DMF) using the ClSO₃H/DMF complex as the sulphonation agent. In this work, the obtained polyelectrolytes with a substitution degree (DS) above 0.38 showed good water solubility. Svensson et al.⁸⁰ also obtained water soluble cellulose sulphate by using NH₂SO₃H in DMF (DS 0.57). Furthermore, sulphonation agents, such as sulphuric acid, SO₃, chlorosulphuric acid, SO₂Cl₂, and complexes of these agents such as SO₃/DMF and SO₃/Pyridine were also applied in order to obtain cellulose sulphate.^{81,82}

In order to increase cellulose reactivity, it has been reported by Liimatainen et al.⁸³ a potential modification way through the introduction of aldehyde groups into the cellulose backbone. In this modification, the vicinal hydroxyl groups at positions 2 and 3 in the cellulose are oxidized to aldehyde groups with sodium metaperiodate to produce DAC (**Figure 8**). The reaction requires using high excess of oxidant and a long reaction time. However, it has been reported that reaction efficiency can be improved, for instance, by mechanical milling, heating and metal salts, as cellulose activators. Aminin et al.⁸⁴ also reported ultra-sonication pre-treatment as one potential way to improve the cellulose reactivity to periodate oxidation. Starting from DAC many further derivatizations can be performed: sulphonates can be obtained by bisulfite addition, carboxylic acid derivatives through further oxidation and imines can come from the Schiff base reaction.

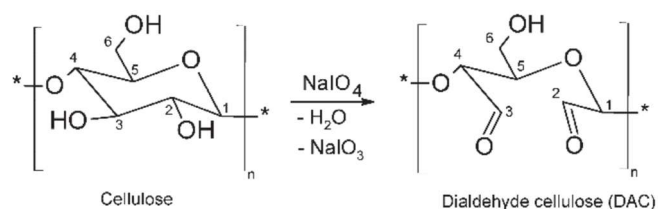


Figure 8 - Periodate oxidation of cellulose.⁸³

Anionic dicarboxyl acid cellulose (DCC) derivatives with variable charge densities were synthesized from DAC using chlorite oxidation (**Figure 9**).⁸⁵ During the reaction, periodate and chlorite-oxidized celluloses are suspended in deionized water at a consistency of 0.5%, and the pH of the suspensions is adjusted to approximately 7.5 using dilute NaOH. In Zhu et al.⁸⁶ work a series of natural dicarboxyl cellulose flocculants (DCCs) were synthesized in one-step via

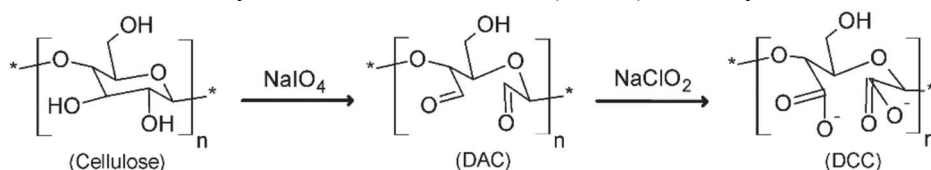


Figure 9 - Periodate and chlorite oxidation of cellulose.⁸⁵

Schiff-base route. The cellulose solvent (NaOH/Urea solution) was utilized during the synthesis process and the positive results showed that the NaOH/Urea solvent effectively promoted the dialdehyde cellulose (DAC) conversion to DCC. Moreover, it has been demonstrated that DCCs with a carboxylate content more than 1 mmol/g exhibit steady flocculation performance to kaolin suspension in the broad pH range from 4 to 10. Its flocculation capacity in an effluent from paper mill also showed excellent efficiency.

Anionic sulphonated cellulose (ADAC) derivatives, with variable charge densities can be synthesized from the DAC using a sulphonation reaction with sodium metabisulfite in an aqueous solution for 24-72 h at room temperature (**Figure 10**).⁸⁷ This periodate oxidation and sulphonation of cellulose leads to obtaining an effective flocculant for kaolin suspensions.

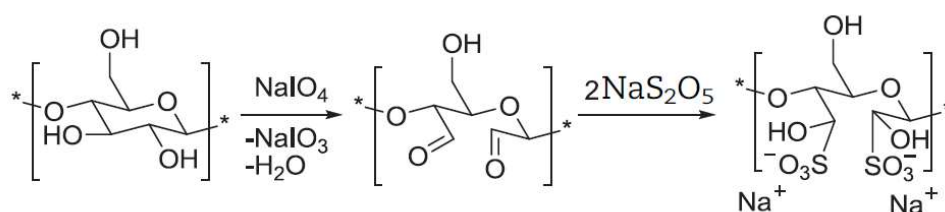


Figure 10 - Periodate oxidation of cellulose followed by the metabisulfite sulphonation reaction.⁸⁷

In Sirviö et al.⁸⁸ studies, a highly cationic charged cellulose was obtained by modification of DAC using Girard's reagent T (**Figure 11**). The quaternary ammonium modification of cellulose lead to a novel biopolymeric flocculation agent that showed a good performance on calcium carbonate and kaolin suspensions. Sirviö et al.⁸⁹ also introduced some modifications on a previously described procedure by using higher temperatures and applying metal salts (such as LiCl , ZnCl_2 , CaCl_2 , MgCl_2) as cellulose activators in order to improve the reaction efficiency. It has been found, that LiCl over all the studied metal salts, is the most successful to reduce the amount of inter and intra molecular hydrogen bonds between cellulose molecules and thus significantly improve the periodate oxidation of cellulose. Moreover, using higher temperatures with LiCl yields high cellulose aldehyde content within shorter oxidation time and lower amount of periodate. Although periodate is toxic and relatively expensive, through its

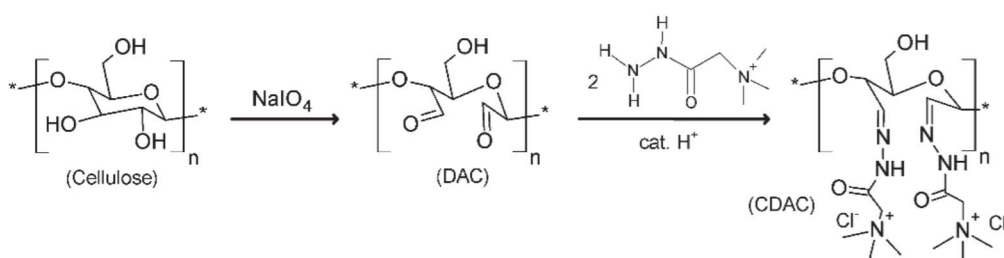


Figure 11 - Cationization of cellulose by Girard's reagent T.⁸⁸

regeneration and recycling, the process is brought into a sustainable/environmentally friendly level.⁸⁹

Amphoteric natural polyelectrolytes also come into focus as potential effective flocculant agents. In a polymeric backbone, cationic and anionic charged groups improve the solubility across the entire pH range, which entails their wide range of applicability. It was proved by Kono and Kusumoto⁹⁰ that amphoteric cellulose with a high degree of cationic substitution presented excellent flocculation ability in a wide pH range toward kaolin suspensions. The reported synthesis of amphoteric molecules, starting from carboxymethylcellulose (as an anionic group) and EPTMAC (2,3-epoxypropyltrimethylammonium chloride, as a cationic part of molecule) in NaOH solution at 60 °C allows to obtain polyelectrolytes with several different cationic and anionic degree of substitution (**Figure 12**).⁹⁰

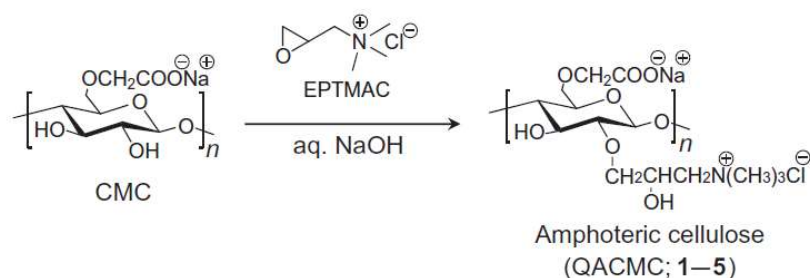


Figure 12 - Synthesis of amphoteric cellulose (QACMC) via etherification of CMC with EPTMAC.

3 Experimental work

3.1 Overview

This chapter refers to the materials used for the experiments as well as the methods applied in each phase of the work. Three different routes were selected for the synthesis of cationic and anionic cellulose-based flocculants: cationization of cellulose and of dialdehyde cellulose by using an etherifying agent, anionization of dialdehyde cellulose by using sodium metabisulfite. A two-step synthesis process was used to produce the cellulose-based flocculants. In the former route, was first treated in alkaline conditions and further cationized with 3-chloro-2-hydroxypropyl-trimethylammonium chloride (CHPTAC). In the latter route: first, cellulose was modified to dialdehyde cellulose (DAC) by periodate oxidation, then, the resultant DAC was tentatively cationized. Similarly, for the synthesis of anionic cellulose-based flocculant, cellulose was first modified to DAC and further anionized. The characterization of synthesized flocculants was based on a series of analysis: FTIR spectra, zeta potential, average hydrodynamic diameter, molecular weight, proton NMR spectra. The performance of the new cellulose-based flocculants was evaluated on synthetic effluents (colour removal tests).

3.2 Materials and chemicals

3.2.1 Cellulose

Cellulose was the raw material for the synthesis of cellulose-based flocculants. It was extracted from bleached eucalyptus pulp, derived from dry sheets of paper mill in Portugal. It was stored and used in dried form with a residual calculated percentage of moisture, as described in the section 3.6.

3.2.2 Chemicals and solvents

The most part of chemicals used for the synthesis of cationized and anionized cellulose flocs were obtained as p.a. grade from Sigma-Aldrich and used without further purification. The pure urea pearls, used in preliminary experiments, were purchased from AppliChem Panreac. Sodium hydroxide in pearls was purchased from PRONALAB. Hydrochloric acid 37%, Sodium acetate, Dimethyl sulphoxide and 2-Propanol, Acetone were supplied by VWR. Ethanol absolute was purchased from Fisher Chemical. The solvents *n*-Hexane and *n*-Heptane were supplied from Riedel-de Haen. All chemicals used for aldehyde content analysis of DACs ($\text{NH}_2\text{OH}\cdot\text{HCl}$, CH_3COOH and $\text{CH}_3\text{COONa}\cdot 3\text{H}_2\text{O}$) were obtained as p.a. grade from Sigma-Aldrich and used without further purification.

3.2.3 Color removal materials

Dyes for color removal tests were used to prepare model coloured effluents and used without further purification. Crystal Violet (liquid), Malachite Green (liquid) and Duasyn Direct Red 8 BLP (liquid) were supplied from Feldkirch Inc. Flora red 4bs (solid) was supplied from Flora. Orange 2 (solid) and Acid Black 2 (solid) were purchased from Roth. Basic Green 1 (solid) was supplied from Alfa Aesar. Brilliant Yellow (solid) was supplied by CHT-R Beitlich. The dyes were further characterized and the results are reported in the relative section 4.4.

As complexing agents for the flocculation, sodium bentonite and Aluminium sulfate-18-hydrate of extra purity supplied by Riedel-de Haen were used. Cationic polyacrylamide (CPAA) supplied by AQUA+TECH, with commercial name SnowFlake E2, was also used in experiments for color removal as a reference.

3.3 Synthesis of cationic cellulose-based flocculants

3.3.1 Cationization of cellulose in NaOH aqueous solution

The procedure reported in this section is an adaptation of a work by Zhang et al.⁹¹ The different nature of starting material respect of the one reported in the article has required several modifications in order to carry out the synthesis and maintain the principles of the project. The cationic cellulose-based flocculants were synthesized by a reaction between cellulose and CHPTAC in a 13 wt% NaOH aqueous solution.

Alkalization of cellulose

The first step of the synthesis aims to increase the cellulose dissolution in water. This was pursued by dispersing in a round-bottom flask a weighted amount of cellulose in a precise volume of 13 wt% NaOH aqueous solution pre-cooled to 0 °C. The cellulose-NaOH solution was stirred for 1 hour at room temperature. The molar ratio between NaOH and cellulose was fixed at 12.9 (mol NaOH/ mol AGU). Raw cellulose was broken into small pieces before the dispersion in NaOH solution.

Cationization with CHPTAC

The same round-bottom flask was collocated in a paraffin oil bath pre-heated at 60 °C. A certain amount of CHPTAC aqueous solution (60 wt%) was added dropwise to the reaction solution, continuously stirred with a magnetic stirrer. The molar ratio between CHPTAC and AGUs has been fixed at 9 in all reactions. After the addition of the reagent, the flask was closed with a rubber cap and kept on stirring for the amount of time required. The temperature was kept

constant during the reaction with an ON/OFF temperature controller connected to the paraffin oil bath. After the reaction, the mixture was left to cool down to room temperature and then it was neutralized with aqueous acetic acid 1 M. The mixture was transferred into centrifuge tubes and centrifuged at mild conditions (2500 rpm for 10 min) in order to separate the dissolved cationized cellulose (CC) from the undissolved part. The supernatant containing the dissolved CC was further recovered, transferred into other centrifuge tubes, precipitated with ethanol and centrifuged again at 9000 rpm for 5 min. The precipitated product was finally oven-dried at 60 °C and stored in sealed containers. The undissolved CC was filtered with a 1 µm paper filter using 300 mL of distilled water. It was oven-dried at 60 °C and stored in sealed containers.

3.3.2 Attempt of cationization of DAC with CHPTAC

By the time this work is written it is not reported in literature any route of synthesis of cationic cellulose-based flocculants from DAC. The idea on the basis of this synthesis is that CHPTAC could eventually react with DAC to give a higher molecular weight polyelectrolyte respect to the one obtained by cationizing DAC with cationic Girard's reagent T.⁹² This is a two-step reaction that required first, the preparation of DAC by periodate oxidation of cellulose and second, the attempt of synthesis of cationic DAC (CDAC) by reaction with CHPTAC in alkaline conditions.

Preparation of dialdehyde cellulose by periodate oxidation of cellulose

Highly oxidized cellulose was produced by weighing 100 g of cellulose suspension with a consistency of 4% into a 500 mL round-bottom flask and adding 300 mL of deionized water containing 7.2 g of LiCl and 8.2 g of NaIO₄. The reaction vessel was covered with aluminium foil to prevent the photo-induced decomposition of periodate and placed in a paraffin oil bath. The reaction mixture was stirred with a magnetic stirrer at 75 °C. After a desired time of reaction, the product was filtered and washed several times with deionized water to remove iodine-containing compounds.^{92,93}

Attempt of cationization of DAC

In a hypothesized reaction procedure, non-dried DAC (0.5 g on a dry basis) was weighted into a 100 mL beaker and 10 mL of deionized water was added. The mixture pH was adjusted to around 8 with a 13 wt% NaOH aqueous solution. Then, CHPTAC aqueous solution (60 wt%) was added dropwise with CHPTAC/aldehyde molar ratio of 4. The mixture was stirred with a magnetic stirrer at 60 °C till to get a transparent solution. The temperature was kept constant during the reaction with an ON/OFF temperature controller connected to the paraffin oil bath.

In order to isolate the product, precipitation was tried with isopropanol, ethanol, acetone, heptane, hexane and DMSO. The results and discussions about these trials are reported in **Appendix C**.

3.4 Synthesis of anionic cellulose-based flocculant

The route for this synthesis is based on the work of Liimatainen et al.⁹⁴ and Zhang et al.⁹⁵ The preparation of dialdehyde cellulose follows the same procedure reported in the previous section 3.3.2.

Anionization of DAC

Non-dried DAC (0.5 g on a dry basis) was weighted into a 100 mL round-bottom flask with 20 mL of deionized water. Then, sodium metabisulfite was added into the mixture with a ratio (mmol bisulfite/g DAC) of 14 or 28. The reaction mixture was kept for 32-72 h at room temperature (24 °C) and stirred with a magnetic stirrer. The flask was closed with a rubber cap during the reaction. The transparent reaction solution was transferred to centrifuge tubes, centrifuged at 4500 rpm for 20 min and washed twice with a water/isopropanol solution (1/9 vv.). The precipitated anionic DAC (ADAC) was oven-dried at 60 °C.

3.5 Determination of the aldehyde content of DAC and assessment of carboxyl's

The aldehyde content of DAC was determined based on the oxime reaction between aldehyde groups and $\text{NH}_2\text{OH}\cdot\text{HCl}$ (**Figure 13**). The non-dried DAC (0.1 g on a dry basis) was placed in a 250 mL beaker containing 1.39 g of $\text{NH}_2\text{OH}\cdot\text{HCl}$ dissolved in 100 mL of 0.1M acetate buffer (pH=4.5).¹ The beaker was covered with a thin rubber foil and the mixture was stirred 48h at room temperature with a magnetic stirrer. The product was filtered and washed with 600 mL of deionized water after which it was oven-dried at 60 °C. Since 1 mol of aldehyde reacts with 1 mol of $\text{NH}_2\text{OH}\cdot\text{HCl}$ giving 1 mol of the oxime product, the aldehyde content in DAC can be calculated directly from the nitrogen content of the product.

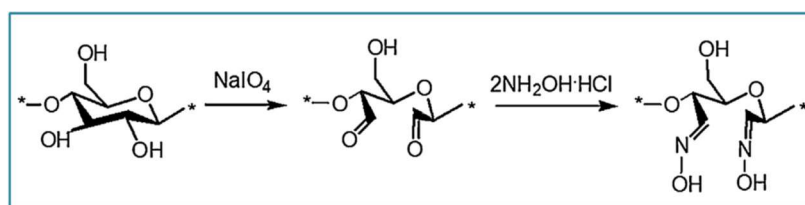


Figure 13 - Schematic of cellulose oxidation and oxime reaction.

¹ Acetate buffer (pH=4.5) solution used in the oxime reaction was made by charging a 2.0 L volumetric flask with 27.4 g of sodium acetate trihydrate and adding 15 mL of glacial acetic acid to the flask and diluting the resulting mixture to 2.0L with deionized water.

An oxidation reaction of hydroxyl's is also prone to give carboxyl's. The latter were determined by a conductometric titration following the Scandinavian standard method reported for pulp, paper and board. The intent was to detect if carboxylic acid groups were present on DACs. Non-dried DAC (0.1 g on a dry basis) was weighted in a 100 mL beaker, to which 45 mL of distilled water and 5 mL of NaCl 0.01M were added. The mixture was stirred for 1 h and subsequently, the pH was adjusted to ca. 3 with HCl 0.01M. After, it was titrated with NaOH 0.01M and the conductivity measured with a Crison conductimeter Basic 30. The step of each addition was of about 0.5 mL and the time between the additions was from 10 s to 30 s. The use of conductometric titration in the attempts of synthesis of cationic DAC is reported in **Appendix C**.

3.6 Characterization procedures

Moisture content

The moisture of extracted cellulose was determined by drying a sample of approximately 2 g overnight in the oven at 105 °C.

Fourier transform infrared (FTIR) spectroscopy

FTIR spectra of cellulose, DACs, CCs, and ADACs were obtained in the Attenuated Total Reflectance (ATR) mode, on a JASCO 4200 (Tokyo, Japan) spectrometer, equipped with a high-intensity ceramic light source, Ge/KBr beam splitter and DLATGS detector. 120 scans were averaged in the range of 550-4000 cm^{-1} .

The theory at the base of infrared spectroscopy states that the positions of atoms within molecules do not remain constant, but undergo continual periodic movement (vibration) relative to each other.⁹⁶ For any given vibrational motion, only certain energies are possible for the vibrational energy states; that is, the energy levels are quantized. Transitions between the energy levels of the vibrational motions can be induced by the absorption of electromagnetic radiations in the infrared region. For a given molecule, most of the independent vibrations motions called *normal modes* are highly localized in a given bond or functional group. In this way, the adsorption bands of individual functional groups are localized in limited portions of the infrared region, allowing for the development of spectra-structure correlations.

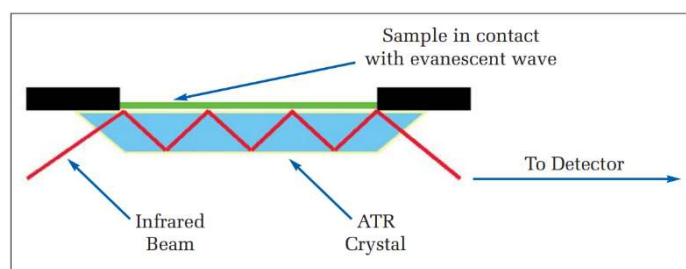


Figure 14 - A multiple reflection ATR system.⁹⁷

ATR technique permits a faster sample preparation and higher spectral reproducibility with respect to traditional measurements in transmission mode. An attenuated total reflection accessory operates by measuring the changes that occur in a totally internally reflected infrared beam when the beam comes into contact with a sample (**Figure 14**).⁹⁷ An infrared beam is directed onto an optically dense crystal with a high refractive index at a certain angle. Thanks to internal reflectance, an evanescent wave that extends beyond the surface of the crystal into the sample held in contact with the crystal can be created. This evanescent wave protrudes only a few microns ($0.5 \mu - 5 \mu$) beyond the crystal surface and into the sample. It is fundamental in this sense a good contact between the sample and the crystal surface. The evanescent wave will be attenuated or altered according to the regions of the infrared spectrum where the sample absorbs energy. The attenuated energy from each evanescent wave is passed back to the IR beam, which then exits the opposite end of the crystal and is passed to the detector in the IR spectrometer. The system then generates an infrared spectrum.

Elemental Analysis (EA)

Elemental Analysis of CCs, ADACs and of the oxime derivative of DACs was performed using an element analyzer EA 1108 CHNS-O from Fisons. A tiny capsule with a weighed amount of sample was introduced into a vertical quartz tube reactor heated at $900 \text{ }^\circ\text{C}$ with a constant flow of helium stream. Before the sample drops into the combustion tube, the helium stream was enriched with a measured amount of oxygen to achieve a strongly oxidizing environment which guarantees complete combustion/oxidation. The resulting four components of the combustion mixture were eluted into a chromatographic column and then detected by a thermal conductivity detector, in the sequence N_2 , CO_2 , H_2O and SO_2 . BBOT - 2,5-Bis (5-*tert*-butyl-benzoxazol-2-yl) thiophene, was used as standard.

Refractive index measurement

The refractive index (RI) is a dimensionless number defined as the ratio of the speed of light in the vacuum and the speed of light in the targeted medium. RI was determined using a refractometer from Atago (RX-5000D). For the determination of RI, the first step was the calibration with the solvent used (distilled water). After this, two drops of the sample were placed on the measuring cell for each tested concentration. The temperature of the measurements was 25 °C. Between each reading, the measuring cell should be cleaned with optical paper to avoid scratching.

Molecular weight, zeta potential and average hydrodynamic diameter

The Zetasizer Nano ZS from Malvern Instruments UK, was used to measure the zeta potential, average hydrodynamic diameter and molecular weight of the CC and the ADAC molecules in aqueous solution. The equipment allows these measurements based on three different techniques⁹⁸:

- Dynamic light scattering (DLS) to perform molecular size analysis, for the enhanced detection of particle aggregates and measurement of molecules of diluted samples;
- Static light scattering (SLS) to perform molecular weight analysis. Molecular weight measurement range is possible from a few g/mol to 500 for linear polymers to 20000 kg/mol for near spherical polymers and proteins;
- Electrophoretic light scattering (ELS) to perform the zeta potential analysis for particles, molecules and surfaces.

DLS

Dynamic Light Scattering (sometimes referred to as Photon Correlation Spectroscopy or Quasi-Elastic Light Scattering) is a technique for measuring the size of particles typically in the sub-micron region.⁹⁹ DLS measures Brownian motion and relates this to the size of the particles. Brownian motion is the random movement of particles due to the bombardment by the solvent molecules that surround them. Normally DLS is concerned with the measurement of particles suspended within a liquid. The larger the particle, the slower the Brownian motion will be. Smaller particles are “kicked” further by the solvent molecules and move more rapidly. The velocity of the Brownian motion is defined by a property known as the translational diffusion coefficient (usually given by the symbol, D). The translational diffusion coefficient is calculated by fitting the correlation curve with a proper function. The correlation curve contains all the information regarding the diffusion

of particles in the measured sample. The fitting of the correlation curve is done with an exponential function (cumulants analysis) or by a sum of exponential functions (CONTIN analysis, adequate to more complex samples). The hydrodynamic diameter distribution of a particle is calculated from the translational diffusion coefficient by using the Stokes-Einstein equation (**Equation 1**):

$$d(H) = \frac{k T}{3\pi\eta D} \quad (\text{Eq. 1})$$

where:

$d(H)$ = hydrodynamic diameter,

D = translational diffusion coefficient,

k = Boltzmann's constant,

T = absolute temperature,

η = viscosity.

The diameter that is measured by DLS is a value that refers to how a particle diffuses within a fluid so it is referred to as a hydrodynamic diameter. The diameter that is obtained by this technique is the diameter of a sphere that has the same translational diffusion coefficient as the particle.

D_z (or Z-Average) is the intensity weighted harmonic mean size of the hydrodynamic diameter distribution. The D_z increases as the particle size increases. Therefore, it provides a reliable measure of the average size of a particle size distribution measured by DLS. The software assumes that the dispersion of the particles obeys the Rayleigh theory (intensity of scattered light proportional to D_i^6) and the value of the average diameter of a distribution (corresponding to D_z) can be determined by **Equation 2**:

$$D_z = \frac{\sum(I_i)}{\sum\left(\frac{I_i}{D_i}\right)} \quad (\text{Eq. 2})$$

Where:

D_z = intensity weighted harmonic mean size of the hydrodynamic diameter distribution;

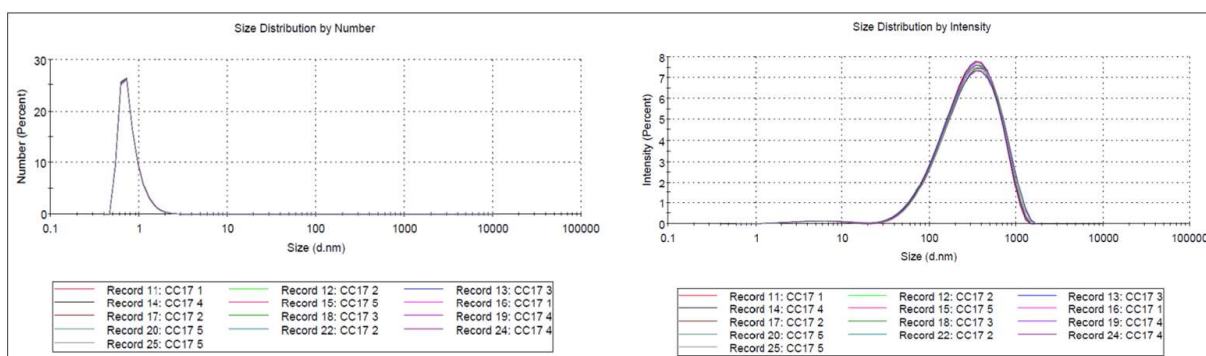
I_i = scattered light intensity of class i ;

D_i = is the hydrodynamic diameter of class i .

Therefore, the D_z is the measured variable that defines the averaged molecular particle size of a suspension. For the determination of this variable, it is necessary to prepare a solution with an optimum diluted concentration. The concentration chosen should guarantee enough particles scattered light for the analysis, guaranteeing a good signal/noise ratio, as well as, avoid the formation of aggregates and multiple scattering. This information is provided by the parameter *count-rate* reported in Zetasizer software which should be always greater than 50. With the increase in concentration, there is a greater probability that inter-particles effects like multiple scattering occur or that lesser free space between particles leads to the rise of friction forces between nearby particles. The latter is an error factor because in DLS measurements it is assumed that the particles are moving only due to Brownian motion. In this sense, the software allowed us to detect situations of multiple scattering through the *quality report*. Anyway, some measurements can be accepted even if the *quality report* is not good. In these cases, the *particle size distribution* (PSD) by number has to be carefully evaluated to observe if the number of aggregates is not relevant as for instance in **Figure 15**.

SLS

Static light scattering (SLS) is a technique to measure absolute molecular weight for a polymer using the relationship between the intensity of light scattered by a molecule and its molecular weight and size, as described by the Rayleigh theory. According to the Rayleigh theory, larger molecules scatter more light than smaller molecules for a given light source, and the intensity of the scattered light is proportional to the molecule's molecular weight.¹⁰⁰ Instead of measuring the time-dependent fluctuations in the scattering intensity like in DLS,



SLS uses the time-averaged intensity of scattered light. From this information, the 2nd Virial coefficient and Molecular Weight could be determined. The molecular weight is determined

Figure 15 – Example of the PSD by number required when there is not good *quality report*, on the left. The corresponding PSD by intensity, on the right.

by applying the Rayleigh equation (**Equation 3**) on the sample measured at different concentrations:

$$\frac{K C}{R_{\theta}} = \left(\frac{1}{MW} + 2A_2 C \right) P_{\theta} \quad (\text{Eq. 3})$$

Where:

- K = optical constant as defined in **Equation 4**;
- C = the concentration;
- R_{θ} = Rayleigh ratio – the ratio of scattered light to incident light on the sample;
- MW = sample molecular weight;
- A_2 = the 2nd Virial coefficient;
- P_{θ} = angular dependence of the sample scattering intensity.

$$K = \frac{2\pi^2}{\lambda_0^4 N_A} \left(\eta_0 \frac{dn}{dc} \right)^2 \quad (\text{Eq. 4})$$

Where:

- N_A = Avogadro's constant;
- λ_0 = laser wavelength;
- n_0 = solvent refractive index;
- $\frac{dn}{dc}$ = is the differential refractive index increment. It is the slope of the straight line obtained by plotting refractive indices versus sample concentration.

Commonly, for molecular weight measurements, the scattering intensity of the analyte used is measured first and compared to that of a well described (standard) pure liquid with a known Rayleigh ratio. The standard used in this work was toluene because it is suitable for precise measurements and is well known over a wide range of wavelengths and temperatures. The expression used to calculate the sample Rayleigh ratio from a toluene standard is (**Equation 5**):

$$R_{\theta} = \frac{I_A \eta_0^2}{I_T \eta_T^2} R_T \quad (\text{Eq. 5})$$

Where:

- I_A = residual scattering intensity of the analyte;
- I_T = is the toluene scattering intensity;

- = toluene refractive index;
- = Rayleigh ratio of toluene.

The angular dependence of the sample scattering intensity (ρ) is a shape correction parameter that depends on the different positions of the same particle (cylinder, coil or sphere). This happens when particles are large enough to cause multiple scattering. On the opposite, multiple scattering is avoided when particles in solution are much smaller than the wavelength of incident light. Under these conditions, ρ is reduced to 1 and **Equation 3** becomes a straight line in which the ordinate at the origin is $1/MW$.

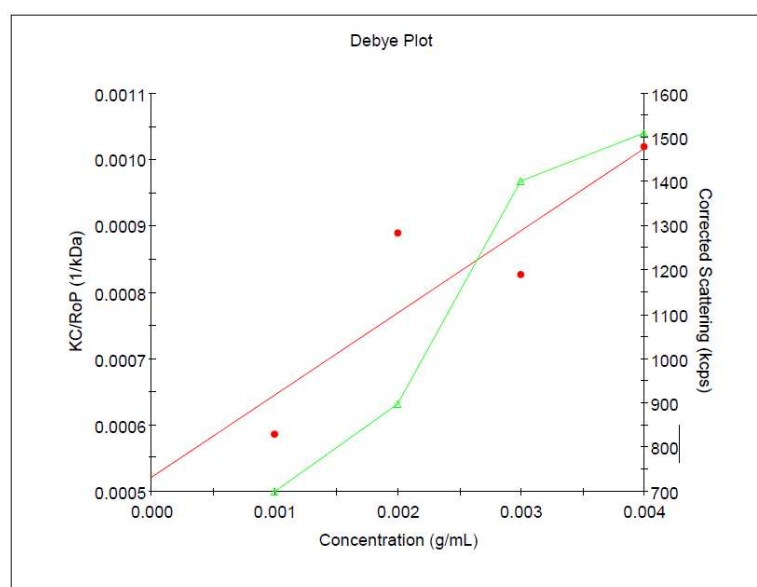


Figure 16– Example of Debye Plot.

At the end, the MW measured with this technique is represented in a Debye plot (**Figure 16**). The Debye graph is a dual axes plot of Kc/RoP and intensity versus concentration. The intercept of the line extrapolated to zero concentration gives the reciprocal molecular weight and the gradient of the line gives the second virial coefficient A_2 . This plot has two lines, Debye line (red) and Intensity line (green). Both must have a growing direction and the higher the correlation coefficient, the better the quality of the test. The intersection of Debye line with the ordinate axis gives the MW. On the other hand, if the intensity of the scattered light decreases between two consecutive points of the intensity line, it means that multiple scattering effects are present. To avoid that, a new solution must be prepared with intermediate concentration.

It can be seen that most of the parameters used in these calculations are constant, with the exception of the differential refractive index increment and dynamic viscosity, which must be introduced in the Zetasizer software. Information about the hydrodynamic diameter of

the molecules can be introduced as well and then can have different values according to the shape of particle expected.

ELS

Electrophoretic Light Scattering (ELS) is a technique used to measure the electrophoretic mobility of particles in dispersion, or molecules in solution. This mobility is often converted to Zeta potential to enable comparison of materials under different experimental conditions.¹⁰¹ The fundamental physical principle is that of electrophoresis. A dispersion is introduced into a cell containing two electrodes. Thus, it is the migration of molecules or particles, which have a net charge or a net zeta potential, in an electric field generated by two electrodes. The migration velocity towards the oppositely charged electrode, known as the mobility, is related to their zeta potential. The concept of zeta potential is related to the presence of ions in the liquid. The ions close to the surface of the particle will be strongly bound while ions that are further away will be loosely bound forming what is called a *Diffuse layer*.¹⁰¹ Within the diffuse layer, there is a boundary and any ions within this boundary will move with the particle when it moves in the liquid, but any ions outside the boundary will stay where they are and this boundary is called the *shearing plane*. A potential exists between the particle surface and the dispersing liquid which varies according to the distance from the particle surface. This potential at the shearing plane is called the zeta potential.

The conversion of the measured electrophoretic mobility data into zeta potential is done using Henry's equation (**Equation 6**):

$$U_E = \frac{2\varepsilon z f(ka)}{3\eta} \quad (\text{Eq. 6})$$

Where:

- z = zeta potential;
- U_E = electrophoretic mobility;
- ε = dielectric constant;
- η = sample viscosity;
- $f(ka)$ = Henry's function.

Electrophoretic determinations of zeta potential are most commonly made in aqueous media and moderate electrolyte concentrations. The Henry's function in this case is 1.5, and this

is referred to as the *Smoluchowski* approximation. Therefore, calculation of zeta potential from the mobility is straightforward for systems that fit the *Smoluchowski* model, i.e. particles larger than about 0.2 microns dispersed in electrolytes containing more than 10^{-3} molar salt. For small particles in low dielectric constant media $f(\kappa a)$ becomes 1.0 and allows an equally simple calculation. This is referred to as the *Hückel* approximation.

To measure zeta potential it was used a concentration of the samples around 0.1 wt% in ultrapure water. Samples were prepared at least half an hour before the measurement and kept on stirring on a magnetic stirrer. Dilutions or ultrasounds were applied on the sample in order to improve the measurement. In the Zetasizer software was settled the measurement in “*automatic*” and number of measurement at 5. The analysis model chose in *data processing* was “*general purpose*”. The cell selected was “*disposable folded capillary cell*” with the code DTS1070.

For hydrodynamic diameter measurement it was used a concentration of the samples around 0.01 wt% in ultrapure water. Samples were prepared one hour before the measurement and kept on stirring on a magnetic stirrer. Dilution or a certain time of ultrasounds were applied on the sample in order to improve the measurement if necessary. For the measurements were used a glass cell cuvette with square aperture, prewashed with ultrapure water and dried. The samples were filtered through a 0.45 μm nylon filter for syringes (Teknokroma). In the Zetasizer software it was settled the measurement in “*automatic*” and the number of measurements at 5. The cell selected was “*glass cuvettes*” with the code PCS1115. The measurement angle was “*173° backscattered*”, measurement duration “*automatic*”. The analysis model chosen in *data processing* was “CONTIN”.

For the measurements of molecular weight, a stock solution of the sample was prepared at 0.4 wt% and stirred overnight on a magnetic stirrer. Then, by the dilution of stock solution, 5 different concentrations were prepared. In order to obtain a good dispersion of the particles, the solutions with different concentrations were magnetically stirred for 1 hour and then submitted to ultrasounds during 5 minutes at 50 kHz. Refractive index was measured for the targeted concentrations determined, a regression of these values was made (refractive index versus surfactant concentrations) and the slope of straight line corresponds to the value of the dn/dc [mL/g]. Samples were filtered with 0.45 μm nylon filter for syringes (Teknokroma). In the Zetasizer software was selected toluene as standard. In *general options* was introduced the “*refractive index increment -dn/dc* [mL/g]” and the *shape correlation model* was selected “*Coil*($R_g=1.56 \cdot R_h$)”. The cell selected was “*glass cuvettes*”

with the code PCS1115. Both SLS run duration and run repetition were settled to “automatic”. The analysis model chose in *data processing* was “Protein analysis”. The size of the molecules was introduced afterwards to recalculate the data and obtain the final molecular weight.

Nuclear Magnetic Resonance (NMR) spectroscopy

Nuclear Magnetic Resonance spectroscopy is a powerful and theoretically complex analytical tool. It is applied for the identification of the carbon/hydrogen framework of organic structures.

The nuclei of many elemental isotopes have a characteristic spin (I). Some nuclei have integral spins (e.g. $I = 1, 2, 3 \dots$), some have fractional spins (e.g. $I = 1/2, 3/2, 5/2 \dots$), and a few have no spin, $I = 0$ (e.g. ^{12}C , ^{16}O , ^{32}S , ...). Isotopes of particular interest and use to organic chemists are ^1H , ^{13}C , ^{19}F and ^{31}P , all of which have $I = 1/2$. A spinning charge generates a magnetic field and the resulting spin-

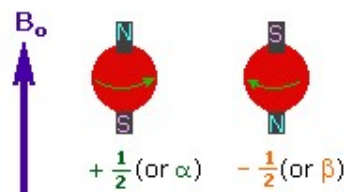


Figure 17 – Spin energy state.¹⁰²
The arrow representing B_0 points North.

magnet has a magnetic moment (μ) proportional to the spin.¹⁰² In the presence of an external magnetic field (B_0) two spin states are possible: $+1/2$ (α -spin state) and $-1/2$ (β -spin state) (**Figure 17**). The lower energy α -spin state is characterized by a magnetic moment aligned with the external field. Instead, the one of the higher energy β -spin state is opposed to the external field. The difference in energy (ΔE) between the two spin states is dependent on the external magnetic field strength and is always very small. Two spin states have the same energy when the external field is zero, but ΔE increases when B_0 grows, as shown in the

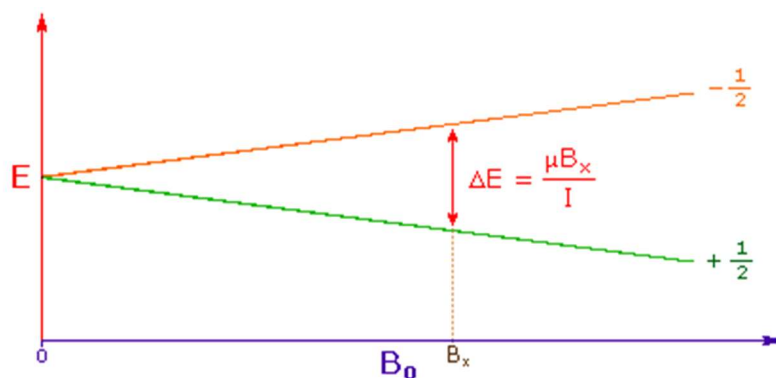


Figure 18 - As the applied magnetic field increases, so does the energy difference between α - and β -spin state.¹⁰²

diagram (**Figure 18**).¹⁰² At a field equal to B_x a formula for the energy difference is given ($I = 1/2$ and μ is the magnetic moment of the nucleus in the field).

When the sample is subjected to a pulse of radiation whose energy corresponds to the difference in energy between the α - and β -spin states, nuclei in the state α -spin are promoted to the β -spin state. This transition is called “flipping” the spin. The radiation required for

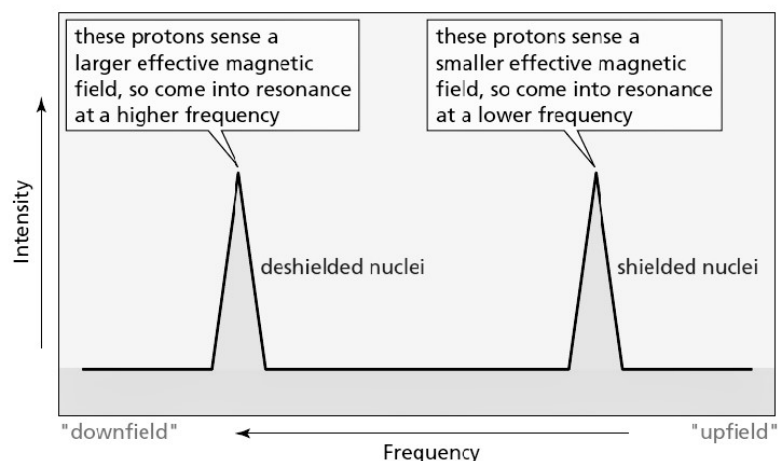


Figure 19 – NMR spectrum: shielded nuclei come into resonance at lower frequencies than deshielded nuclei. Upfield means farther to the right-hand side of the spectrum, and downfield means farther to the left-hand side of the spectrum.¹⁰³

the flipping is in the radiofrequency (rf) region of the electromagnetic spectrum and is called *rf radiation*. When the nuclei return to their original state, called relaxation, they emit electromagnetic signals whose frequency depends on the difference in energy between the α - and β -spin states. These signals are detected by the spectrometer which displays them as a plot of signal intensity versus signal frequency (magnetic field), generating an NMR spectrum (**Figure 19**).¹⁰³ The term “nuclear magnetic resonance” comes to the fact that the nuclei are in resonance with the *rf radiation*. In this context, “resonance” refers to the flipping back and forth of nuclei between the α - and β -spin states in response to the *rf radiation*.¹⁰³

The phenomenon of shielding derives from the local magnetic field, generated by the electrons circulating around the nuclei, which opposes to the applied magnetic field. The effective magnetic field, therefore, is what the nuclei “sense” through the surrounding electronic environment:

$$B_{\text{effective}} = B_{\text{applied}} - B_{\text{local}}$$

This means that B_{local} is greater as greater is the electron density of the environment in which the nucleus is located. Consequently, the nucleus is more shielded from the applied magnetic

field. Thus, nuclei in electron-dense environments sense a *smaller effective magnetic field*. Even more, they will require a *lower frequency* to come into resonance because ΔE is smaller (**Figure 18**). On the other hand, nuclei in electron-poor environments sense a *larger effective magnetic field* and they will require a *higher frequency* to come into resonance (**Figure 19**).

In proton NMR (^1H NMR) spectroscopy, the spectrometer must be tuned to a specific nucleus, in this case the proton. For each proton in a different environment it is possible to see a signal in ^1H NMR. Protons in the same magnetic environment are called *chemically equivalent protons*.¹⁰³ The number of signals that appear on a ^1H -NMR spectrum, stands thus for set of chemically equivalent protons of that compound. The position at which a signal occurs in an NMR spectrum is called the *chemical shift*.¹⁰³ The *chemical shift* is a measure of how far the signal is from the reference tetramethylsilane (TMS) signal. The most common scale for chemical shifts is the δ (delta) scale. The TMS signal is used to define the zero position on this scale. The area under each signal is proportional to the number of protons that gives rise to the signal. Therefore, the relative intensities of the signals are proportional to the relative number of equivalent protons. In fact, the integration only provides *ratios* of protons, not the *absolute* number. For convenience in calculating the relative signal strengths, the smallest integration is set to 1 and the other values are converted accordingly. Furthermore, NMR signals are not usually single triangles, but a complex pattern of split triangles labeled as doublets (2 peaks), triplets (3 peaks), quartets (4 peaks) and so on. The distance between the split peaks is called *coupling constant*, denoted by J .¹⁰² The interaction between nearby protons produce different spin flip energies as they can orient themselves in a pattern of parallel or anti-parallel to the applied magnetic force. This phenomenon, where the spin of the nucleus of one proton is close enough to affect the spin of another, is called *spin-spin coupling*.¹⁰³ Splitting is always reciprocated between the protons and provides information on the neighbors of a proton within the molecule.

Briefly, the kind of information that can be obtained from an ^1H NMR spectrum is:¹⁰³

1. The number of signals indicates the number of different types of protons that are in the compound.
2. The position of a signal indicates the types of proton(s) responsible for the signal (methyl, methylene, methine, allylic, vinylic, aromatic, etc.) and the types of

neighboring substituents. The integration of the signal tells the relative number of protons responsible for the signal.

3. The multiplicity of the signal ($N + 1$) tells the number of protons (N) bonded to adjacent carbons.
4. The coupling constants identify coupled protons.

The samples for ^1H NMR were prepared by solubilizing the anionic cellulose-based flocculants in D_2O at a concentration of 10 mg/ml. The cationic cellulose-based flocculants were prepared at a concentration of 2.5 mg/ml. The solubilization was performed in a beaker by stirring the sample with a magnetic stirrer for a certain time, being then the solution transferred to the NMR tube. The deuterium oxide and the NMR tubes were purchased from Sigma-Aldrich. The spectra were collected at room temperature in a Bruker Avance III 400 MHz NMR spectrometer using a Bruker standard pulse program. Sodium 3-(trimethylsilyl)propionate- d_4 (TMSP, δ 0.00) was used as internal standard.

3.7 Characterization of dyes

The dyes used to prepare the colored effluents were characterized in order to have basic information to conduct the performance tests. The characterization included: full wavelength UV-VIS spectra, conductivity measurements, zeta potential, average hydrodynamic diameter. From the full wavelength UV-VIS spectra, the wavelength corresponding to absorption maximum of each dye was obtained. UV-VIS spectra of dyes were measured on a Jasco spectrophotometer, model V550, in the 800-200 nm wavelength range, with a scanning speed of 200nm/min.

3.8 Performance tests: color removal

Performance tests were performed using the CCs, undissolved CCs and ADACs. Typically, it was prepared a solution of the flocculant chosen at a concentration of 0.8 mg/mL in distilled water which was stirred with magnetic stirrer before the test. For each test, it was prepared a stock solution of dye at 15 mg/L as model wastewater. To change the pH, HCl 1M or NaOH 1M were used. Only the solid dyes were tested in the present work.

In the case of CCs, the performance tests with cellulose-based flocculants were compared with those using a CPAM solution at the same concentration (0.8 mg/mL) and dosage, prepared one hour before the test. It was also used sodium bentonite as the complexing agent. Tests consisted of the following passages:

- 1) Preparation of a volume of 150 mL of model wastewater in a beaker.

- 2) Addition of sodium bentonite and sustained stirring on a magnetic stirrer to disperse the bentonite.
- 3) Addition of the flocculant using a 1 mL syringe, adding dropwise and mixing slowly for 10-20 s.
- 4) Change of the pH with HCl 1M, mixing slowly for 10-20 s.
- 5) Collection of a sample from the supernatant water of the model wastewater at different times (5 min, 1 h, 24 h).
- 6) Take pictures of the beakers after 24 h.
- 7) Measurement of the final pH of the treated model wastewater.

For the tests with ADACs, aluminium sulfate-18-hydrate was used as the complexing agent.

Tests consisted of the following passages:

- 1) Preparation of a volume of 150 mL of model wastewater in a beaker.
- 2) Change of the pH with NaOH 1M, mixing slowly for a few seconds.
- 3) Addition of aluminium sulfate, mixing slowly for a few seconds and waiting 2-3 minutes.
- 4) Addition of the ADAC using a 1 mL syringe, adding dropwise and mixing slowly for 10-20 s.
- 5) Collection of a sample from the supernatant water of the model wastewater at different times (5 min, 1 h, 24 h).
- 6) Take pictures of the beakers after 24 h.
- 7) Measurement of the final pH of the treated model wastewater.

The tests with the undissolved CCs were conducted without using a complexing agent and without preparing a solution of polymer. The polymer was added directly to the test sample in dry form. A magnetic stirring at 200 rpm was applied to well disperse the fibers. In some cases, after the agitation, the model wastewater was filtered. Tests consisted of the following passages:

- 1) Preparation of a volume of 150 mL of model wastewater in a beaker.
- 2) Addition of the undissolved CC.
- 3) Change of the pH with HCl 1M.
- 4) Stirring with a magnetic stirrer at 200 rpm for a certain time.
- 5) Collection of a sample from the supernatant water of the model wastewater right after stirring.
- 6) Pictures of the beaker after 24 h.

7) Measurement of the final pH of the treated model wastewater.

The color removal over time for all tests conducted was calculated based on absorbance measurements at a fixed wavelength (typically at the absorption maximum of each dye). Measurements of the supernatant waters were made on the Jasco spectrophotometer, model V550. Samples were analyzed in triplicate and the results averaged on them. The color removed was then calculated from the reduction of the absorbance of the supernatant water as:

Where:

- = absorbance of the initial model wastewater;
- = absorbance of the sample after treatment.

4 Results and discussion

4.1 Synthesis of cationic cellulose-based flocculants

4.1.1 Preliminary experimental work

This section deals with the experimental work done before the definition of the synthesis procedure reported in section 3.3.1.

Dissolution of cellulose in NaOH-based aqueous system

The first step of the synthesis route described by Zhang et al.⁹¹ concerns with the dissolution of cellulose in a NaOH-based aqueous solution. This step is itself divided into two sub-steps. The first one is the addition of a 14 wt% NaOH aqueous solution to cellulose. The second one is the addition of a 24 wt% urea aqueous solution, both pre-cooled at 0 °C. As claimed in the studies conducted by Qi et al.,¹⁰⁴ this dissolution process can lead to a complete transparent cellulose solution in a certain range of conditions. It is reported in the literature that urea can improve cellulose dissolution in water thanks to its “hydrophobic part”.¹⁰⁵ Anyway, the degree of polymerization (DP) of cellulose poses an important thermodynamic limit to the dissolution process in water. As molecular weight increases, the entropic driving force contribution to dissolution is weaker.¹⁰⁵ The fundamental point in Qi et al.’s work is that the starting material was cotton linters with a DP of 570. Therefore, they got those results starting from a material with specific characteristics quite favorable for the dissolution. However, in the same article, they stated that is possible to dissolve cellulose in aqueous NaOH/Urea solution, even with a relatively high DP (500-900).

In order to achieve cellulose dissolution, several trials were conducted by changing two variables: time of dissolution (both sub-steps) and concentration of NaOH aqueous solution (**Table 5**). Starting from the trial C4, it was also added a pretreatment of swelling with a solution of EtOH/H₂O (1:1 v/v). The mixture was kept on stirring on a stirring plate for 20 min, at ambient temperature. After that, it was filtrated with distilled water to remove the ethanol. To maintain the temperature of the cellulose-NaOH-urea mixture around 0 °C the beaker was kept in an ice bath protected by a polystyrene container. In all trials, the mass ratio of NaOH solution and urea solution was always 1. The concentration of urea solution was fixed at 24 wt%. In the trials reported in **Table 5**, it was never reached complete cellulose dissolution. The separation process by centrifugation performed after cellulose dissolution showed that it was partially dissolvable. Even the introduction of a pretreatment did not improve significantly the cellulose

solubility. Even more, this pretreatment introduced an incalculable amount of water which eventually diluted the concentration of NaOH and urea solution in the subsequent steps. This could influence positively the dissolution sub-step with NaOH since too high NaOH concentration (C_{NaOH}) has an opposite effect as reported by Porro et al.¹⁰⁶ This is the reason why the C_{NaOH} was additionally decreased from 14 to 13 wt% (trials C6 and C7). Even so, there was no significant change in the dissolution process. For these reasons, the complete cellulose dissolution was no longer pursued and it was accepted the result of a partial dissolution.

Table 5 – Trials for cellulose dissolution in NaOH-based aqueous solution.*

Name	type cell	Dry cell weight [g]	Vol. sol. EtOH/H ₂ O [mL]	NaOH conc. [wt%]	vol. NaOH [mL]	initial T [°C]	Stirring time	vol. Urea [mL]	initial T [°C]	Stirring time
C1	KG-1	1	∅	14	20.1	0	10 min	21.4	0	20 min
C2	KG-1	0.5	∅	14	20.1	1	20 min	21.4	0	20 min
C3	KG-1	1	∅	14	20.1	1	1 h	21,4	2	2 h
C4	KG-2	0.5	40	14	10	0.6	3.18 h	10.7	0.5	4 h
C5	KG-2	0.5	40	14	10	0.5	2 h	10.7	0	4 h
C6	KG-2	0.5	60	13	10	1	1 h	107	0	2 h
C7	KG-2	0.5	40	13	10	0	2 h	10.7	0	4 h

*The type of cellulose differs only in the moisture content: KG-2=2.62 wt %, KG-1=4.93 wt %. The volume of solution of EtOH/H₂O is the total added for the cellulose swelling. Initial temperature refers to the one of the solution when it was added.

Cationization of cellulose with CHPTAC

The cellulose in the cellulose-NaOH-urea mixture was cationized after separating the dissolved and undissolved cellulose parts by centrifugation. Only the dissolved part was kept for the cationization. However, this step of separation posed another issue. Since the amount of CHPTAC to add for the reaction is based on the molar ratio CHPTAC/AGU, it is supposed to know exactly the amount of dissolved cellulose. Basically, this implies to solve the system of 5 equations in 6 unknowns composed by the partial mass balance of urea, cellulose, water, total mass balance and the sum of initial masses. The resolution is mathematically impossible, but, in practice, can be solved by measuring the water present in the undissolved cellulose part. It is necessary to filtrate the undissolved cellulose to remove the excess of water and then dry it.

From the volume of water filtrated and the weight difference before and after drying it can be deduced the mass of water in the undissolved cellulose. The main problem of this procedure is that the amount of time required for this determination is longer than 48 hours. Such a long time between the dissolution treatment and the beginning of the reaction is not reasonable. Therefore, the additional variation to the route of synthesis proposed by Zhang et al.⁹⁴ was that the centrifugal separation was postponed till after the cationization with CHPTAC. In this way, the amount of CHPTAC added is calculated based on all the cellulose present in the cellulose-NaOH-urea solution.

With the variation introduced, it was performed another series of trials reported in **Table 6** and **Table 7**. Basically, the reaction conditions in **Table 7** are derived from Zhang et al.⁹¹ From C11 the pretreatment was eliminated for the reason explained beforehand. The C_{NaOH} was fixed at 13 wt % and the stirring time was 1 and 2 h respectively for the sub-steps of alkalization and urea treatment. The time of 1 h was chosen considering the capability of NaOH to break the crystalline structure of cellulose with the passing time. In the recent study of Moral et al.¹⁰⁷ it was showed the influence of the C_{NaOH} and reaction time on the alkalization. In this sense, 1 h is more than sufficient to get a satisfying alkalization. Unfortunately, the C_{NaOH} cannot be increased too much in the present work because it plays an important role in the successive reaction step. The sodium hydroxide is necessary for the cationization reaction with CHPTAC because the latter has to be taken to the more reactive form: epoxypropyltrimethylammonium chloride (EPTAC). In fact, the process of cationization with CHPTAC is carried out in two steps: first, the formation of EPTAC by reaction with hydroxide ions, and second, the nucleophilic substitution of the hydroxyl groups in the AGU (**Figure 20**). However, the reaction efficiency is less than perfect due to a competing hydrolysis reaction¹⁰⁸: the EPTAC is hydrolyzed to a diol which is unable to react with cellulose, and this increases the cost of the cationic modification.¹⁰⁷ Prado and Matilewicz¹⁰⁹ states also that the increase in NaOH to some extent, also increases the degree of substitution (DS); as one equivalent of NaOH is necessary to generate the epoxide EPTAC from the chlorohydrin CHPTAC (that amount is called stoichiometric alkali and is consumed in the reaction). However, an excess of NaOH favors polysaccharide degradation and epoxide degradation towards the diol.¹⁰⁹ Thus, the stoichiometric alkali was the amount used in the present study. The stability of EPTAC is strongly influenced by pH and temperature. The equation resulting from a kinetic model of this system may be used to estimate half-life values within the specified pH and temperature limits (**Equation 7**):¹¹⁰

$$\log(\text{half - life, days}) = -0.943(\text{pH}, 10.5 - 12.5) - 0.04(\text{Tem}, 20 - 50 \text{ }^\circ\text{C}) + 12.808 \quad (\text{Eq. 7})$$

In the model, the influence of the pH is much higher than that of temperature. Just applying the model, for a pH of 12.5 and 11.6 (usual pH measured after cationization) at a temperature of 50 °C we get a half-life range between about 2.5 and 17.7 hours. But this range is overestimated because, in the present work, the temperature during cationization was 60 °C and the initial pH usually around 12.8. Thus, in order to not affect too much EPTAC half-life and not even compromise its formation from CHPTAC, the C_{NaOH} was fixed at 13 wt%. Supposing a complete consumption of NaOH for alkalization, the remaining part is in a molar ratio with CHPTAC almost equal to unity (mol NaOH/mol CHPTAC=0.99). This molar ratio is sufficient to form the epoxide (stoichiometric alkali) even if, according to Hashem et al.¹⁰⁸, the optimum molar ratio of NaOH:CHPTAC is 1.8 or greater.

Table 6 – Trials for cellulose dissolution in NaOH-cased aqueous solution*

Name	type cell	Dry cell weight [g]	Vol. sol. EtOH/H ₂ O [mL]	NaOH conc. [wt%]	vol. NaOH [mL]	initial T [°C]	Stirring time	vol. Urea [mL]	initial T [°C]	Stirring time
C8	KG-2	0.5	40	13	10	0	2 h	10.7	0	4 h
C9	KG-2	1	60	13	20.1	0	1 h	21.4	0	2 h
C10	KG-2	1	60	13	20.1	0	1 h	21.4	0	2 h
C11	KG-2	1.35	∅	13	27.2	1	1 h	28.9	0	2 h
C12	KG-1	1	∅	13	20.1	1	1 h	21.4	0	2 h

*More information are reported in Table 5.

Table 7 – Trials of cationized cellulose starting from Cellulose-NaOH-Urea solution of Table 6.*

Name	Mol. Ratio	Time [h]	T [°C]	Solubility	Analysis
CC8	9	8	60	soluble	FTIR,EA
CC8u	9	8	60	not sol.	FTIR,EA
CC9	9	8.2	60	soluble	∅
CC9u	9	8.2	60	not sol.	∅
CC10	9	9	60	soluble	FTIR,EA
CC10u	9	9	60	not sol.	FTIR,EA
CC11	9	8.25	60	soluble	FTIR
CC11u	9	8.25	60	not sol.	FTIR
CC12	9	8	60	soluble	FTIR
CC12u	9	8	60	not sol.	FTIR

*Molar ratio refers to mol CHPTAC/mol AGU. EA=elemental analysis, CC=dissolved CC, CCu=undissolved CC.

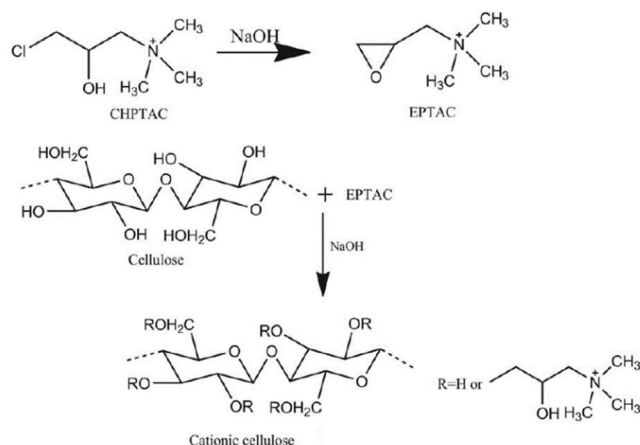


Figure 20 – Reaction scheme of the two-step cellulose cationization with CHPTAC.⁹¹

As shown in **table 7**, the dissolved and undissolved CC samples were characterized by FTIR spectroscopy and some by EA. What is emerged from FTIR spectra of both CCs are two unexpected peaks, together with those attributable to cellulose modification. As can be noticed on **Figure 21**, there are two quite intense peaks numbered as 7 and 8 respectively at the wavenumbers of 1659 and 1619 cm⁻¹. The other peaks are referred to cellulose backbone or due to its modification like peak 9 at 1474 cm⁻¹ and peak 10 at 1415 cm⁻¹, respectively of methyl groups of ammonium and C-N stretching vibration.⁹¹ The peaks 7 and 8 were not reported in Zhang et al. work, so they are an indication of product contamination. They were attributed to urea which can remain in the final CC. Since urea is very water soluble, it was tried to wash CC10, CC11 and CC12 in distilled water by vigorous stirring. The washed CC10, CC11 and CC12 named as CC10w, CC11w and CC12w were analyzed again by FTIR and the spectra have shown a significant decrease of the urea peaks intensity but

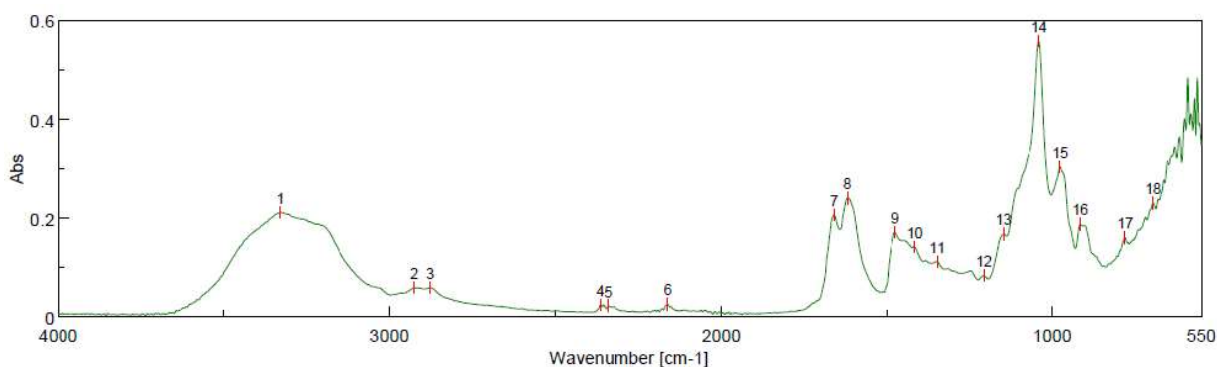


Figure 21 – FTIR spectrum of CC10.

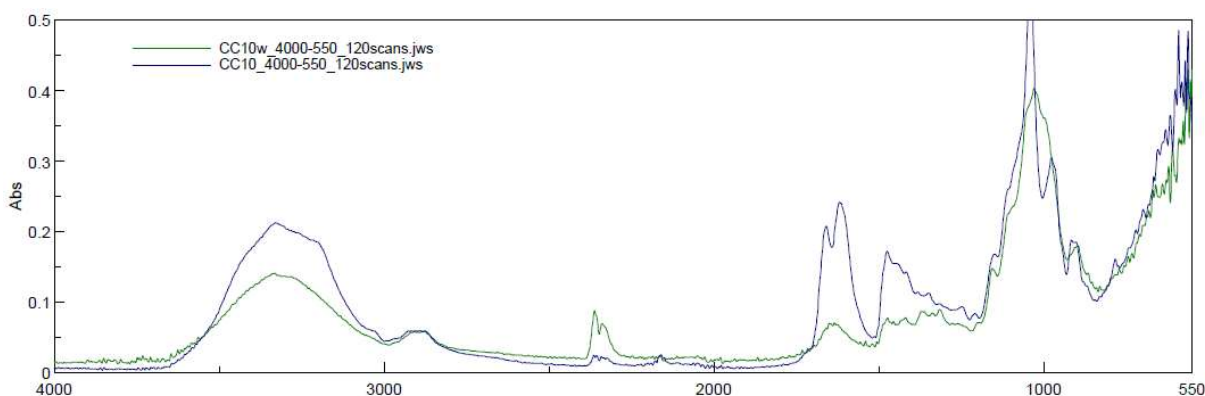


Figure 22 – Overlay FTIR spectra of CC10 and CC10w.

also those of cellulose modification **Figure 22**. Therefore, it was decided to remove the sub-step with urea for the cellulose dissolution. The rest of the synthesis route is the one reported in section 3.3.1.

4.1.2 Definitive Experimental work

According to the route of synthesis reported in section 3.3.1, several experiments were set up just changing the time of reaction. The products were characterized following the methods reported in section 3.6. For the obtained undissolved CC, only FTIR spectra and EA were performed. All the reaction data of these trials are reported in **Table 8** and the results from the characterization of CC are in **Table 9**. The degree of substitution was calculated from the nitrogen content, based on EA, according to the following equation (**Equation 8**):

$$DS = \frac{162 N\%}{14 - 1.5 N\%} \quad (\text{Eq. 8})$$

where 162 is the molecular weight of AGU, 14 is the atomic weight of nitrogen, 151.5 is the molecular weight of the cationic substituent group and N% is the averaged percentage of nitrogen by weight in the sample. The yield was calculated considering the undissolved CC as the side product (**Equation 9**):

$$Yield = \frac{m_{CC_i}}{m_{C_i} + m_{CC_{iu}}} \times 100 \quad (\text{Eq. 9})$$

Where:

- = mass of dissolved CC number i;
- = mass of undissolved CC number i.

The range reported for the zeta potential was calculated as the half difference between the higher and the lower value of measured zeta potential.

Table 8 – Reaction data for synthesis of cationic cellulose-based flocculant.*

Name	mass cell. [g]	Mol. Ratio	Time [h]	T [°C]	Solubility	Analysis
CC13	0,5	9	3	60	soluble	FTIR,EA,zeta,size
CC13u	0,5	9	3	60	not sol.	FTIR,EA
CC14	1	9	2	60	soluble	FTIR,EA,zeta,size,MW
CC14u	1	9	2	60	not sol.	FTIR,EA
CC15	1	9	4	60	soluble	FTIR,EA,zeta,size
CC15u	1	9	4	60	not sol.	FTIR,EA
CC16	3	9	3.15	60	soluble	FTIR,EA,zeta,size
CC16u	3	9	3.15	60	not sol.	FTIR,EA
CC17	2	9	4	60	soluble	FTIR,EA,zeta,size
CC17u	2	9	4	60	not sol.	FTIR,EA
CC19	3	9	3	60	soluble	FTIR,EA,zeta,size,NMR,MW
CC19u	3	9	3	60	not sol.	FTIR;EA
CC20	3	9	2	60	soluble	FTIR,EA,zeta,size,
CC20u	3	9	2	60	not sol.	FTIR;EA
CC21	3	9	4	60	soluble	FTIR,zeta,EA,size
CC21u	3	9	4	60	not sol.	FTIR;EA
CC22	3	9	5	60	soluble	FTIR,EA,zeta,size,NMR
CC22u	3	9	5	60	not sol.	FTIR;EA
CC23	3	9	6	60	soluble	FTIR,EA,zeta,size
CC23u	3	9	6	60	not sol.	FTIR;EA
CC24	3	9	7	60	soluble	FTIR,EA,zeta,size
CC24u	3	9	7	60	not sol.	FTIR;EA

*Zeta=zeta potential, Size=averaged hydrodynamic diameter, NMR=proton NMR, time= reaction time, Mol. ratio= molar ratio CHPTAC/AGU, mass cell.=initial mass of dried cellulose, MW=molecular weight.

It can be noticed in **Table 9** that from CC19 to CC22 both zeta potential and DS increase with the increasing reaction time. The trend, however, changes for reaction time larger than 5 hours. This trend is clearer in the diagram reported in **Figure 23**. It seems that after 5 hours the CC faces some degradation which has not allowed zeta potential and DS to increase. In general, the DS is quite high since it is over 0.2.¹⁰⁹ Another remarkable aspect is the reaction yield which was not high enough. The mean yield is $2.96 \pm 1.06\%$. It was not possible to confirm reproducibility since when the reaction was repeated with the same reaction time did not lead to the same DS and consequently zeta potential. For example, the products obtained with a reaction time of 4 h (CC15, CC17 and CC21) showed different values of DS. The only difference between them was the amount of reagents involved. The CC15, CC17, and CC21 started respectively from 1 g, 2 g, and 3 g of dried cellulose and

consequently all the other reagents were scaled according to the ratios. What is more, the zeta potential was similar between CC15 and CC21 even if their DS was quite different.

Table 9 – Characterization results of CC and undissolved CC.*

Name	Size [nm]	PDI	MW [kDa]	Zeta pot. [mV]±σ	DS	Yield [wt%]
CC13	184.9	0.202	∅	26.2	0.63	∅
CC13u					0.26	
CC14	246.25	0.505	3190±515	44.6±2.9	0.63	∅
CC14u					0.62	
CC15	156.6	0.46	∅	51±1.5	0.94	2.71
CC15u					0.80	
CC16	172.9	0.483	∅	44.1±2,05	0.62	3.4
CC16u					1.27	
CC17	213.8	0.448	∅	45,5±2.75	0.70	3.59
CC17u					0.47	
CC19	128.3	0.373	1920±380	47.3±1.8	1.05	3.82
CC19u					0.60	
CC20	211.8	0.51	∅	47.6±1.25	0.92	3.64
CC20u					0.93	
CC21	235	0.382	∅	51.4±1.8	1.24	2.73
CC21u					0.85	
CC22	134.7	0.212	∅	59.2±1.5	1.30	1.7
CC22u					0.74	
CC23	144.5	0.411	∅	50.9±2.55	0.87	2.03
CC23u					1.10	
CC24	134.6	0.47	∅	54.1±1.9	0.94	3.02
CC24u					0.81	

*PDI=polydispersity index of the hydrodynamic diameter, DS=degree of substitution.

The difference on the DS was also observed between CC16 and CC19 even if the reaction time and mass of starting material were almost the same. An explanation could be that the

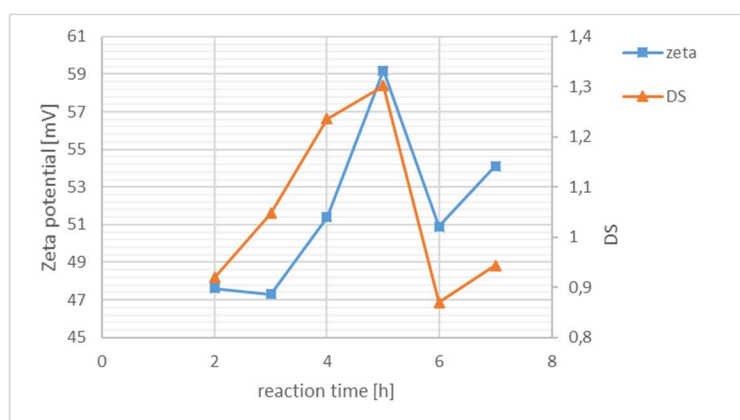


Figure 23 – Diagram of DS and zeta potential of CC samples in function of time from CC19 to CC24.

reaction system is heterogeneous, so the efficiency is lower than that in homogeneous conditions. In heterogeneous reactions, the charged groups accumulate on the surface of the polysaccharide particles, and diffusion of other reagent molecules to the inner parts is increasingly hindered. Instead, in homogeneous processes the polysaccharide dissolves, and reactions are less hindered.¹⁰⁹ Moreover, the mixing during the reaction was far from perfect. The heterogeneity of the system, which embodied a certain stiffness, combined with a scarce mixing could explain the lack of reproducibility. This effect can be more predominant when the amount of cellulose is high. Anyway, all the CC are soluble in water which is confirmed by the transparency of the supernatant after centrifugation, as reported in **Figure 24**. The FTIR spectra of the CCs show some new peaks respect to the spectra of cellulose. As it is noticed in **Figure 25** the spectra of CC17 showed an additional

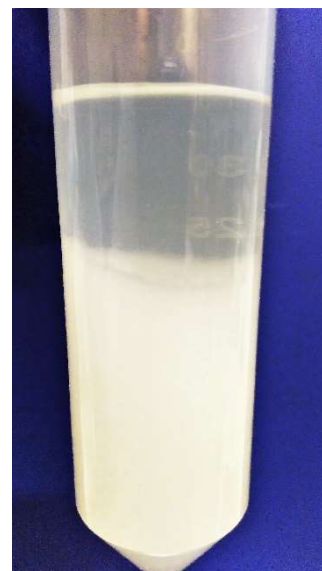


Figure 24– Centrifuge tube after centrifugation of reaction solution with CHPTAC. Note the difference between supernatant CC24 and precipitated CC24u.

peak at 1478 cm^{-1} and another at 1413 cm^{-1} . As previously stated in section 4.1.1, these new peaks indicate that CHPTAC was successfully introduced onto the cellulose backbone. Furthermore, the ^1H NMR spectra confirmed the cellulose modification (**Figure 26**). The spectrum of CC22 showed a strong peak at 3.15 ppm, which is related to the methyl protons of the alkylammonium group. Other minor peaks were observed between 3.2 and 4.5 ppm which can be assigned to the protons of the cellulose backbone and other protons of the substituent moiety. All the other FTIR and ^1H NMR spectra listed in **Table 9** are reported in Appendix A. It is not possible to draw any conclusion regarding the influence of DS on MW of CC because it was not possible to do all the measurements for lack of time. Consequently, it is also not possible to draw any conclusion about size since it is related to zeta potential and MW. Debye plots of CC14 and CC19 are showed respectively in **Figure 1B** and **Figure 2B**

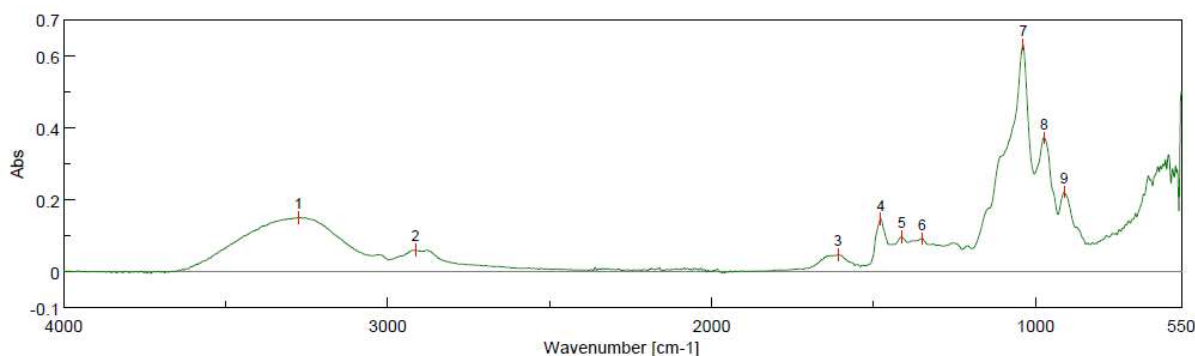


Figure 25 – FTIR spectrum of CC17.

(**Appendix B**). About the DS of undissolved CC, it can be noticed that almost all values are different from the corresponding CC. The DS of undissolved CC is sometimes higher or lower than the DS of dissolved CC. The reason may be the heterogeneity of reaction system that leads to a substitution not well distributed on the undissolved CC.

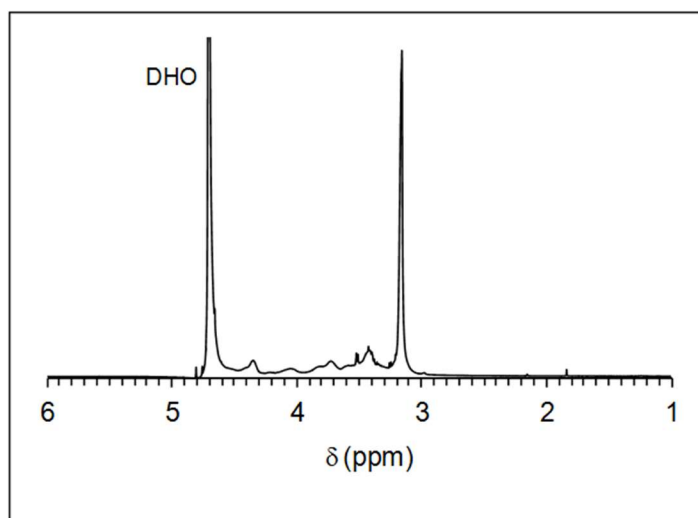


Figure 26 - ^1H NMR spectrum of CC22.

4.1.3 Attempt to synthesis of cationic DAC

The route of synthesis started from the synthesis of DAC. It was used the same DACs synthesized for the ADAC and reported in **Table 21**. The attempts of cationization with CHPTAC as well as the conductometric titration are explained in **Appendix C**.

4.1.4 Color removal tests of CC

Performance tests for the CC were performed on some selected dyes: Acid Black, Flora red 4bs, Orange 2, Basic green 1, Methylene blue and Brilliant yellow. The test on Acid Black will be showed entirely, while for the other only the best results will be presented. The dyes have been characterized according to the analyses reported in section 3.7. The results are presented in **Table 10**.

Table 10 – Data from dyes characterization.*

Dye	Zeta potential [mV]	λ_{max} [nm]	Conductivity [$\mu\text{S}/\text{cm}$]
Acid Black 2 solid	-20.4	574	9.3
Basic Green 1 solid	+6,12	624	14.2
Crystal Violet liquid	+45.7	589	Ø
Duasyn Direct Red liquid	-34.9	511	30.4
Flora Red 4bs solid	-54.6	500	31.4
Malachite Green liquid	+50.2	252	Ø
Methylene Blue solid	+2.5	663	11.4
Orange 2 solid	-25.6	485	19.3
Brilliant Yellow solid	-26.9	410	49.0

* λ_{max} = wavelength of absorption maximum in the VIS-UV spectrum

Acid Black

The CC tested was CC19 and all the experimental conditions are summarized in **Table 11**. The picture of the effluents after 24 h of treatments are shown in **Figure 27**.

Table 11 – Color removal test of Acid Black with CC19. Experimental conditions and performance after 5 min, 1 h, 24 h.*

Sample	Bentonite [wt%]	ppm CPAA	ppm CC19	pH	5 min	1 h	24 h
0	∅	∅	∅	5.6	∅	∅	∅
1	0.133	∅	∅	8.42	turbidity	turbidity	turbidity
2	0.133	21.20	∅	8.36	turbidity	turbidity	turbidity
3	0.133	∅	21.20	8.43	turbidity	turbidity	13.4
4	0.133	21.20	∅	2.68	turbidity	turbidity	92.6
5	0.133	∅	21.20	2.57	43.8	85.4	98.2
6	0.067	15.90	∅	2.73	turbidity	turbidity	28.1
7	0.067	∅	15.90	2.83	56.8	71.9	92.5
8	0.133	15.90	∅	2.80	turbidity	turbidity	82.0
9	0.133	∅	15.90	2.79	88.6	90.7	96.3
10	∅	15.90	∅	2.85	37.7	∅	∅
11	∅	∅	15.90	2.83	9.8	∅	∅

*turbidity=absorbance higher than the blank 0; 5 min,1 h, 24 h=performance after 5 minutes, 1 h, 24 h.

The results have demonstrated that CC19 can remove significantly the color. Compared to CPAA the performance is even better in two situations (7 and 9). For sample 9 the color removed in 5 minutes is remarkable, more than 88%. The change of pH is necessary because samples 3 and 5 with exactly the same dosages show completely different results: removal is much better at pH acid. Also, according to the test 9 a very high removal can be achieved with a very low concentration of CC. The addition of bentonite is important to achieve a good color removal. In fact, the complexation of CC with bentonite is essential for the removal process. The samples of 10 and 11 at 1 h and 24 h were not collected since there was an evident ineffectiveness of CC19 and CPAA as can be noticed in **Figure 27**.

Also the CC21 was tested with Acid Black in order to compare the performance with CC21u in the next section. The best results are reported in **Table 12**. As with the CC19 the color removal is quite good even if the results are slightly inferior. It has to be underlined that in this test the order of the additions was inverted respect to the one used in the previous test. The reason is that the color was removed only with the inverted order, so: first the pH was adjusted, second the CC21 was added and last the bentonite.

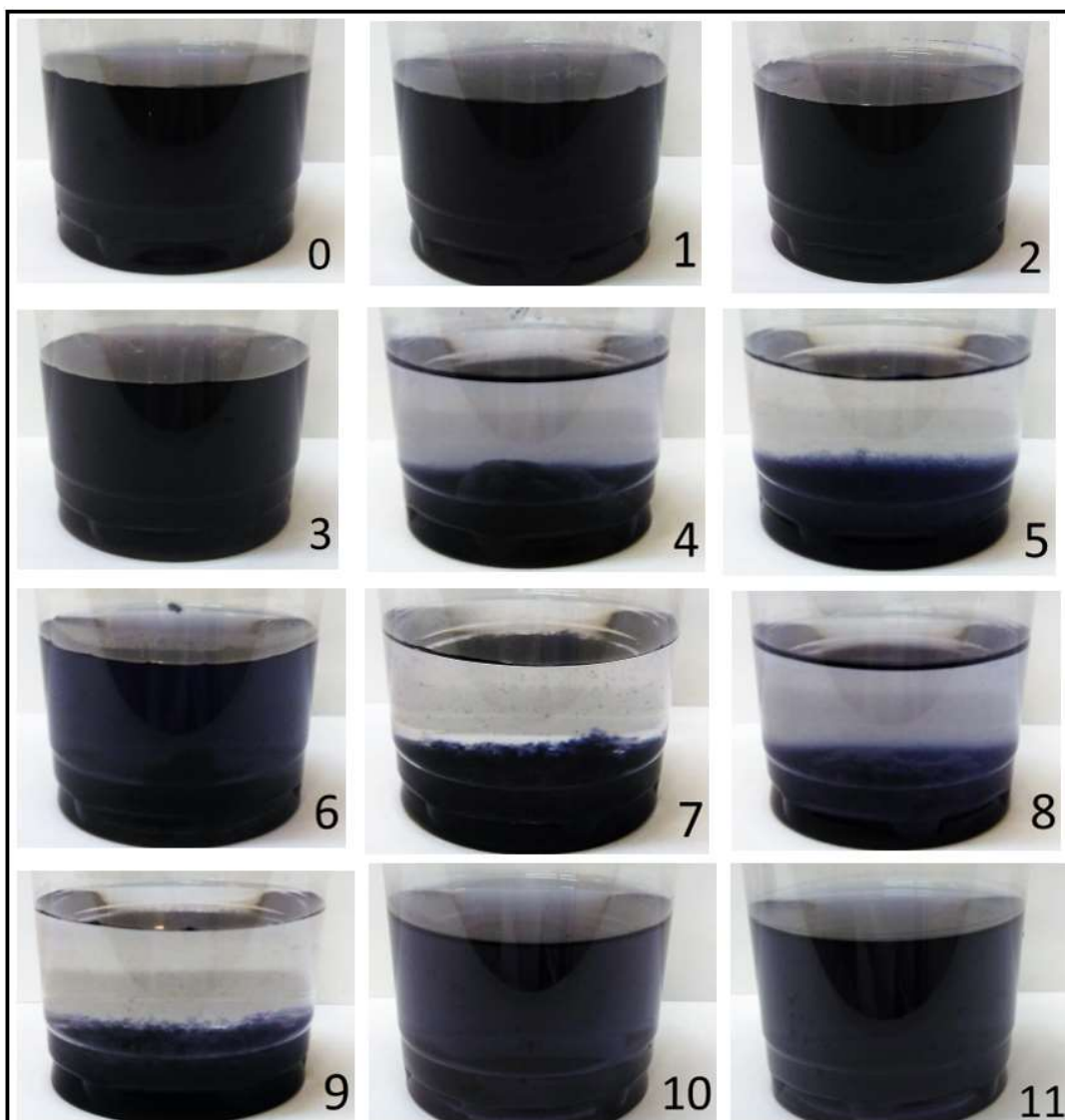


Figure 27 – Pictures of color removal tests of CC19 with Acid Black. The numbers correspond to the samples in Table 10 (0 is the initial effluent).

Table 12 - Color removal test of Acid Black with CC21. Experimental conditions and performance after 5 min, 1 h, 24 h.

Sample	Bentonite [wt%]	ppm CC21	pH	5 min	1 h	24 h
12	0.067	15.90	3.82	72.4	67.8	90.4
13	0.067	10.60	3.33	68.3	86.7	88.5
15	0.133	15.90	3.81	78	85.6	91.9

Methylene Blue

The CC19 was tested with Methylene Blue and the best results together with the experimental conditions are reported in **Table 13**. The CC19 has performed very well in the color removal

of this dye, even under different conditions of pH. In particular, it has not been necessary to change the pH after the addition of bentonite and CC19. Compared to CPAA, the CC19 worked slightly better especially in the short time, as it is noticed between sample 6 and 7 at 5 min. Even a very low concentration of C19 and bentonite allowed very high color removal.

Table 13 - Color removal test of Methylene Blue with CC19. Experimental conditions and performance after 5 min, 1 h, 24 h.

Sample	Bentonite [wt%]	ppm CPAA	ppm CC19	pH	5 min	1 h	24 h
6	0.133	21.20	Ø	8.40	71.8	76.0	77.6
7	0.133	Ø	21.20	8.04	98.7	99.6	99.8
8	0.067	15.90	Ø	7.70	96.5	98.5	99
9	0.067	Ø	15.90	7.60	99	99.8	99.8

Basic Green 1

The CC19 was tested with Basic Green 1 and the best results together with the experimental conditions are reported on **Table 14**. The CC19 has performed very well with high and low flocculant dosage (samples 3 and 7). At lower dosage it has been necessary to change the pH to acidic conditions differently from the higher dosage. The CC19 worked better than CPAA in those trials in which the pH remained unchanged, reaching a high color removal in short time.

Table 14 - Color removal test of CC19 with Basic Green 1. Experimental conditions and performance after 5 min, 1 h, 24 h.

Sample	Bentonite [wt%]	ppm CPAA	ppm CC19	pH	5 min	1 h	24 h
2	0.133	26.50	Ø	8.50	70.5	77.1	81.6
3	0.133	Ø	26.50	7.72	98.7	99.4	99.6
4	0.067	21.20	Ø	8.90	39.8	67.1	65.2
5	0.067	Ø	21.20	8.32	82.4	84.1	82.8
6	0.067	10.60	Ø	3.01	93.6	96.4	100
7	0.067	Ø	10.60	2.90	99.4	99.5	99.9

Brilliant Yellow

The CC16 was tested with Brilliant Yellow and the best result is reported in **Table 15**. The flocculant has not worked well with this dye. Many different conditions were tried, but the results were never remarkable. With the dosage referred to the sample 16 the color removal

is quite significant. Even more, CPAA for the same conditions resulted in worst performance. It was noticed that the dosage required was pretty higher than the one in the other tests.

Table 15 - Color removal test of Brilliant Yellow with CC16. Experimental conditions and performance after 5 min, 1 h, 24 h.

Sample	Bentonite [wt%]	ppm CPAA	ppm CC16	pH	5 min	1 h	24 h
10	0.333	31.80	∅	6.92	turbidity	turbidity	35.4
16	0,333	∅	31.80	7.12	4.4	30.3	74.4

Orange 2

The CC17 was tested with Orange 2, but in any case good results were obtained. In the different conditions tried the color removed was always lower than 30%. Also CC21 was tested in order to be compared with CC21u in the next section. Also in this case the performances are not significant. An inverted order of additions as well as with Acid Black was also tested without success.

Flora Red 4bs

The CC17 was tested with Flora Red 4bs and the best results are reported in **Table 16**. The best result has been obtained by changing the pH (sample 9). In any case, the CC17 has worked better than CPAA.

Table 16 - Color removal test of Flora Red 4bs with CC17. Experimental conditions and performance after 5 min, 1 h, 24 h.

Sample	Bentonite [wt%]	ppm CPAA	ppm CC17	pH	5 min	1 h	24 h
4	0.133	15.90	∅	4.69	turbidity	turbidity	41.2
5	0.133	∅	15.90	4.71	10.1	18.6	84.9
8	0.067	21.20	∅	3.50	69.3	77.9	79.2
9	0.067	∅	21.20	3.54	43.3	88.0	94.3

General considerations

In general, the bentonite has never worked alone, but it has just increased the turbidity. The flocculant alone is not able to remove the color in any case. Only with Basic Green 1 the color removal only with flocculant has given a result over 90%, but it was due to a color variation caused by the pH change. The CCs worked better than CPAA for the removal of Acid Black

2, Methylene Blue, Basic Green 1 and Flora Red 4bs once the conditions were well tuned. In general, good color removal was achieved with only low concentration of CC.

4.1.5 Color removal tests with undissolved CC

In order to check the availability of using the undissolved CC, it was tested for color removal similarly to the CC, but without adding bentonite and introducing a stirring time to compensate its insolubility in water. The CC21u was tested with negatively charged dyes: Acid Black 2, Brilliant Yellow, Orange 2 and Flora Red 4bs.

Acid Black

The experimental conditions and best results of the test are shown in **Table 17**. The results are quite remarkable even without changing the pH to the acidic condition. The effect of the stirring time is quite controversial because comparing samples 6, 7, and 8, it is not clear if increasing stirring time, the color removed is higher or not. Without stirring the color removed is, in any case, already good, even without changing the pH to acid (samples 5 and 13). Even more, the higher dosage of CC21u has not improved significantly the final performance. Some variations are within experimental error

Table 17 - Color removal test of Acid Black with CC21u. Experimental conditions and performance after stirring.

Sample	ppm CC21u	stirring speed [rpm]	stirring time [min]	pH	performance
5	133.34	manual	Ø	5.32	98.1
6	133.34	200	5	4.85	95.3
7	133.34	200	15	4.86	85
8	133.34	200	30	4.71	99.3
9	200.00	200	40	2.48	92.5
10	266.67	200	30	2.65	84.7
11	333.33	200	30	2.86	90.5
12	333.33	200	30	4.91	78.3
13	333.33	manual	Ø	4.94	97

Brilliant Yellow

The experimental conditions and best results of the test are shown in **Table 18**. In contraposition to the previous test, in this one the stirring had a slightly positive effect. The color removed in sample 20 is higher than sample 19 at same CC21u dosage. The sample 20 compared to 21 has revealed that a pH change does not improve the performance.

Table 18 - Color removal test of Brilliant Yellow with CC21u. Experimental conditions and performance after stirring.

Sample	ppm CC21u	stirring speed [rpm]	stirring time [min]	pH	performance
19	33.33	manual	Ø	5.40	82.8
20	33.33	200	30	5.23	88.2
21	33.33	200	30	3.21	87

Flora Red 4bs

The experimental conditions and best results of the test are shown in **Table 19**. The CC21u has shown quite good results at different dosages. It was noticed that increasing the stirring time the color removed is higher, for example comparing samples 11 and 13. The highest dosage is not improving the performance. The color removed without stirring is not significant in this case.

Table 19 - Color removal test of Flora Red 4bs with CC21u. Experimental conditions and performance after stirring.

Sample	ppm CC21u	stirring speed [rpm]	stirring time [min]	pH	performance
4	266.67	manual	Ø	5.57	19.2
11	200.00	200	30	3.43	82.9
12	133.33	200	30	3.43	86.5
13	200.00	200	60	4.09	94.6
14	133.33	200	60	3.94	96.6

Table 20 - Color removal test of Orange 2 with CC21u. Experimental conditions and performance after stirring.

Sample	ppm CC21u	stirring speed [rpm]	stirring time [min]	pH	performance
9	66.67	200	15	not changed	95.4
10	133.33	200	15	not changed	96.1
11	100.00	200	15	not changed	95.6
12	66.67	200	30	not changed	91.6
14	66.67	manual	Ø	not changed	turbidity

Orange 2

The experimental conditions and best results of the test are shown in **Table 20**. These results are quite remarkable considering that the soluble CC is not working with this dye. It seems that the performance is stable even changing the dosage. Without stirring no removal was achieved.

Also, increasing the stirring time at same dosage (samples 9 and 12) did not improve the performance. The pH was not changed in any sample.

Considerations on tests with undissolved CC

In all the tests there have been difficulties of settling of the particles/fibers formed. Even after 24 h, there were unsettled particles suspended on the surface of the treated model wastewater. In some cases, the fibers of CC21u were aggregated in big settling flocs of particles, in other cases, they have remained isolated and suspended. For this reason, the mechanism of color removal with the undissolved CC has to be clarified. Since it is not water soluble and required stirring in some cases, the flocculation is excluded. What is more probable is the adsorption of the dye on the fibers surface. After all, the fibers are cationized and there may be some positive charges along the fibers. These charges may attract the negatively charged molecules of the dyes and adsorb them. Furthermore, the fact that the particles/fibers are not settling may require a filtration after the treatment. In this sense, some samples have been filtrated to remove the suspended particles and clarify them. The UV absorbance of the samples after filtration has not changed so much. Even if the dosage of CC21u is quite high its application in color removal is possible, but an additional step of filtration can increase the costs of the treatment. The application of these cationized fibers in other fields is not excluded and has to be explored more deeply.

Comparing the performance of CC21 and CC21u with the dyes Orange 2 and Acid Black, what emerged is that CC21u is able to remove the Orange 2 without pH change and any other complexing agent, while CC21 is not working with this dye. About Acid Black, both have demonstrated good performances even if the results of CC21u are slightly better, especially the sample 8 in **Table 15**.

4.2 Synthesis of anionic cellulose-based flocculant

4.2.1 Synthesis of DAC

It was synthesized 4 different DACs which have been used in the subsequent anionization reactions. The DACs were prepared in different reaction conditions, but the DS of the different obtained samples (except sample 2) were not very different (**Table 21**). The DS was calculated from the nitrogen content derived from EA after oximation reaction (Section 3.5). The FTIR spectrum of DAC3 in **Figure 28** showed a characteristic band at 1727 cm^{-1} (peak 4) which is assigned to the aldehyde carbonyl stretching. Additionally, the characteristic C1-H bending band of cellulose (at 897 cm^{-1}) was shifted (to 876 cm^{-1} , peak 10) in DAC. This is certainly the

result of the ring opening and oxidation of OH groups at C2/C3 positions; new hemiacetal linkages can also be established between the aldehyde groups and the alcohol groups of different chains which would be held responsible for the observed spectroscopic changes.⁹⁴

Table 21 – Reaction data and substitution degree for synthesis of DACs

Name	Time [h]	Temp [°C]	Periodate/Cell	DS	Analysis
DAC1	4	68	2.05	1.73	FTIR,EA
DAC2	4	75	1.81	1.56	FTIR,EA
DAC3	2.5	70	2.66	1.73	FTIR,EA
DAC4	4	75	2.05	1.70	FTIR,EA

4.2.2 Synthesis of ADACs

The ADACs synthesized are reported in **Table 22**. As in the work of Liimatainen et al.⁹⁴ varied reaction conditions were tried in terms of the amount of sodium metabisulfite and reaction time. The anionic DACs derived from the same DAC3 (ADAC3-1, ADAC3-2, ADAC3-3) have shown that is possible to obtain flocculants with a different zeta potential. The higher DS in these three flocs is in accordance with the value of zeta potential since a higher DS leads to a higher polyelectrolyte charge. Furthermore, ADACs synthesized at different conditions (ADAC2-1 and ADAC3-3) and from different DACs can lead to flocculants with almost the same charge and similar DS. It means that by starting from a DAC with higher DS a flocculant with the similar charge of one derived from a DAC with lower DS can be synthesized, by reducing the reaction time. It seems reasonable because DAC2 has fewer dialdehyde units relatively to DAC3 and to compensate this, in order to obtain a similar product, the reaction time should be increased (at the same metabisulfite/cellulose ratio). This aspect is not confirmed if compared ADAC1-1 with ADAC3-3. The reason why ADAC1-1 shows a lower zeta potential and DS is practical. The reaction to obtain ADAC1-1 was performed in a 100 mL beaker closed with aluminium foil and parafilm and, instead, ADAC3-

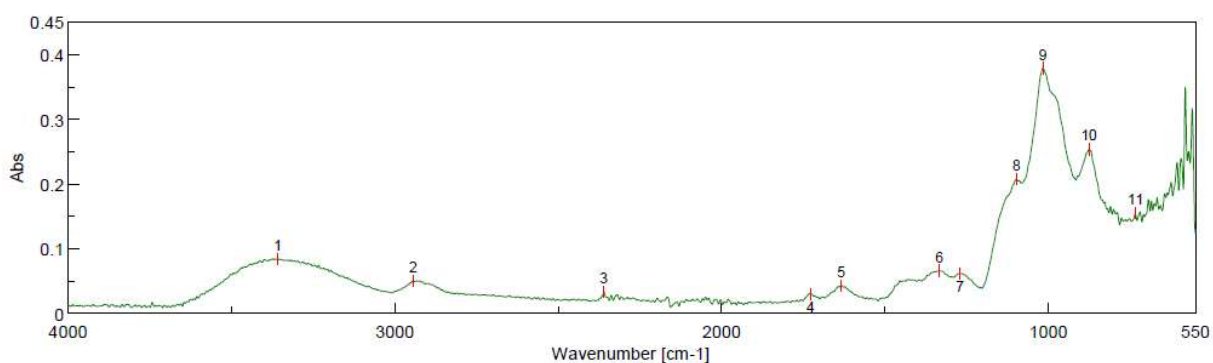


Figure 28 – FTIR spectrum of DAC3.

1 was synthesized according to the procedure reported in section 3.4. The different ambient of reaction probably determined a lower reaction efficiency in the case of ADAC1-1. Starting from ADAC2-1 the procedure is the one more accurate and, in effect, ADAC2-1 obtained under the same reaction conditions of ADAC1-1 showed a higher DS and charge than ADAC1-1, even if the DAC2 is less substituted than DAC1. The solubility was confirmed by the total transparency of the reaction solution at the end of the synthesis. Just for ADAC4-1 it was noticed that some DAC were still unreacted, so it was not totally soluble.

Table 22 – Reaction conditions and some characterization results of ADACs*

Name	NaS ₂ O ₅ /cell	time [h]	solubility	Size [nm]	PDI	MW [kDa]	Zeta pot. [mV]±σ	DS	Analysis
ADAC1-1	28	72	soluble	221.8	0.269	∅	-33.9±3.3	0.69	FTIR,EA,size,zeta
ADAC2-1	28	72	soluble	132.75	0.468	∅	-46.2±1.3	0.77	FTIR,EA,zeta,size
ADAC3-1	14	72	soluble	91.02	0.237	232±3,64	-50.5±4.1	0.90	FTIR,EA,zeta,size,NMR,MW
ADAC3-2	14	34	soluble	76.17	0.379	692±310	-37.6±1.6	0.68	FTIR,EA,zeta,size,NMR,MW
ADAC3-3	28	38	soluble	94.48	0.533	∅	-47.5±2.3	0.83	FTIR,EA,zeta,size
ADAC4-1	14	32.2	not total	80.72	0.527	∅	-49.5±2	0.41	FTIR,EA,zeta,size

*NaS₂O₅/cell = mmol sodium metabisulfite/ g cellulose, time= reaction time.

FTIR spectroscopy showed the modification of DACs by the introduction of new bands. In the spectrum of ADAC3-1 new peaks appeared at 1095 cm⁻¹ (peak 4) and 611 cm⁻¹ (peak 8) (**Figure 29**). These peaks are associated with SO₂ vibrations of sulfonic acid groups.⁹⁴ Even more, the modification of DAC was confirmed by the disappearance of the aldehyde peaks. It is not possible to draw any conclusion regarding the influence of DS on MW of ADAC because it was not possible to do all the measurements for lack of time. Consequently, it is also not possible to draw any conclusion about size since it is related to zeta potential and MW. Debye plots of ADAC3-1 and ADAC3-2 are showed respectively in **Figure 3B** and **Figure 4B (Appendix B)**. The ¹H NMR spectrum (Figure 34) was also measured however the signals were highly overlapped with the signal from water. A new additional peak

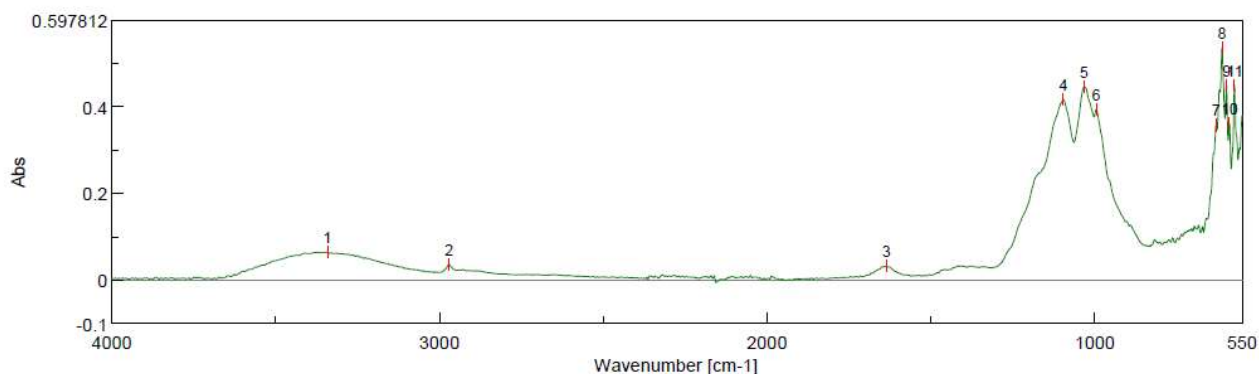


Figure 29 – FTIR spectrum of ADAC3-1.

appeared at 1.09 ppm (doublet) which is yet to be identified (**Figure 30**). All the other FTIR and ^1H NMR spectra of samples listed in **Table 21** are reported in **Appendix A**.

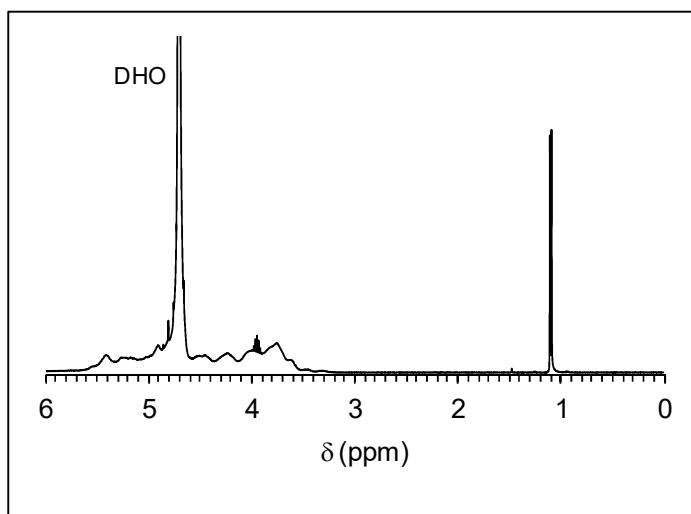


Figure 30 – ^1H NMR spectrum of ADAC3-1.

4.2.3 Color removal tests with ADAC

Color removal tests with ADAC3-1 were performed on Methylene Blue, Acid Black, Brilliant Yellow, Flora Red 4bs and Orange 2. Since the test on Methylene Blue was a preliminary test, it has been used bentonite as complexing agent. For the other tests it has been used aluminium sulfate. The different dyes were characterized according to the strategy reported in section 3.7, the results being shown in **Table 10**.

Methylene Blue

The ADAC3-1 was tested with Methylene Blue and the best results are reported in **Table 23**. As can be noticed, the performance is not remarkable. This was quite foreseeable because both bentonite and the flocculant have a negative charge. These negative charges combined do not allow the formation of flocs because of the charge repulsion. Also because the dye is slightly positively charged and easily neutralized by both bentonite and ADAC3-1.

Table 23 - Color removal test of Methylene Blue with ADAC3-1. Experimental conditions and performance after 5 min, 1 h, 24 h.

Sample	Bentonite [wt%]	ppm ADAC3-1	pH	5 min	1 h	24 h
2	∅	31.80	3.60	55.5	∅	68.5
6	0.133	31.80	6.30	48.6	∅	79
7	0.133	15.90	5.95	70.4	∅	76.1

Following this test, the choice was to use aluminium sulfate as complexing agent because of its positive charge. As bentonite works well with CC since they have opposite charges, in the same way aluminium sulfate with ADACs can favor the flocs complexation. Aluminium sulfate is one of the most important papermaking chemicals, but it has also been used as water clarification coagulant.¹¹¹ It was chosen to test ADAC3-1 only with negatively charged dyes.

Acid Black

The experimental conditions and best results of the test are reported in **Table 24**. The color removed is quite high in each sample, even at different pH and dosage. It was noticed, comparing sample 10 and 11, that aluminium sulfate is working even alone. The ADAC3-1 seems only to improve the velocity of sedimentation but not final performance after 24 h. The pictures representing the best results are reported in **Figure 31**.

Table 24 - Color removal test of Acid Black with ADAC3-1. Experimental conditions and performance after 5 min, 1 h, 24 h.

Sample	Alum. Sulf. [wt%]	ppm ADAC3-1	pH	5 min	1 h	24 h
8	0.033	2.65	5.10	78.8	88.1	97.6
9	0.033	1.06	6.60	80.9	88.1	96.7
10	0.047	∅	3.90	64.6	81.9	96.6
11	0.047	1.59	4.00	77.2	87.1	96.5
14	∅	15.90	5.80	14.4	∅	11.5

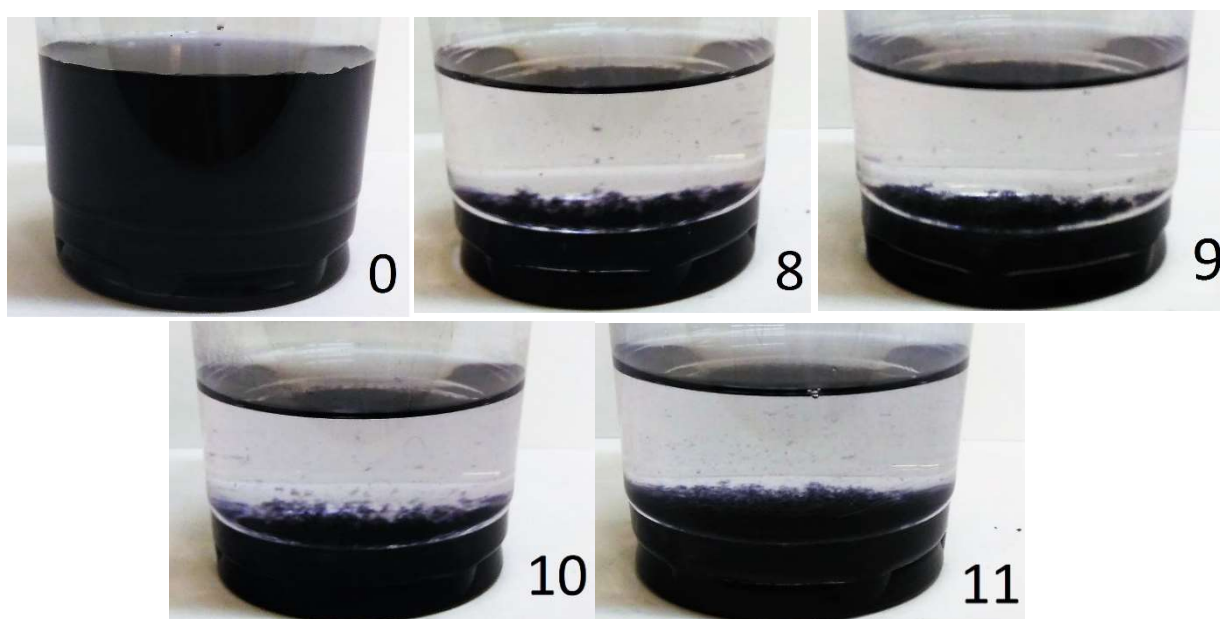


Figure 31 – Pictures of color removal tests of Acid Black with ADAC3-1.

Flora Red 4bs

The experimental conditions and best results of the color removal test of this dye are showed in **Table 25**. The results have revealed a good performance with this dye. Even in this case, the aluminium sulfate is working alone and the ADAC3-1 tends to increase the settling velocity of the flocs. The color removed after 5 min is higher with the higher dosage (both alum and ADAC3-1), but the final value is roughly the same. Also the pH does not seem to influence so much the color removal.

Table 25 - Color removal test of Flora Red 4bs with ADAC3-1. Data and performance after 5 min, 1 h, 24 h.

Sample	Alum. Sulf. [wt%]	ppm ADAC3-1	pH	5 min	1 h	24 h
1	0.067	Ø	3.93	72.4	87.8	98.8
2	0.067	2.65	3.87	89	93.9	96.6
3	0.067	5.30	3.79	83	91.4	96.8
4	0.033	Ø	6.71	70.5	90.5	98.9
5	0.033	1.06	6.75	77.6	93.7	92.8
6	0.033	2.12	6.71	74.6	93.9	98.9
12	Ø	15.90	5.05	46	Ø	46.9

Brilliant Yellow

From the best results reported in **Table 26** it can be noticed that the color removed was not as good as the other dyes. The performance at 5 min was not sufficient in all samples even if the results are better than with aluminium sulfate was working alone. Also, better results were obtained for the lower dosage of ADAC3-1

Table 26 - Color removal test of Brilliant Yellow with ADAC3-1. Experimental conditions and performance after 5 min, 1 h, 24 h.

Sample	Alum. Sulf. [wt%]	ppm ADAC3-1	pH	5 min	1 h	24 h
1	0.067	Ø	3.72	43.1	71.2	73.4
2	0.067	2.65	3.67	56	55.7	84.7
3	0.067	5.30	3.66	59.9	67.4	77
10	Ø	15.90	4.82	26.8	Ø	Ø

Orange 2

ADAC3-1 tested with this dye did not achieved significant results.

General considerations

In general, the ADAC3-1 is not able to remove the color alone however it improves the performance especially in the short time. It has to be notice that ADAC-1 worked better in color removal of Brilliant Yellow than CC. Only negative charged dyes were tested in order to favor the initial aggregation with the aluminium sulfate and secondly the complexation with the flocculant. For this reason, there was no sense to test positively charged dyes. Furthermore, in all tests the pH was changed to alkaline in order to favor the cationic behaviour of aluminium sulfate. The final pH is in some cases very acid because of aluminium sulfate. It was not possible to test ADACs with different DS for a lack of time.

5 Conclusions and future work

5.1 Conclusions

In this work, cationic and anionic cellulose-based flocculants were synthesized and applied on color removal tests.

In the synthesis of the CC it has been discovered that a complete cellulose dissolution in NaOH-based aqueous solution is not possible. Consequently, the reaction of cationization was occurring in heterogeneous conditions. These conditions combined with the inefficient mixing can explain the low reaction yield obtained around 3 wt%. Anyway, the CC flocculants were successfully synthesized as confirmed by FTIR spectra and ¹H NMR spectra. The CC flocculants were water soluble and it was possible to modulate their charge and the degree of substitution - DS, by changing the reaction time. The minimum charge was around +47 mV with 2 h of reaction, and the maximum charge around +59 mV at 5 h of reaction. Over 5 h there has not been an increase of the charge and the DS probably due to degradation of cellulose. However, the reactions were affected by a lack of reproducibility which must be related with the difficulty of mixing. The CC tested has shown good results with color removal, over 90 %, with almost all the dyes. The removal was more effective using a dual system in combination with bentonite. Only with Orange 2 and Brilliant Yellow the color removed was not sufficient. In general, an acid pH can favor the flocculation, but with Methylene Blue the CC19 has worked without changing the pH. The color removal has worked both for negatively and positively charged dyes. The order of addition could make a difference in the efficiency of removal as it was noted for the CC21 in the test with Acid Black. Even more, a right dosage of flocculant and bentonite can lead to a fast complexation and sedimentation of the flocs.

The undissolved CC is not a valuable product for this work, but it can have some applications. The undissolved CC21 tested only with negatively charged dyes has shown pretty good results. The effect of stirring time is not well defined since, for instance, for Orange 2 it has been relevant, but not with Acid Black. The optimum dosage of the undissolved CC21 must vary according to the dye, but a dosage of 133,33 ppm has worked well with all dyes except for the Brilliant Yellow. In any case, the dosage of the undissolved CC is quite high, even if it has not been required any other additional complexing agent. The acid pH can favor the color removal in all tests. The main drawback is the unsettled

fibers/particles that still remain after the treatment. To remove them and clarify the supernatant water it may be necessary a filtration step. However, this additional step increases the cost of the treatment. The possible applications of the undissolved CC remain an open field to be explored in the future.

The ADAC was successfully synthesized as confirmed by the FTIR spectra and the ^1H NMR spectra. The ADAC flocculants are water soluble as noticed from the transparency of the reaction solution. The DS and the zeta potential of the ADACs can be modulated in two ways: varying the DS of DAC or playing with reaction conditions, as the time and the amount of sodium metabisulfite. The higher zeta potential obtained was around -50 mV while the lower around -34 mV. Again a dual system had to be used in color removal (combination of ADAC with aluminium sulfate). The color removal tests on negatively charged dyes have demonstrated that the flocculant is not fundamental, but it can improve the performance in terms of settling velocity. The results are very good for Acid Black and Flora Red 4bs, which has shown a removal efficiency value over 90% even after 1 h in the case of for Flora Red. For Brilliant Yellow, the results are quite good, with around 85% of but not over 90% of color removed after 24 h, contrary to what happened with the cationic cellulose. For Orange 2 the performance is not significant with values under 30%.

In the future it is necessary to perform removal tests with the two types of modified cellulose testing the effect of the degree of substitution, which was not possible in this work due to lack of time.

In summary, it can be referred that the cellulose based polyelectrolytes produced represent promising alternatives for the treatment of harsh colored waste waters, substituting the usual oil based synthetic polyelectrolytes which are not biodegradable.

5.2 Future works

The present work is not definitive and it leaves open many doors for future improvements. Regarding the synthesis of CC the proposals are:

- Characterize the starting material;
- Improve cellulose dissolution in order to have a reaction in homogeneous conditions and doing so to increase the reaction yield;
- Improve the separation of CC from the undissolved part to avoid contaminations of the product;
- Vary the molar ratio CHPTAC:AGU to understand its influence in the reaction;

- Improve the mixing during both steps of synthesis;
- Verify the residual content of reagents in the final product;
- Improve the reproducibility.

Furthermore, valorize the undissolved CC, not only for applications in color removal.

Regarding the synthesis of ADAC the proposals are:

- Vary the DS of DAC in order to understand better the influence on the final product;
- Change the amount of sodium metabisulfite and reaction time in a wider range;
- Verify the residual content of reagents in the final product;
- Improve reproducibility.

Both for CC and ADAC, the MW should be measured for all the samples. Regarding the color removal tests the proposals are:

- Study more deeply the influence of pH and dosage of both flocculants and complexing agent;
- Analyze the COD of the supernatant water;
- Try other complexing agents with ADAC;
- Test other model wastewaters;
- Check the influence of the DS of both CC and ADAC on removal efficiency.

6 References

- ¹ Bratby, J., **2006**. *Coagulation and Flocculation in Water and Wastewater Treatment*, 2nd ed. IWA Publishing, London.
- ² Sharma, B.R., Dhuldhoya, N.C., Merchant, U.C., **2006**. *Flocculants—an ecofriendly approach*. *J. Polym. Environ.* 14, 195–202.
- ³ Lee, C. S., Robinson, J., Chong, M. F., **2014**. *A review on application of flocculants in wastewater treatment*, *Process Safety and Environmental Protection* 92, 489-508.
- ⁴ Singh, R.P., Karmakar, G.P., Rath, S.K., Karmakar, N.C., Pandey, S.R., Tripathy, T., Panda, J., Kanan, K., Jain, S.K., Lan, N.T., **2000**. *Biodegradable drag reducing agents and flocculants based on polysaccharides: materials and applications*. *Polym. Eng. Sci.* 40, 46–60.
- ⁵ Song, Y.B., Zhang, J., Gan, W.P., Zhou, J.P., Zhang, L.N., **2010**. *Flocculation properties and antimicrobial activities of quaternized celluloses synthesized in NaOH/Urea aqueous solution*. *Industrial & Engineering Chemistry Research* 49 (3), 1242e1246.
- ⁶ Bohuslav Dobias, H.S., **2005**. *Coagulation and Flocculation*, 2nd ed. CRC Press, Taylor & Francis Group, United States of America.
- ⁷ W. Kern, *Z. Physik. Chem. Part A*, **1938**, 181, 249.
- ⁸ <http://goldbook.iupac.org/P04728> (Retrieved July 18th, 2016).
- ⁹ Moudling, B.M., and Shah, B., *Advances in solid-liquid separation*, H.S. Muralidhara (ed.), **(1986)**, p.192.
- ¹⁰ Ayyala, S., Pugh, R.J., and Forssberg, E., *Mineral processing and extract*. *Metallurgy Review*, 12 **(1995)** 115.
- ¹¹ Somasundaran, P., Das, K.K., and Yu, X., *Current options in colloid and interface sciences*, 1 **(1996)** 530.
- ¹² Chong, M., **2012**. *Direct flocculation process for wastewater treatment*. In: Sharma, S.K., Sanghi, R. (Eds.), *Advances in Water Treatment and Pollution Prevention*. Springer, Netherlands, pp. 201–230.
- ¹³ Bolto, B., Gregory, J., **2007**. *Organic polyelectrolytes in water treatment*. *Water Res.* 41, 2301–2324.
- ¹⁴ Renault, F., Sancey, B., Badot, P.M., Crini, G., **2009a**. *Chitosan for coagulation/flocculation processes – an eco-friendly approach*. *Eur. Polym. J.* 45, 1337–1348.
- ¹⁵ Caskey, J.A., Primus, R.J., **1986**. *The effect of anionic polyacrylamide molecular conformation and configuration on flocculation effectiveness*. *Environ. Prog.* 5, 98–103.

-
- ¹⁶ Biggs, S., Habgood, M., Jameson, G.J., Yan, Y.-d., **2000**. *Aggregate structures formed via a bridging flocculation mechanism*. Chem. Eng. J. 80, 13–22.
- ¹⁷ Blanco, A., Fuente, E., Negro, C., Tijero, J., **2002**. *Flocculation monitoring: focused beam reflectance measurement as a measurement tool*. Can. J. Chem. Eng. 80, 1–7.
- ¹⁸ Razali, M.A.A., Ahmad, Z., Ahmad, M.S.B., Ariffin, A., **2011**. *Treatment of pulp and paper mill wastewater with various molecular weight of polyDADMAC induced flocculation*. Chem. Eng. J. 166, 529–535.
- ¹⁹ Sher, F., Malik, A., Liu, H., **2013**. *Industrial polymer effluent treatment by chemical coagulation and flocculation*. J. Environ. Chem. Eng. 1, 684–689.
- ²⁰ Kleimann, J., Gehin-Delval, C., Auweter, H., Borkovec, M., **2005**. *Super-stoichiometric charge neutralization in particle–polyelectrolyte systems*. Langmuir 21, 3688–3698.
- ²¹ J. Duan, J. Gregory / *Advances in Colloid and Interface Science* 100–102 (**2003**) 475–502.
- ²² Ahmad, A.L., Wong, S.S., Teng, T.T., Zuhairi, A., **2008**. *Improvement of alum and PACl coagulation by polyacrylamides (PAMs) for the treatment of pulp and paper mill wastewater*. Chem. Eng. J. 137, 510–517.
- ²³ Blanco, A., Fuente, E., Negro, C., Tijero, J., **2002**. *Flocculation monitoring: focused beam reflectance measurement as a measurement tool*. Can. J. Chem. Eng. 80, 1–7.
- ²⁴ Somasundaran, P., and Ramachandaran, R., *Inflocculation and dewatering and engineering foundation*, NY, (**1988**) p.217
- ²⁵ Henderson, J.M., and Wheatley, A.D., *J. Applied Polymer Science* 33 (**1987**) 669.
- ²⁶ S. Lu, R.J. Pugh, E. Forssberg, *Interfacial separation of particles*, Study in interface science, **2005**.
- ²⁷ Özacar, M., Sengil, I.A., **2003**. *Evaluation of tannin biopolymer as a coagulant aid for coagulation of colloidal particles*. Colloids Surf. A: Physicochem. Eng. Aspects 229, 85–96.
- ²⁸ Rinaudo, M., **2006**. *Chitin and chitosan: properties and applications*. Progr. Polym. Sci. 31, 603–632.
- ²⁹ Szyguła, A., Guibal, E., Palacín, M.A., Ruiz, M., Sastre, A.M., **2009**. *Removal of an anionic dye (Acid Blue 92) by coagulation–flocculation using chitosan*. J. Environ. Manage. 90, 2979–2986.
- ³⁰ E. Guibal, J. Roussy, *React. Funct. Polym.*, **2007**, 67, 33.
- ³¹ No, S. Meyers, *Application of chitosan for treatment of wastewaters*, Springer, New York, **2000**, 1.
- ³² Bolto, B., Dixon, D., Eldridge, R., King, S.J., **1998**. *The use of cationic polymers as primary coagulants in water treatment*. In: Hahn, H.H., Hoffmann, E., Odegaard, H. (Eds.), Proceedings

of the Fifth Gothenburg Symposium. Chemical Water and Wastewater Treatment. Berlin, Springer, pp. 173–182.

³³ Bolto, B., Dixon, D., Eldridge, R., King, S., **2001**. *Cationic polymer and clay or metal oxide combinations for natural organic matter removal*. *Water Res.* 35 (11), 2669–2676.

³⁴ Eikebrokk, B., Saltnes, T., **2002**. *NOM removal from drinking water by chitosan coagulation and filtration through lightweight expanded clay aggregate filters*. *J. Water Supply: Res. Technol. Aqua* 51 (6), 323–332.

³⁵ Guibal, E., Roussy, J., **2007**. *Coagulation and flocculation of dye-containing solutions using a biopolymer (chitosan)*. *React. Funct. Polym.* 67, 33–42.

³⁶ Rodrigues, A.C., Boroski, M., Shimada, N.S., Garcia, J.C., Nozaki, J., Hioka, N., **2008**. *Treatment of paper pulp and paper mill wastewater by coagulation–flocculation followed by heterogeneous photocatalysis*. *J. Photochem. Photobiol. A: Chem.* 194, 1–10.

³⁷ Pariser, E.R., Lombardi, D.P., **1989**. *Chitin Sourcebook: A Guide to the Research Literature*. Wiley, New York.

³⁸ Özacar, M., Sengil, I.A., **2000**. *Effectiveness of tannins obtained from valonia as a coagulant aid for dewatering of sludge*. *Water Res.* 34, 1407–1412.

³⁹ Beltrán Heredia, J., Sánchez Martín, J., **2009**. *Removing heavy metals from polluted surface water with a tannin-based flocculant agent*. *J. Hazard. Mater.* 165, 1215–1218.

⁴⁰ L. Wang, W. Liang, J. Yu, Z. Liang, L. Ruan, and Y. Zhang, *Flocculation of Microcystis aeruginosa Using Modified Larch Tannin*, *Environ. Sci. Technol.* **2013**, 47, 5771–5777.

⁴¹ Roussy, J., Chastellan, P., Vooren, M.V., Guibal, E., **2005**. *Treatment of ink-containing wastewater by coagulation/flocculation using biopolymers*. *WaterSAManuscript* 31, 369–376.

⁴² Al-Hamadani, Y.A.J., Yusoff, M.S., Umar, M., Bashir, M.J.K., Adlan, M.N., **2011**. *Application of psyllium husk as coagulant and coagulant aid in semi-aerobic landfill leachate treatment*. *J. Hazard. Mater.* 190, 582–587.

⁴³ Anastasakis, K., Kalderis, D., Diamadopoulou, E., **2009**. *Flocculation behavior of mallow and okra mucilage in treating wastewater*. *Desalination* 249, 786–791.

⁴⁴ Mishra, A., Bajpai, M., **2005**. *Flocculation behaviour of model textile wastewater treated with a food grade polysaccharide*. *J. Hazard. Mater.* 118, 213–217.

⁴⁵ Mishra, A., Agarwal, M., Yadav, A., **2003**. *Fenugreek mucilage as a flocculating agent for sewage treatment*. *Colloid. Polym. Sci.* 281, 164–167.

⁴⁶ Mishra, A., Yadav, A., Agarwal, M., Bajpai, M., **2004**. *Fenugreek mucilage for solid removal from tannery effluent*. *React. Funct. Polym.* 59, 99–104.

-
- ⁴⁷ Agarwal, M., Srinivasan, R., Mishra, A., **2001**. *Study on flocculation efficiency of okra gum in sewage waste water*. *Macromol. Mater. Eng.* 286, 560–563.
- ⁴⁸ Wu, C., Wang, Y., Gao, B., Zhao, Y., Yue, Q., **2012**. *Coagulation performance and floc characteristics of aluminum sulfate using sodium alginate as coagulant aid for synthetic dyeing wastewater treatment*. *Sep. Purif. Technol.* 95, 180–187.
- ⁴⁹ Pal, S., Mal, D., Singh, R.P., **2005**. *Cationic starch: an effective flocculating agent*. *Carbohydr. Polym.* 59, 417–423.
- ⁵⁰ C. Y. Teha, T. Y. Wua,* , J. C. Juanb, **2014**, *Potential use of rice starch in coagulation–flocculation process of agro-industrial wastewater: Treatment performance and flocs characterization*, *Ecological Engineering* 71, 509–519.
- ⁵¹ Teh, C.Y., Wu, T.Y., Juan, J.C., **2014**. *Optimization of agro-industrial wastewater treatment using unmodified rice starch as a natural coagulant*. *Ind. Crops Prod.* 56, 17–26.
- ⁵² S. Y. Bratskaya, S. Genest, K. Petzold-Welcke, T. Heinze, S. Schwarz, **2014**, *Flocculation Efficiency of Novel Amphiphilic Starch Derivatives: A Comparative Study*, *Macromol. Mater. Eng.* 2014, 299, 722–728
- ⁵³ . D. Klemm, B. Heblein, H. P. Fink, A. Bohn, *Angew. Chem. Int. Ed.*, **2005**, 44, 3358.
- ⁵⁴ Khiari, R., Dridi-Dhaouadi, S., Aguir, C., Mhenni, M.F., **2010**. *Experimental evaluation of eco-friendly flocculants prepared from date palm rachis*. *J. Environ. Sci.* 22, 1539–1543.
- ⁵⁵ Suopajarvi, T., Liimatainen, H., Hormi, O., Niinimäki, J., **2013**. *Coagulation–flocculation treatment of municipal wastewater based on anionized nanocelluloses*. *Chem. Eng. J.* 231, 59–67.
- ⁵⁶ Solarek D.B. , *Phosphorilated starches and miscellaneous inorganic esters*, in *Modified Starch: Properties and Uses* , Ed.: Wurzburg O.K. , CRC Press , Boca Raton (USA) , **1986** , pp. 97 – 112 .
- ⁵⁷ D. Krentz, C. Lohmann, *Properties and Flocculation Efficiency of Highly Cationized Starch Derivatives*, *Starch/Stärke* 58 (**2006**) 161–169.
- ⁵⁸ Vihervaara T, Bruun HH, Backman R, Paakkanen M. *The effect of different methods of cationisation on the starch granule and its gelatinisation product*. *Starch/Stärke* **1990**; 42:64–8.
- ⁵⁹ Sableviciene D, Klimaviciute R, Bendoraitiene J, Zemaitaitis A. *Flocculation properties of high-substituted cationic starches*. *Colloids Surf A Physicochem Eng Asp* **2005**; 259:23–30.
- ⁶⁰ Kavaliauskaite R, Klimaviciute R, Zemaitaitis A. *Factors influencing production of cationic starches*. *Carbohydr Polym* **2008**; 73:665–75.

-
- ⁶¹ Hebeish A, Higazy A, El-Shafei A, Sharaf S. *Synthesis of carboxymethyl cellulose (CMC) and starch-based hybrids and their applications in flocculation and sizing*. Carbohydr Polym **2010**; 79:60–9.
- ⁶² Ellis H.A., Utah S.I., Martins O. (1982), Water Res 16(9):1433.
- ⁶³ Nishiuchi T, Kobayashi K(1977) Nippon Kogaku Kaishi, 11, 1711;
- ⁶⁴ Lekniute E, Peciulyte L, Klimaviciute R, Bendoraitiene J, Zemaitaitis A. *Structural characteristics and flocculation properties of amphoteric starch*. Colloids Surf A Physicochem Eng Asp **2013**;430:95–102.
- ⁶⁵ Huang, X.; Li, L.; Liao, X. P.; Shi, B. *Preparation of platinum nanoparticles supported on bayberry tannin grafted silica bead and its catalytic properties in hydrogenation*. J. Mol. Catal. A: Chem. **2010**, 320 (1–2), 40–46.
- ⁶⁶ Beltran, H. J.; Sanchez, M. J.; Gomez-Munoz, M. C. *New coagulant agents from tannin extracts: Preliminary optimization studies*. Chem. Eng. J. **2010**, 162 (3), 1019–1025.
- ⁶⁷ Al. Arbenz, L. Avérous, *Chemical modification of tannins to elaborate aromatic biobased macromolecular architectures*, Green Chem., **2015**, 17, 2626–2646.
- ⁶⁸ Quamme, J. E.; Kemp, A. H. *Stable tannin based polymer compound*. Patent number: 4558080, United States Patent, **1985**.
- ⁶⁹ J. Sánchez-Martín*, J. Beltrán-Heredia 1 , C. Solera-Hernández, *Surface water and wastewater treatment using a new tannin-based coagulant. Pilot plant trials*, Journal of Environmental Management 91 (2010) 2051-2058
- ⁷⁰ B. S. Kaith, R. Jindal, R. Sharma, *Study of ionic charge dependent salt resistant swelling behavior and removal of colloidal particles using reduced gum rosin-poly(acrylamide)-based green flocculant*, Iran Polym J (2016) 25:349–362.
- ⁷¹ A. Mishra, M. Bajpai, S. Pal, M. Agrawal, S. Pandey, *Tamarindus indica mucilage and its acrylamide-grafted copolymer as flocculants for removal of dyes*, Colloid Polym Sci (2006) 285: 161–168.
- ⁷² Rudie AW, Ball A, Patel N (2006), *Ion Exchange of H + , Na + , Mg 2+ , Ca 2+ , Mn 2+ , and Ba 2+ on Wood Pulp*. J Wood Chem Technol 26:259–272.
- ⁷³ Constantin M, Asmarandei I, Harabagiu V, et al (2013) *Removal of anionic dyes from aqueous solutions by an ion-exchanger based on pullulan microspheres*. Carbohydr Polym 91:74–84.
- ⁷⁴ T. R. Dawsey, C. L. Mc Cormick, *J. Macromol. Sci. Rev.*, **1990**, 30, 405.
- ⁷⁵ . W. Burchard, N. Habermann, P. Klufers, B. Seger, U. Wilhelm, *Angew. Chem.*, **1994**, 106, 936.

-
- ⁷⁶ Klemm D., Philipp B., (2001b) *Comprehensive cellulose chemistry. Functionalization of cellulose*, Wiley-VCH, Verlag-GmbH, Weinheim, Germany, Vol.2 p. 221-223.
- ⁷⁷ Heinze T., Koschella A.(2005), *Carboxymethyl ethers of cellulose and starch – A review*, *Macromol. Symp.* 223, 13-39.
- ⁷⁸ Borza j., Racz I.,(1995) *Carboxymethylcellulose of fibrous character, a survey*, *Cellulose Chem. Technol.* 29, 657-663.
- ⁷⁹ . L. Zhu, J. Qin, X. Yin, L. Ji, Q. Lin, Z. Qin, *Polym. Adv. Technol.*, **2014**, 25, 168.
- ⁸⁰ . A. Svensson, E. Nicklasson, T. Harrah, B. Panilaitis, D. L. Kaplan, M. Brittberg, P. Gatenholm, *Biomaterials*, **2005**, 26,419.
- ⁸¹ . Z. Wang, L. Li, K. Xiao, J. Wu, *Bioresource Technol.*, **2009**, 100, 1687.
- ⁸² . S. Yao, *Chem. Eng. J.*, **2000**, 78, 199.
- ⁸³ H. Liimatainen, J. Sirviö, O. Sundman, M. Visanko, O. Hormi, J. Niinimäki, *Bioresour. Technol.*, **2011**, 102, 9626.
- ⁸⁴ T. Aimin, Z. Hongwei, C. Gang, X. Guohui, L. Wanzhi, *Ultrasonics Sonochemistry*, **2004**, 12, 467.
- ⁸⁵ Liimatainen H, Visanko M, Sirviö JA, et al (2012b) *Enhancement of the Nanofibrillation of Wood Cellulose through Sequential Periodate–Chlorite Oxidation*. *Biomacromolecules* 13:1592–1597.
- ⁸⁶ Hangcheng Zhu, Yong Zhang, Xiaogang Yang, Hongyi Liu, Lan Shao, Xiumei Zhang, Juming Yao, *One-step green synthesis of non-hazardous dicarboxyl cellulose flocculant and its flocculation activity evaluation*, *Journal of Hazardous Materials* 296 (2015) 1–8.
- ⁸⁷ Liimatainen H, Visanko M, Sirviö J, et al (2013b) *Sulfonated cellulose nanofibrils obtained from wood pulp through regioselective oxidative bisulfite pre-treatment*. *Cellulose* 20:741–749.
- ⁸⁸ J. Sirviö, A. Honka, H. Liimatainen, J. Niinimäki, O. Hormi, *Carbohydr. Polym.*, **2011**, 86, 266.
- ⁸⁹ J. Sirviö, U. Hyvakkö, H. Liimatainen, J. Niinimäki, O. Hormi, *Carbohydr. Polym.*, **2011**, 83, 1293.
- ⁹⁰ H. Konko, R. Kusumoto, *React. Funct. Polym.*, **2014**, 82, 111.
- ⁹¹ H. Zhang, H. Guo, B. Wang, L. Xiong, S. Shi, X. Chen, *Homogeneous synthesis and characterization of polyacrylamide-grafted cationic cellulose flocculants*, *J. APPL. POLYM. SCI.* **2016**.
- ⁹² J. Sirviö, A. Honka, H. Liimatainen, J. Niinimäki, O. Hormi, *Carbohydr. Polym.*, **2011**, 86, 266.

-
- ⁹³ J. Sirviö, U. Hyvakkö, H. Liimatainen, J. Niinimäki, O. Hormi, *Carbohydr. Polym.*, **2011**, *83*, 1293.
- ⁹⁴ H. Liimatainen, J. Sirvio, O. Sundman, O. Hormi, J. Niinimaki, *Use of nanoparticulate and soluble anionic celluloses in coagulation-flocculation treatment of kaolin suspension*, *Water Research* **46** (2012) 2159-2166.
- ⁹⁵ J. Zhang, N. Jiang, Z. Dang, T. J. Elder, A. J. Ragauskas, *Oxidation and sulfonation of celluloses*, *Cellulose* (2008) 15:489–496.
- ⁹⁶ Daniel J. Pasto, Carl R. Johnson, Marvin J. Miller, *Experiments and techniques in organic chemistry*, Prentice Hall, **1992**, 545 pages.
- ⁹⁷ http://www.uts.utoronto.ca/~traceslab/ATR_FTIR.pdf
- ⁹⁸ Malvern, <http://www.malvern.com/en/products/product-range/zetasizer-range/zetasizer-nano-range/zetasizer-nano-zs/default.aspx>, (Retrieved July 8th, **2016**).
- ⁹⁹ Malvern, <http://www.malvern.com/en/support/resourcecenter/technicalnotes/TN101104DynamicLightScatteringIntroduction.aspx>, (Retrieved July 8th, **2016**).
- ¹⁰⁰ Malvern, <http://www.malvern.com/en/products/technology/static-light-scattering/>, (Retrieved July 8th, **2016**).
- ¹⁰¹ Malvern, <http://www.malvern.com/en/products/technology/electrophoretic-light-scattering/default.aspx>, (Retrieved July 8th, **2016**).
- ¹⁰² <https://www2.chemistry.msu.edu/faculty/reusch/virttxtjml/spectrpy/nmr/nmr1.htm>, (Retrieved July 8th, **2016**).
- ¹⁰³ P.Y. Bruice, *Organic Chemistry (5th)*.
- ¹⁰⁴ H. Qi, Q. Yang, L. Zhang, T. Liebert, T. Heinze, *The dissolution of cellulose in NaOH-based aqueous system by two-step process*, *Cellulose* (2011) 18:237–245.
- ¹⁰⁵ B. Medronho, H. Duarte, L. Alves, F. Antunes, A. Roman, B. Lindman, *Probing cellulose amphiphilicity*, *Nordic Pulp & Paper Research Journal* Vol 30 no (1) **2015**.
- ¹⁰⁶ F. Porro, O. Be'due', H. Chanzy, L. Heux, *Solid-State ¹³C NMR Study of Na-Cellulose Complexes*, *Biomacromolecules* **2007**, *8*, 2586-2593.
- ¹⁰⁷ A. Moral, R. Aguado, M. Ballesteros, A. Tijero, *Cationization of Alpha-Cellulose to Develop New Sustainable Products*, *International Journal of Polymer Science* (2015).
- ¹⁰⁸ M. Hashem, P. Hauser, B. Smith, *Reaction Efficiency for Cellulose Cationization Using 3-Chloro-2-Hydroxypropyl Trimethyl Ammonium Chloride*, *Textile research journal*, (2003).
- ¹⁰⁹ H. J. Prado, M. C. Matulewicz, *Cationization of polysaccharides: A path to greener derivatives with many industrial applications*, *European Polymer Journal* **52** (2014) 53–75.

¹¹⁰Dow-chemicals:

https://dowanswer.custhelp.com/app/answers/detail/a_id/9837/kw/kinetic%20model/session/L3RpbWUvMTQ2ODQwNjkwOC9zaWQvZHo2d3RwVm0%3D, (Retrieved July 13th, **2016**).

¹¹¹ Z. Yan, Y. Deng, *Cationic microparticles in Papermaking wet end*, IPST Technucal Paper Series numeber 927, **2002**

Appendix A

FTIR spectra of CC and ADAC

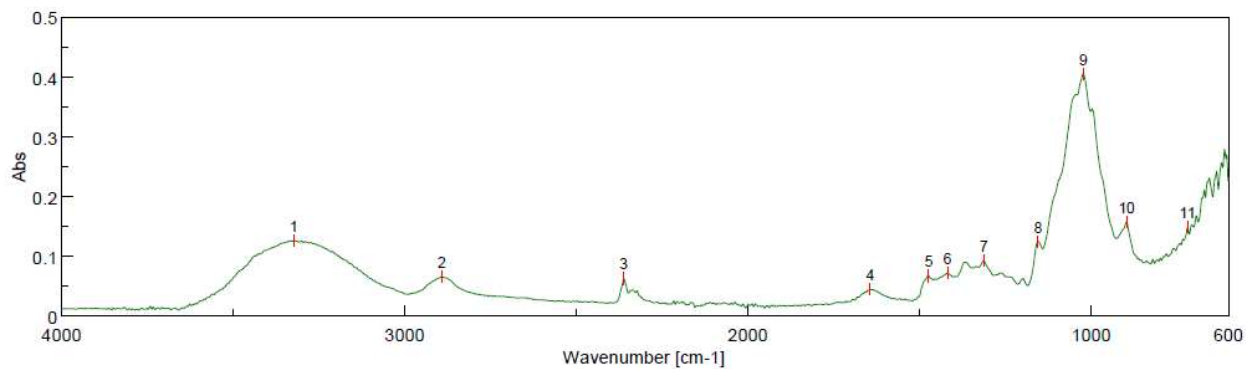


Figure 1A - FTIR spectrum of CC13u.

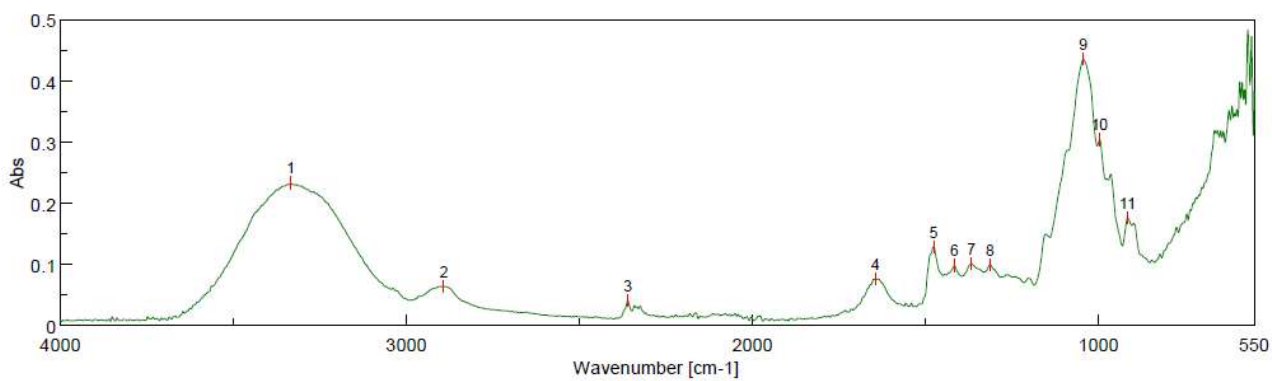


Figure 2A - FTIR spectrum of CC13.

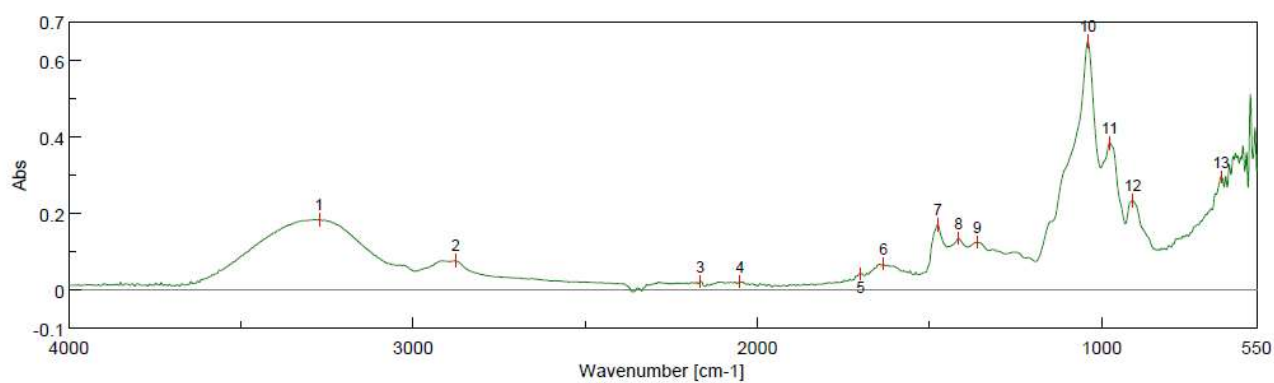


Figure 3A - FTIR spectrum of CC14.

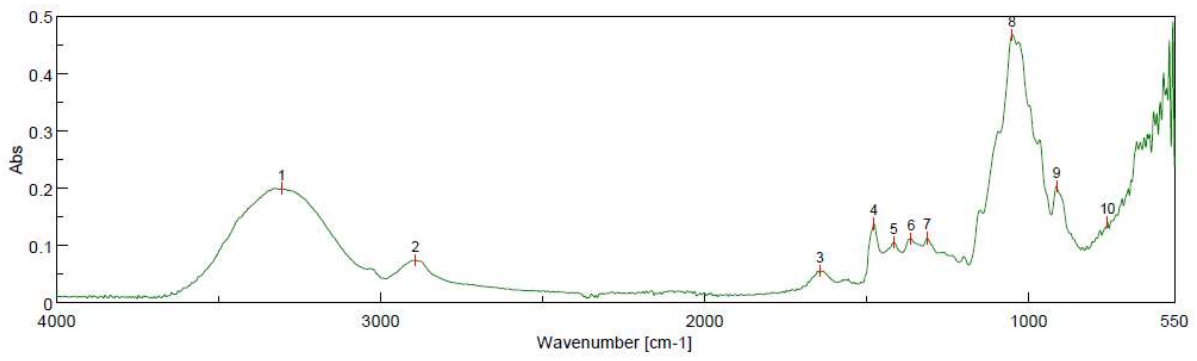


Figure 4A - FTIR spectrum of CC14u.

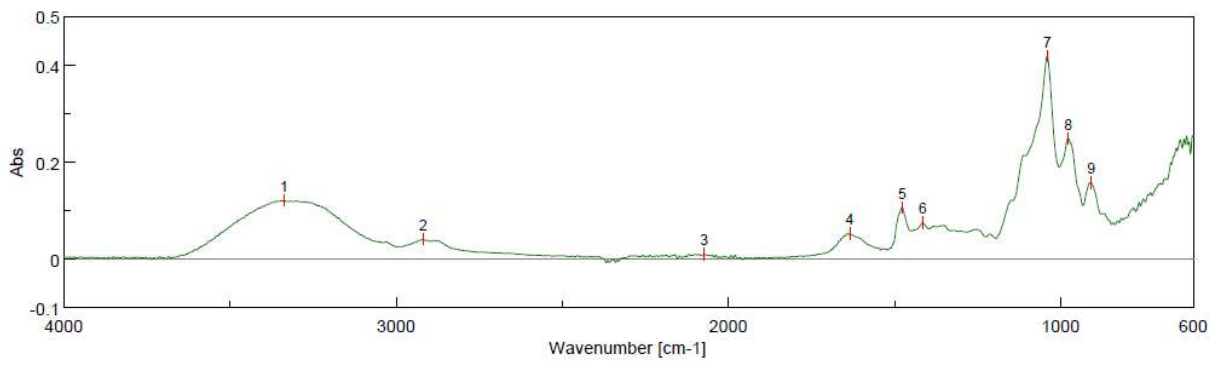


Figure 5A - FTIR spectrum of CC15.

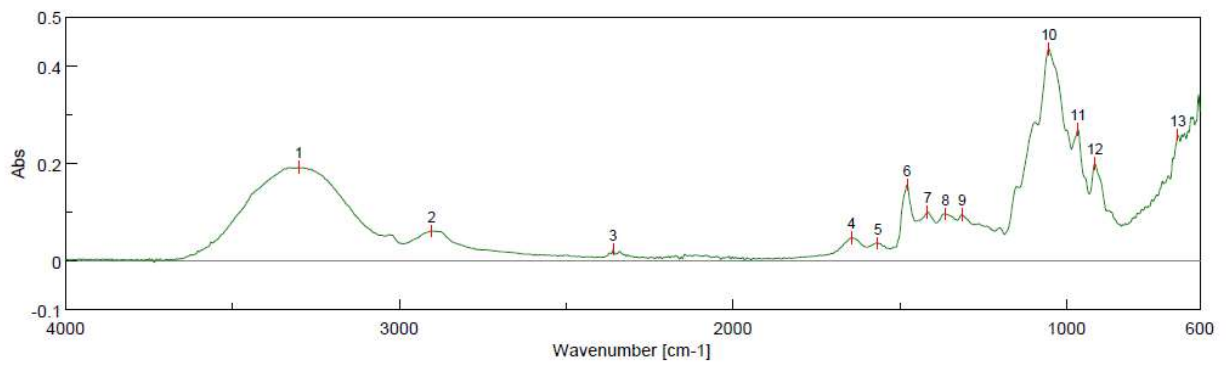


Figure 6A - FTIR spectrum of CC15u.

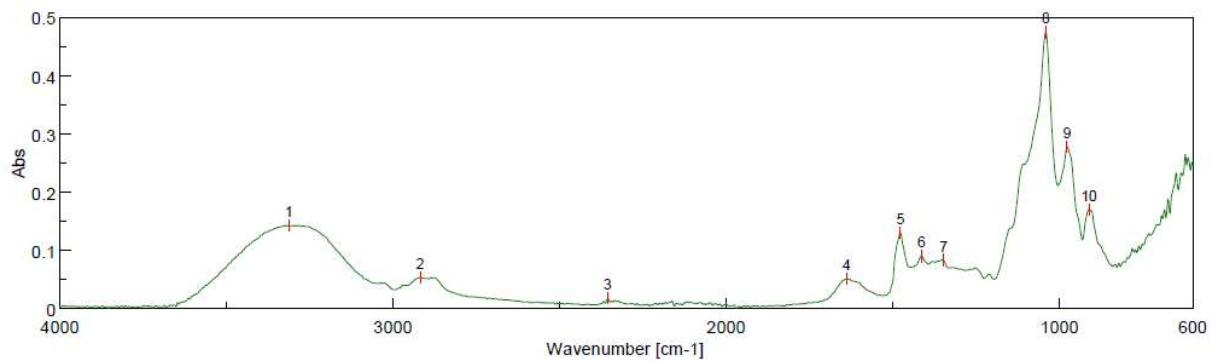


Figure 7A - FTIR spectrum of CC16.

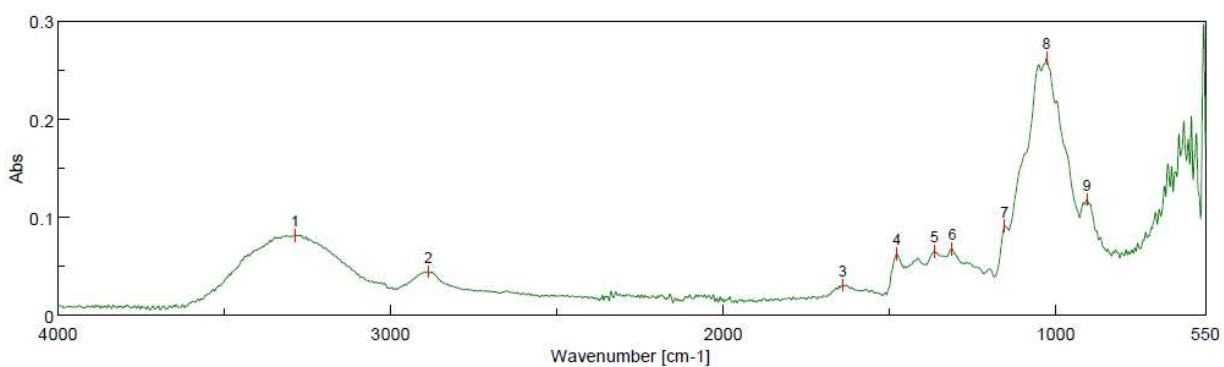


Figure 8A - FTIR spectrum of CC17u.

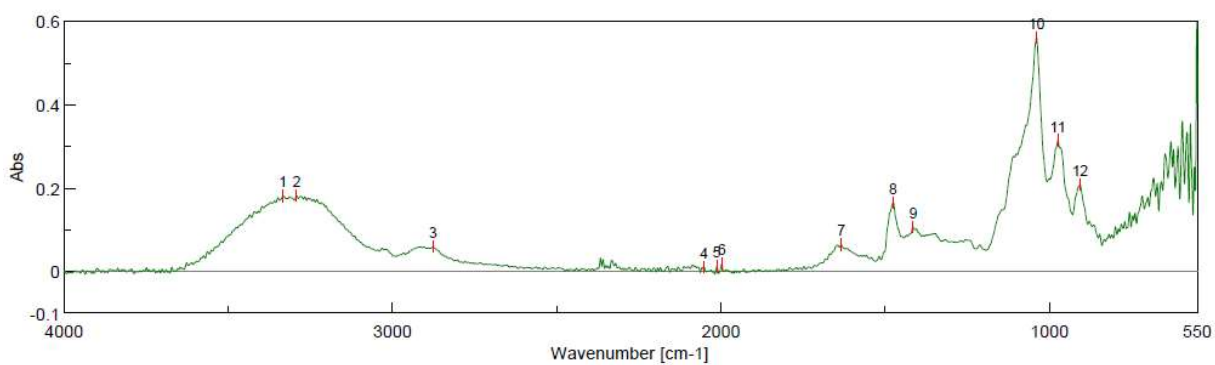


Figure 9A - FTIR spectrum of CC19.

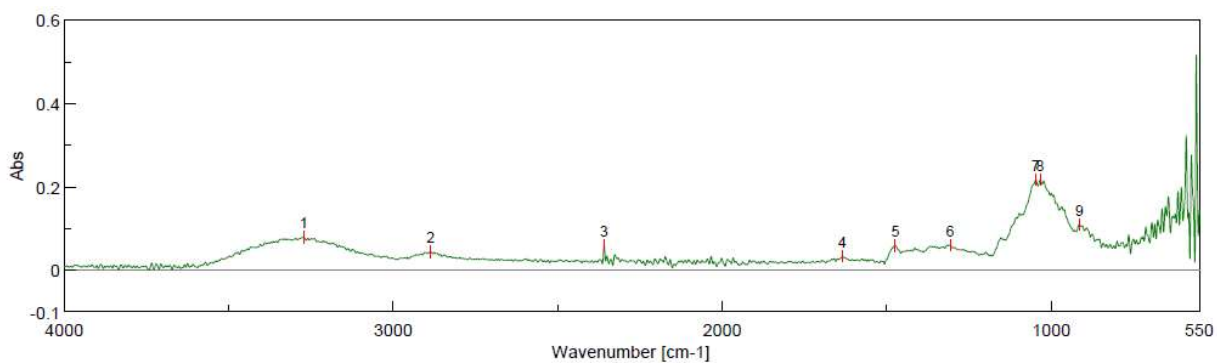


Figure 10A - FTIR spectrum of CC19u.

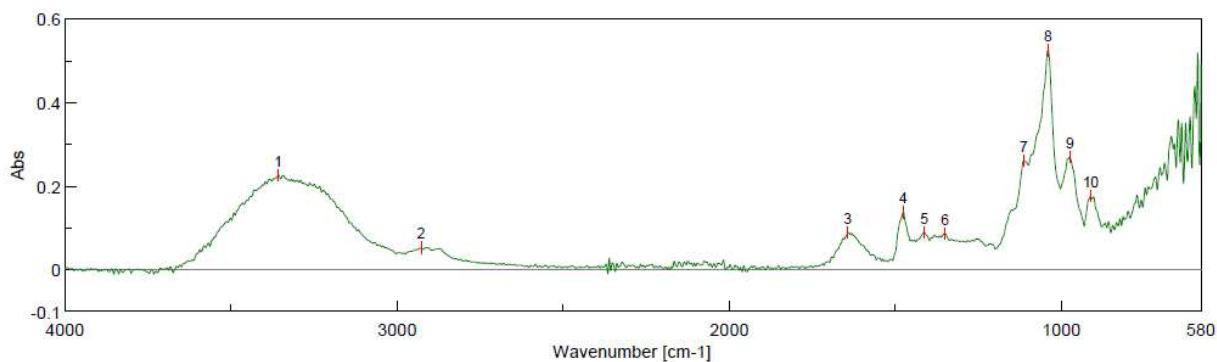


Figure 11A - FTIR spectrum of CC20.

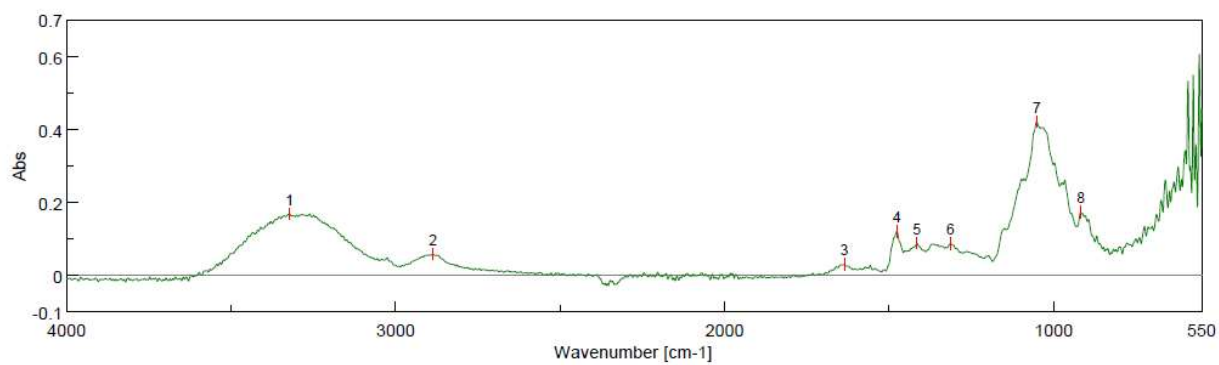


Figure 12A - FTIR spectrum of CC20u.

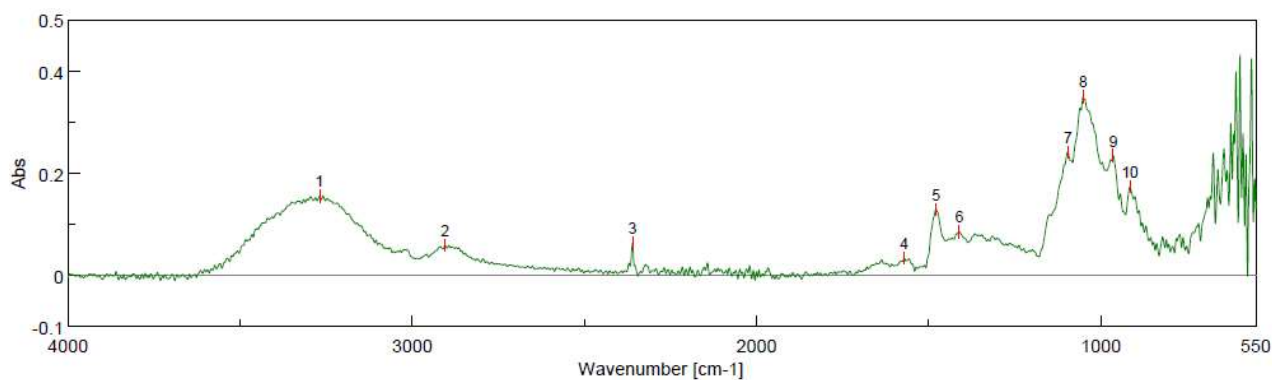


Figure 13A - FTIR spectrum of CC21.

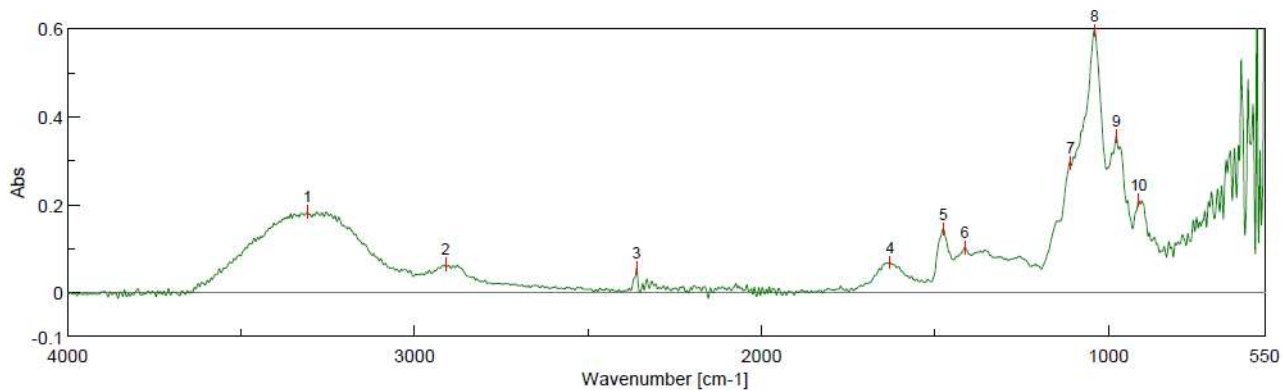


Figure 14A - FTIR spectrum of CC21u

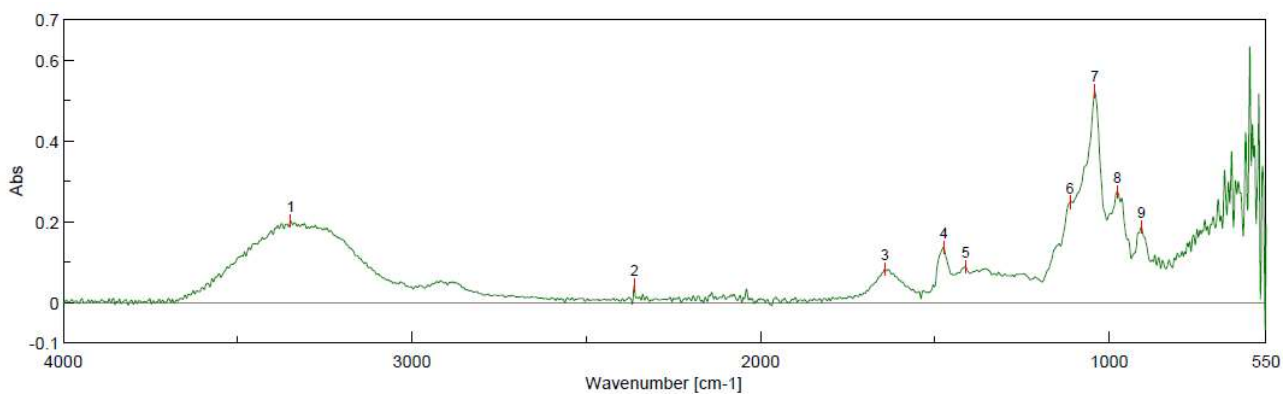


Figure 15A - FTIR spectrum of CC22.

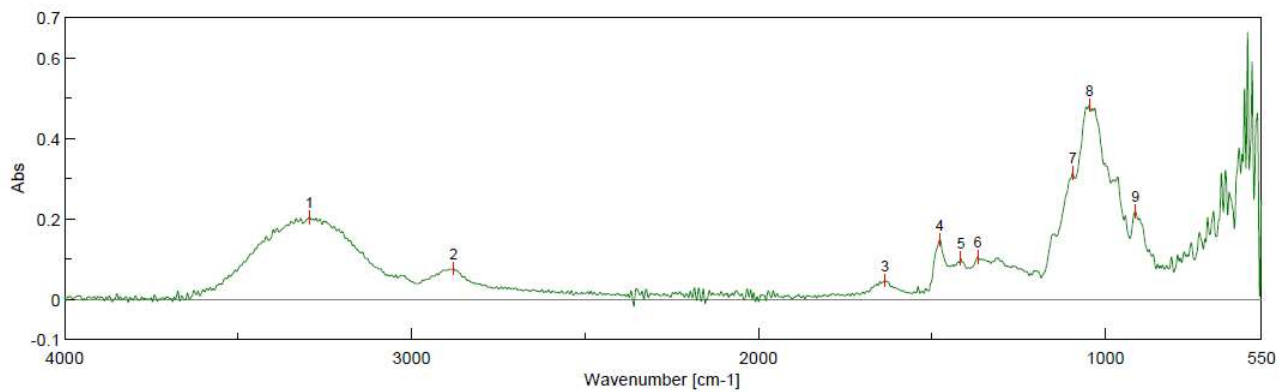


Figure 16A - FTIR spectrum of CC22u.

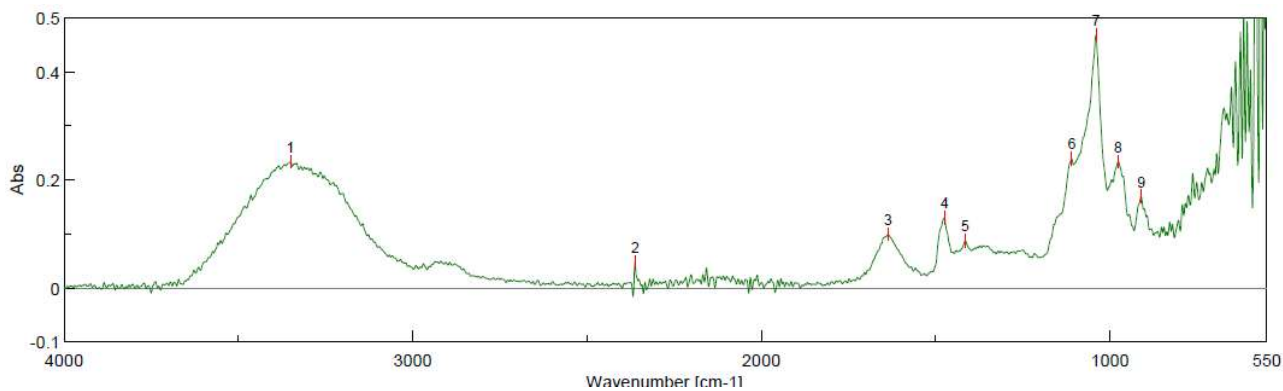


Figure 17A - FTIR spectrum of CC23.

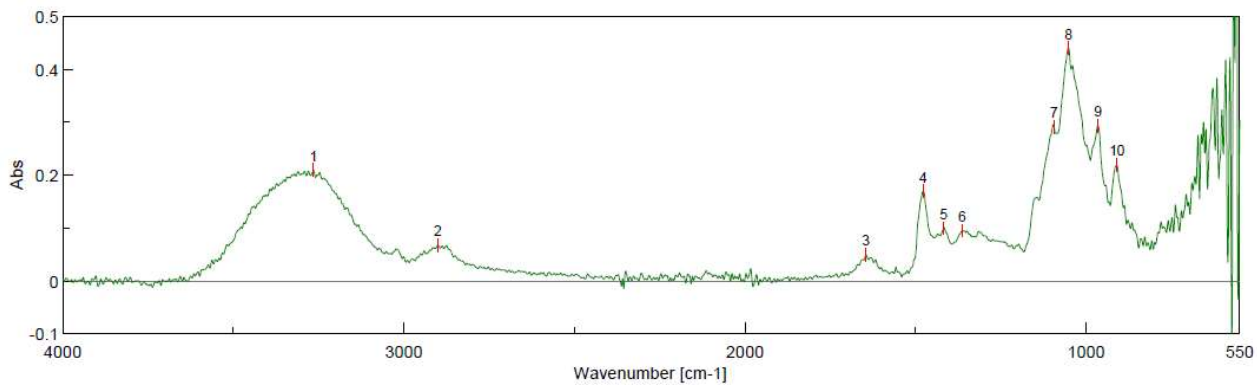


Figure 18A - FTIR spectrum of CC23u.

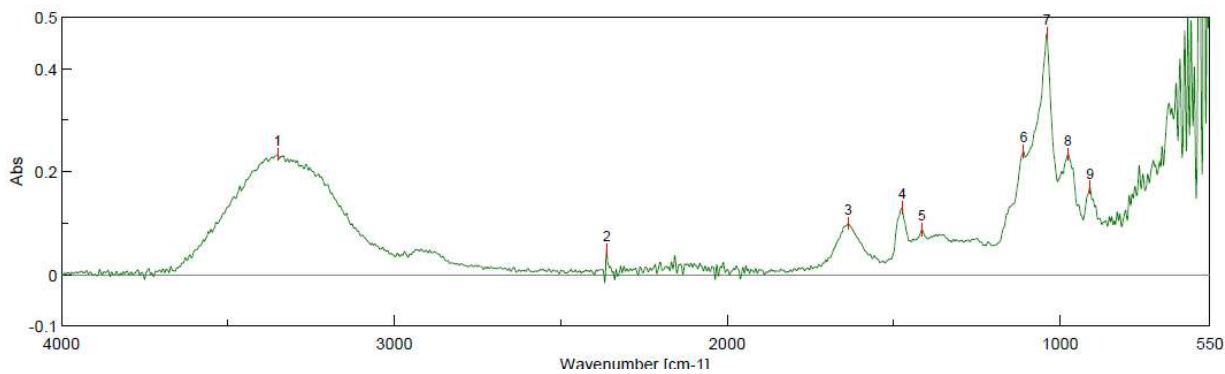


Figure 19A - FTIR spectrum of CC24.

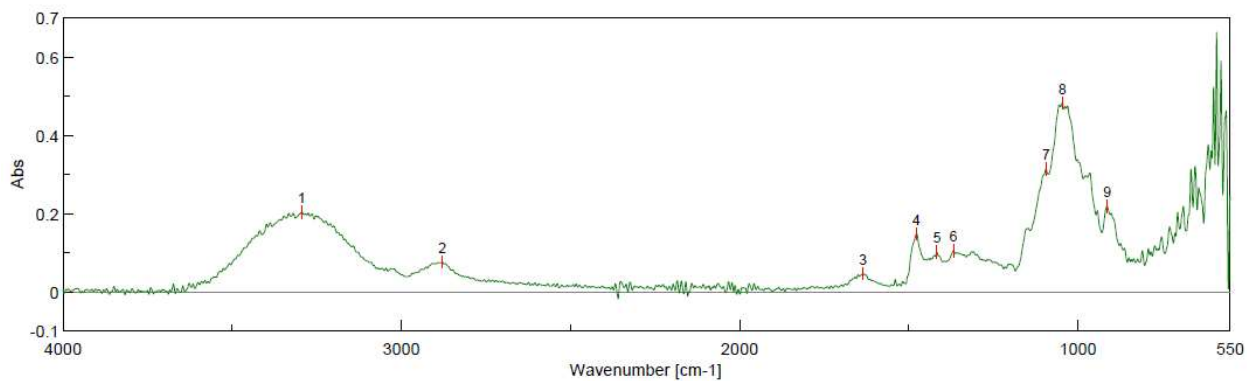


Figure 20A - FTIR spectrum of CC24u.

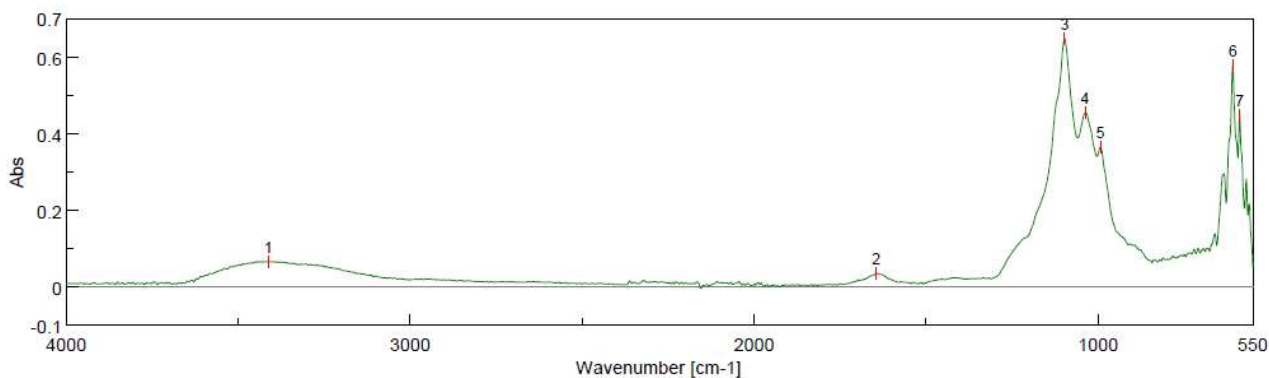


Figure 21A - FTIR spectrum of ADAC1-1.

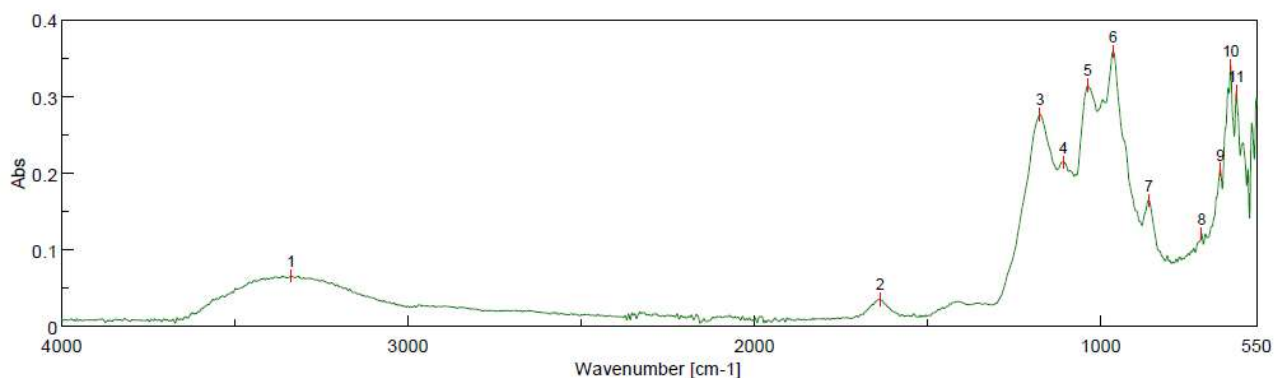


Figure 22A - FTIR spectrum of ADAC2-1.

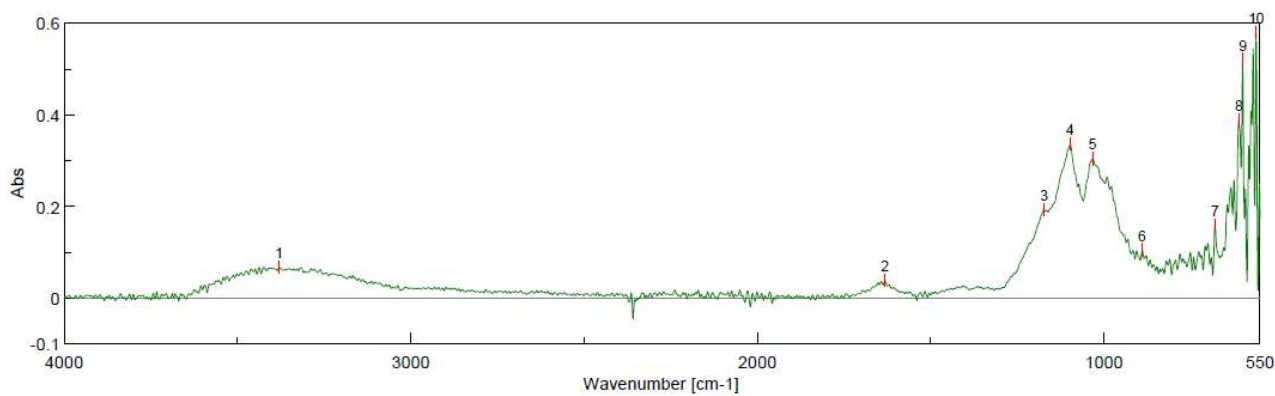


Figure 23A - FTIR spectrum of ADAC3-2.

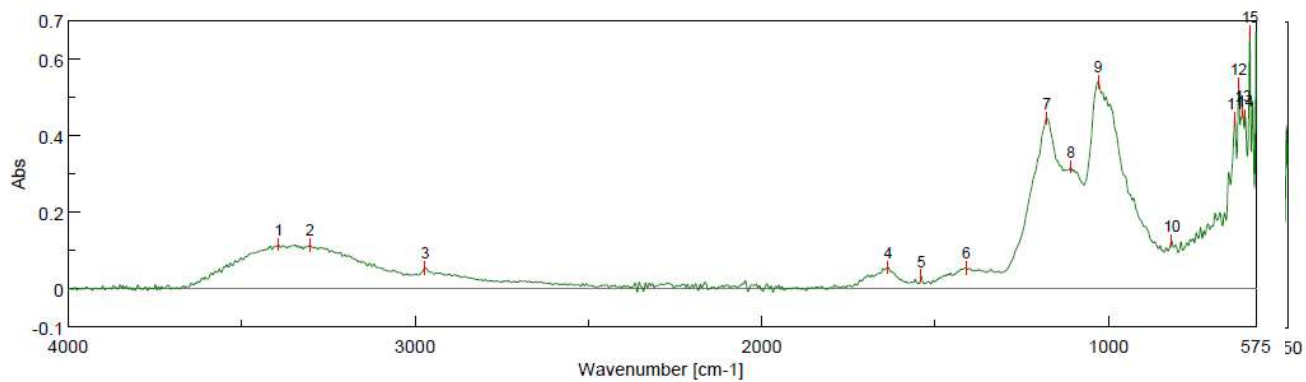


Figure 24A - FTIR spectrum of ADAC3-3.

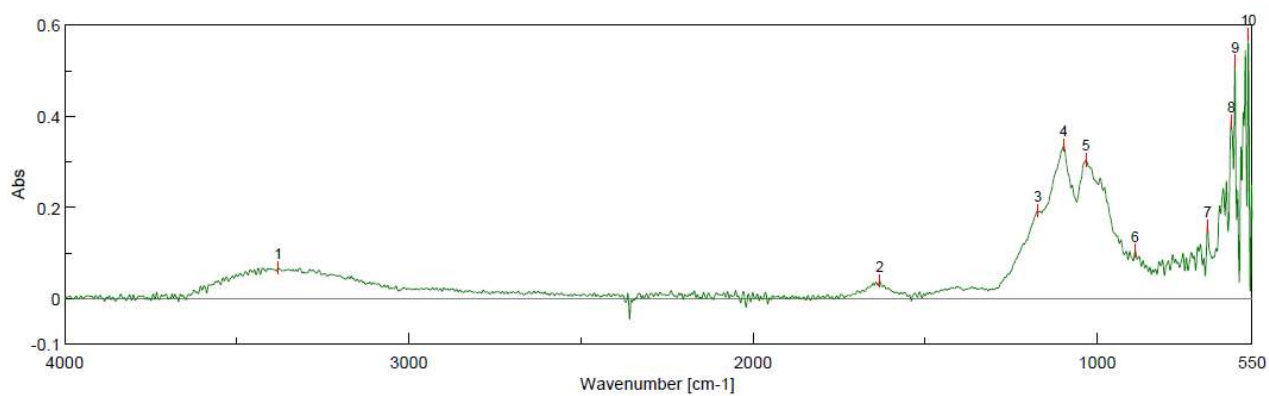


Figure 25A - FTIR spectrum of ADAC4-1.

Appendix B

Debye Plots

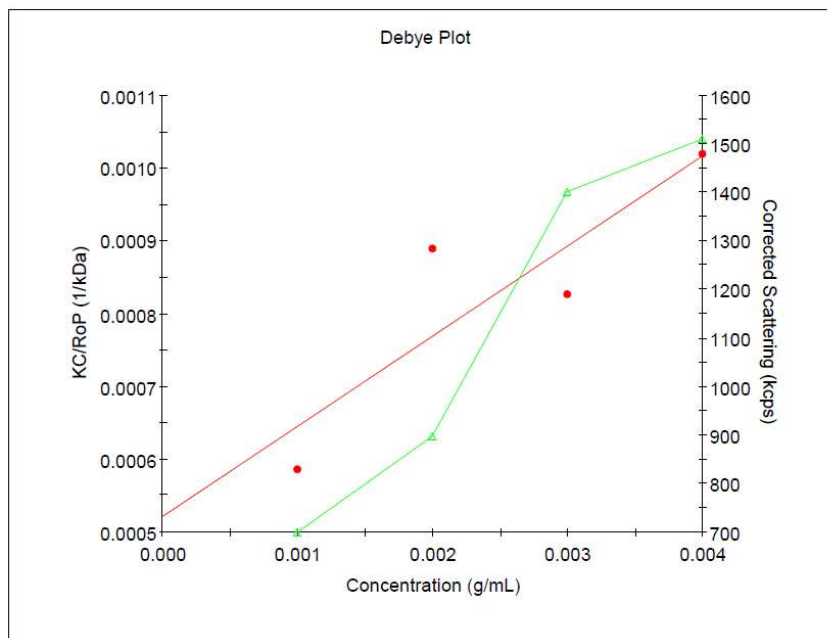


Figure 1B – Debye plot used for molecular weight determination of CC14.

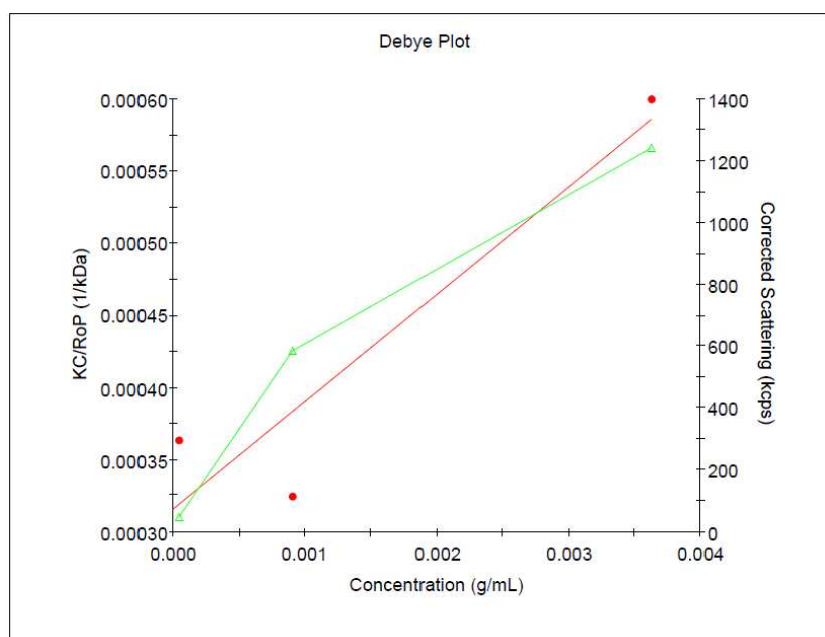


Figure 2B – Debye plot used for molecular weight determination of CC19.

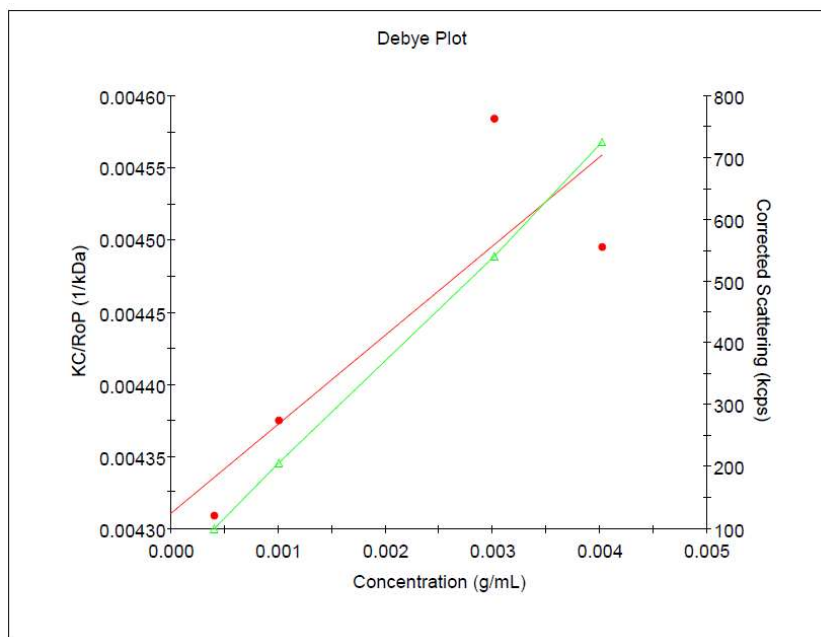


Figure 3B – Debye plot used for molecular weight determination of ADAC3-1.

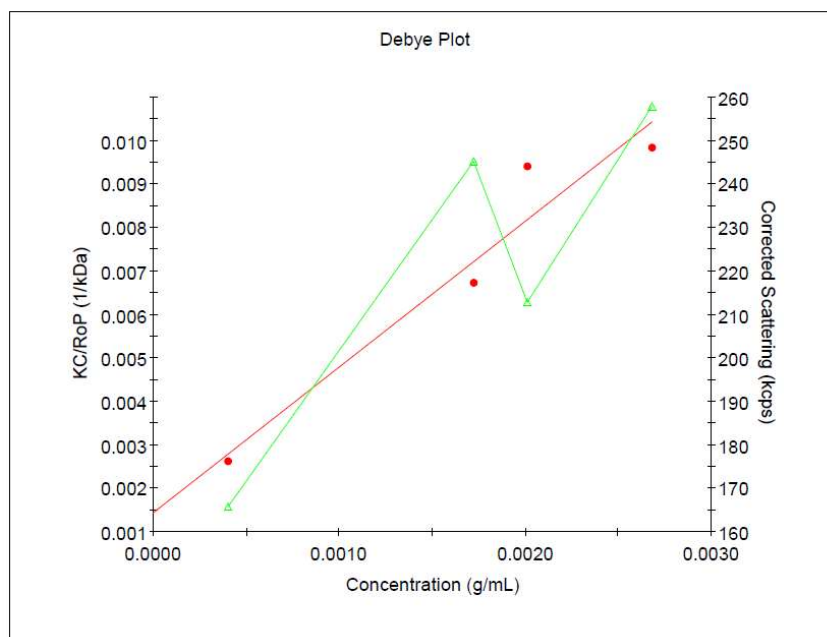


Figure 4B – Debye plot used for molecular weight determination of ADAC3-2.

Appendix C

Synthesis of cationic DAC /Conductometric titration

The basic idea in this route of synthesis was to make CHPTAC react with DAC, but it was necessary to have favorable reactive groups along the chain. The aldehyde groups seem not to be favorable as they are with Girard reagent T. However, it was supposed that the presence of carboxylic acid groups could favor the reaction with CHPTAC. For this reason, it was checked if the oxidation of cellulose could introduce these groups along the molecule. The conductometric titration of DAC1 gave a negative result, i.e., no carboxyl's were detected, since any *plateau* was measured and the graph has a “v” shape (**Figure 1C**). It was tried an over-oxidation of cellulose in DAC3, but the titration gave a negative result as well. The conclusion was that the sodium periodate oxidation of cellulose cannot introduce carboxylic groups. Anyway, the reaction was tried several times. DAC3 was selected and it was used the procedure of section 3.3.2. It was noticed that after roughly 50 min the reaction solution was to get transparent. In order to recover the product by precipitation many solvents were chosen. The direct precipitation adding drop by drop the reaction solution has given no positive results. It was tried to cool down the solvent or stirring it while adding drop by drop the reaction solution, but nothing happened. It was tried to heat up till 40 °C part of the reaction solution in order to evaporate water and concentrate the product. This last trial led to a color variation from transparent to brownish as an indication that some degradation was occurring. It is not clear which reaction was happening and the hypothetic structure of the product. It is supposed that CHPTAC after transformation to epoxide reacts with the alkalized hydroxyl groups of DAC. In

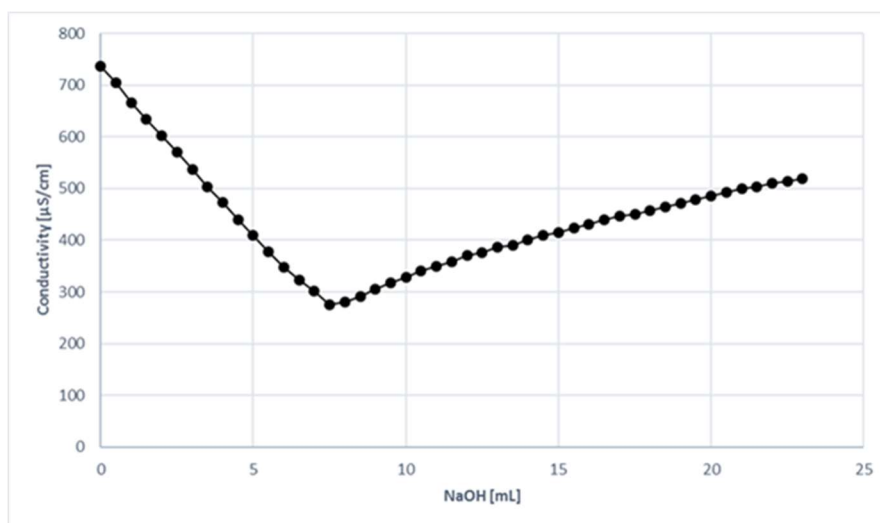


Figure 26A – Diagram of the conductometric titration of DAC1.

fact, hydroxyl groups in DAC and other hydroxyl groups in the non-oxidized AGU may remain after oxidation. Briefly, it is possible that EPTAC reacts with some alkalized hydroxyl groups along DAC.

This route of synthesis remains open to be studied and analysed more in detail in the future since it can lead to a new cellulose-based product.